ADAMA SCIENCE AND TECHNOLOGY UNIVERSITY

SCHOOL OF GRADUATE STUDIES

DEPARTMENT OF CIVIL ENGINEERING

EMPIRICAL CORRELATION BETWEEN ULTIMATE BEARING CAPACITY OF SHALLOW FOUNDATION AND FIELD DYNAMIC CONE PENETRATION INDEX FOR SHORT TERM LOADING (THE CASE OF EXPANSIVE SOILS OF ASELLA TOWN)

A Thesis Submitted to the School of Graduate Studies of Adama Science and Technology University in Partial Fulfillment of the Requirements for the Degree of Master of Science in Civil Engineering (Geotechnical Engineering)

By

Kemal Abdela

Advisor

Dr. Yadeta Chemdesa

July, 2017, Adama, Ethiopia

ADAMA SCIENCE AND TECHNOLOGY UNIVERSITY

SCHOOL OF GRADUATE STUDIES

DEPARTMENT OF CIVIL ENGINEERING

EMPIRICAL CORRELATION BETWEEN ULTIMATE BEARING CAPACITY OF SHALLOW FOUNDATION AND FIELD DYNAMIC CONE PENETRATION INDEX FOR SHORT TERM LOADING (THE CASE OF EXPANSIVE SOILS OF ASELLA TOWN)

By

Kemal Abdela

Approved by board of examiners

Advisor	signature	date
External examiner	signature	date
Internal examiner	signature	date
School dean	signature	date
Department head	signature	date
Chairperson	signature	date

DECLARATION

I hereby declare that the work entitled empirical correlation between ultimate bearing capacity of shallow foundation and field dynamic cone penetration index (DCPI) for short term loading of expansive soils of Asella town has been performed by me to the best of my knowledge towards masters of Science in department of civil engineering, under supervision of Dr. Yadeta Chemdesa. It contains no materials which has been accepted for award of any other degree in university, except where due acknowledgement has been made in the text.

Kemal Abdela ____________________ _______________

Signature date

Certify by:

Dr. Yadeta Chemdesa __________________ _____________

Signature date

ACKNOWLEDGMENT

I am grateful to **ALMIGHT ALLAH** for making it possible for me to complete this study and being with in every stage I pass through.

My sincere appreciation goes to my advisor Dr. Yadeta Chemdesa for his guidance and supervision of all my way through this research study.

Special thanks goes to geotechnical laboratory assistance of civil engineering department Shumi Dame and Solomon Abera for their valuable assistance during laboratory tests and the departments for facilitating the situation.

Finally, my deepest gratitude goes to Bule Hora University for sponsoring me and those who assist me to reach the final of my research work specially my family and friends for their support and encouragements through my journey.

ABSTRACT

Bearing capacity is one of the important parameters to be investigated for design and construction of foundations of civil engineering structures. The conventional method of estimating these parameters is relatively expensive and time consuming specially for small scale projects. Dynamic cone penetrometer (DCP) is one of the in situ test methods widely used in site investigation for estimating the strength and density of soils. This work is, therefore, aimed at predicting ultimate bearing capacity (Q_{ult}) of shallow foundations from field dynamic cone penetration index DCPI (mm/blow). The soil index properties and tri-axial tests were performed on soil samples extracted from different pits. On the same pits, DCP test have been performed in the field to determine DCPI (mm/blow). Then single regression analysis have been performed to determine relationship of Q_{ult} with DCPI and index properties. Single regression analyses results showed that Q_{ult} have strong relation with DCPI (R^2=0.75) than index properties. The comparison between the developed equation and the actual Q_{ult} obtained from Terzagi's bearing capacity equation shows average variations of $\pm$11.7%, suggesting the validity of the developed equation. The footing dimension have little effect on the predicted bearing capacity of foundation as the variation in bearing capacities with width of footing is very small.

TABLE OF CONTENTS

CONTENTS PAGE

List of figures

List of tables

List of symbols and abbreviations

AASHTO	American association of state highway and transportation officials
ASTM	American society of testing materials
B	Width of footing
C	Clay
CBR	Californian bearing ratio
CD	Consolidated drained tri-axial test
CH	High plastic clay
CI	Consistency index
CL	Low plastic clay
Cu	Un-drained cohesion
CU	Consolidated un-drained tri-axial test
D	Penetration per blow
DCP	Dynamic cone penetrometer
DCPI	Dynamic cone penetration index
D_f	Depth of foundation
FS	Factor of safety
G	Gravel
GPS	Global position system
L	Length of footing
Li	Liquidity index
LL	Liquid limit
M	Silt
MDD	Maximum dry density
MH	high plastic silt
ML	Low plastic silt
N	Blow per 100mm
N_c	Bearing capacity factor due to cohesion contribution

NMC	Natural moisture content
N_q	Bearing capacity factor due to overburden pressure contribution
N_γ	Bearing capacity factor due to unit weight contribution
O	Organic materials
OMC	Optimum moisture content
P	Poorly graded
PI	Plasticity index
Q_{all}	Allowable bearing capacity
Q_{ult}	Ultimate bearing capacity
S	Sand
S_c	Bearing capacity shape factor for cohesion component
SPSS	Statistical package for social science
S_q	Bearing capacity shape factor for surcharge component
S_γ	Bearing capacity shape factor for unit weight component
UCS	Unconfined compressive strength
USCS	Unified soil classification system
UU	Unconsolidated un-drained tri-axial test
W	Well graded
W_l	Liquid limit
W_n	Natural moisture content
W_p	Plastic limit
σ_1	Major principal stress
σ_3	Cell pressure/Minor principal stress
σ_d	Deviator stress
Φ_u	Un-drained angle of internal friction
γ_b	Bulk unit weight
γ_d	Dry unit weight
ε_a	Axial strain

CHAPTER ONE

1. INTRODUCTION

1.1. Back ground and Justification

The engineering and geological soil and material investigations are important components in urban planning and designing of every engineering structure. The causes of failure of engineering structures built on clayey soils are mostly related to the expansive nature of the soils and improper estimation of bearing capacities of the soil mass.

Bearing capacity is one of the important parameters to be investigated for design and construction of foundations of civil engineering structures. Improper estimation of these bearing pressure leads to either overestimation or underestimation of soil load carrying ability. The conventional approach to estimate bearing capacity of foundation is through investigation of shear strength parameters such as cohesion (C) and angle of internal friction (Φ).

Determination of the shear strength parameters of soils, which are basic parameters for bearing capacity computation, using aforementioned methods requires relatively more time, effort as well as money. In addition, the application of field tests for determination of bearing capacities are important for professional engineers since present practice is to rely more on field tests as it can avoid some of the problems of disturbance associated with the extraction of soil samples form ground. In light of these challenges there is a need to find time and cost effective ways that can replace shear strength parameters for determination of bearing capacity of shallow foundation for light structures.

Dynamic cone penetrometer (DCP) is one of the in situ test methods widely used in site investigation for estimating the strength and density of soils. The test is simple, quick and the equipment is portable. In combination with the other methods it has potentials to predict the engineering properties of soil. It has recommended to be appropriate technology for use in developing countries (Sanglerat, 1972). Due to this attempts have been made by different researchers to find the empirical relationship between DCP test result and engineering properties for different soil types: DCPI with CBR (Amini, 2003)and (Desalegn, 2012), D-value with UCS (McElvaney et al., 1991), D-value with resilient modulus (George et al., 2000), D-value with allowable bearing pressure (Dzitse-Awuku, 2008). Their results suggests that the engineering properties can be predicted satisfactorily from DCP values. However, engineering properties of soils varies from place to place based topography and climatic condition, so previously developed correlation by different researchers to predict engineering properties of soil have limit application to the study area. Adopting those developed correlation without improvement can leads us to misinterpretation of soil behaviors. In addition, most of the previous attempts focus on DCP use in pavement design and not much research has been conducted on use of DCP in estimating ultimate bearing capacity for shallow foundation design in particular.

The present work is, therefore, aimed at developing correlation between ultimate bearing capacity of shallow foundation and field dynamic cone penetration index (DCPI). The outcome of the present work can be applicable to preliminary assessment and design of shallow foundation on expansive soils.

1.2. Research Objectives

1.2.1. General objectives

The main objective of this research was to establish correlation between ultimate bearing capacity of shallow foundation and field dynamic cone penetration index (DCPI) of expansive soils of the town.

1.2.2. Specific objectives

- Determination of geotechnical index properties for preliminary soil assessment and subsequent analysis.
- Determination of the shear strength parameters (i.e. friction angle (Φ_u) and cohesion **(**C_u)) from UU tri-axial test.
- Checking and come up with Correlations of ultimate bearing capacity of shallow foundation with field dynamic cone penetration index (DCPI).
- Evaluation and validation the developed correlation using a control test results.

1.3. Description of the study area

Asella is the capital of Arsi zone and Tiyo woreda of Oromia regional state located between latitudes of **7^0 54’55”N-8^0 00’05”N**, and longitude of **39^0 06’10”E-39^0 10’00”E**. The altitudes of the town is 2700 meters above sea level in the South east but declines up to 2210 meters above mean sea level in the west direction of the town (Yilma, 2013)**.**

Generally, rugged topographies are common in the eastern parts of the town but almost gentle slopes prevail in the western and northern parts of the town. The presence of steeper gradient in eastern parts of the town is responsible for the presence of deep furrow erosion along most stream and river valleys of the town.

Topography is important in soil formation as it control on surface processes like erosion and drainage. The soil of Asella town ranges from red clay soil which is found in the southern and eastern parts of the town where there is well drained hilly and high downward seepage to black cotton soil which is generally observed in flat, low lying areas of northern and some part of western direction of the town with poor vertical drainage.

The climate of a given place is the reflection of different factors such as latitude, altitude, pressure difference between high lands and low lands and distance from the Sea as well as the impact of topography and cloud cover. Due to the impact of altitude, the agro climatic zone of the town is categorized as temperate climate because temperate climate prevails at the altitudinal limit the town is located. The mean annual rainfall and temperature of the town is 700-850mm and 17.5^0C, respectively (Yilma, 2013). Generally the soil forming factors such as topography, amount of rain, climate and parent rock materials seems to favor formation of red clay soil and black cotton soil in different part of study area.

1.4. Scope of the Investigation

In order to address the aforementioned purposes, fifteen test pits were dug in the town at different locations where expansive soils prevails. The locations (latitude and longitude) of the test pits are included in Figure 1.1 and Table 1.1. Depth of test pit varies from 1.5- 3.0m as it is common on the study area to place the foundation at these depth. Disturbed samples were extracted from all pits for shear strength and index property tests and parametric studies have been done to correlate ultimate bearing capacity (Q_{ult}) of shallow foundation with field DCP tests results (DCPI).

The results from this research can be used in identifying and estimating bearing capacities of the expansive soil of the area and so that possible measures can be taken to reduce the problems arising to the structures during and after construction. It can also be impute for further investigation on expansive clay soil in the other locality of the country.

Table 1.1: Latitude and longitude of test pit location

Location	**Depth(m)**	**Latitude**	**Longitude**
Pit 1:Asella hospital	1.5	$7^0$58’4.39”	$39^0$8’1.13”
Pit 2:Stadium	2.5	$7^0$57’34.77”	$39^0$7’45.17”
Pit 3:Maikel	2.0	$7^0$57’51.31’’	$39^0$8’10.64”
Pit 4: Silingo	1.5	$7^0$58’50.06”	$39^0$7’43.21”
Pit 5: Ars**i** university	2.5	$7^0$59’20.26”	$39^0$7’44.43”
Pit 6: Kebele 2	2.0	$7^0$56’48.16”	$39^0$7’42.13”
Pit 7: Kebele 14;boseta	1.5	$7^0$57’38.20”	$39^0$08’37.5”
Pit 8:Kebele 1; Chilalo college	1.5	$7^0$56’46.34”	$39^0$08’2.16”
Pit 9:Kebele 4 ;mosque	2.0	$7^0$57’30.70”	39^0 06’59.21”
Pit 10: Kebele 10; prep. School	2.5	$7^0$58’30.50”	$39^0$08’4.64”
Pit 11: Welkesa river area	2.0	$7^0$58’59’’	$39^0$07’50.5”
Pit 12: Keb. 10 TTC	1.5	$7^0$58’26.5”	$39^0$07’45.8”
Pit 13:Keb.9,mosque area	1.5	$7^0$58’2”	$39^0$08’14.5”
Pit 14: Keb. 10,condominium	1.5	$7^0$59’2.4”	$39^0$07’51”
Pit 15:bBehind OPDO office	2.0	$7^0$57’58”	$39^0$07’52.6”

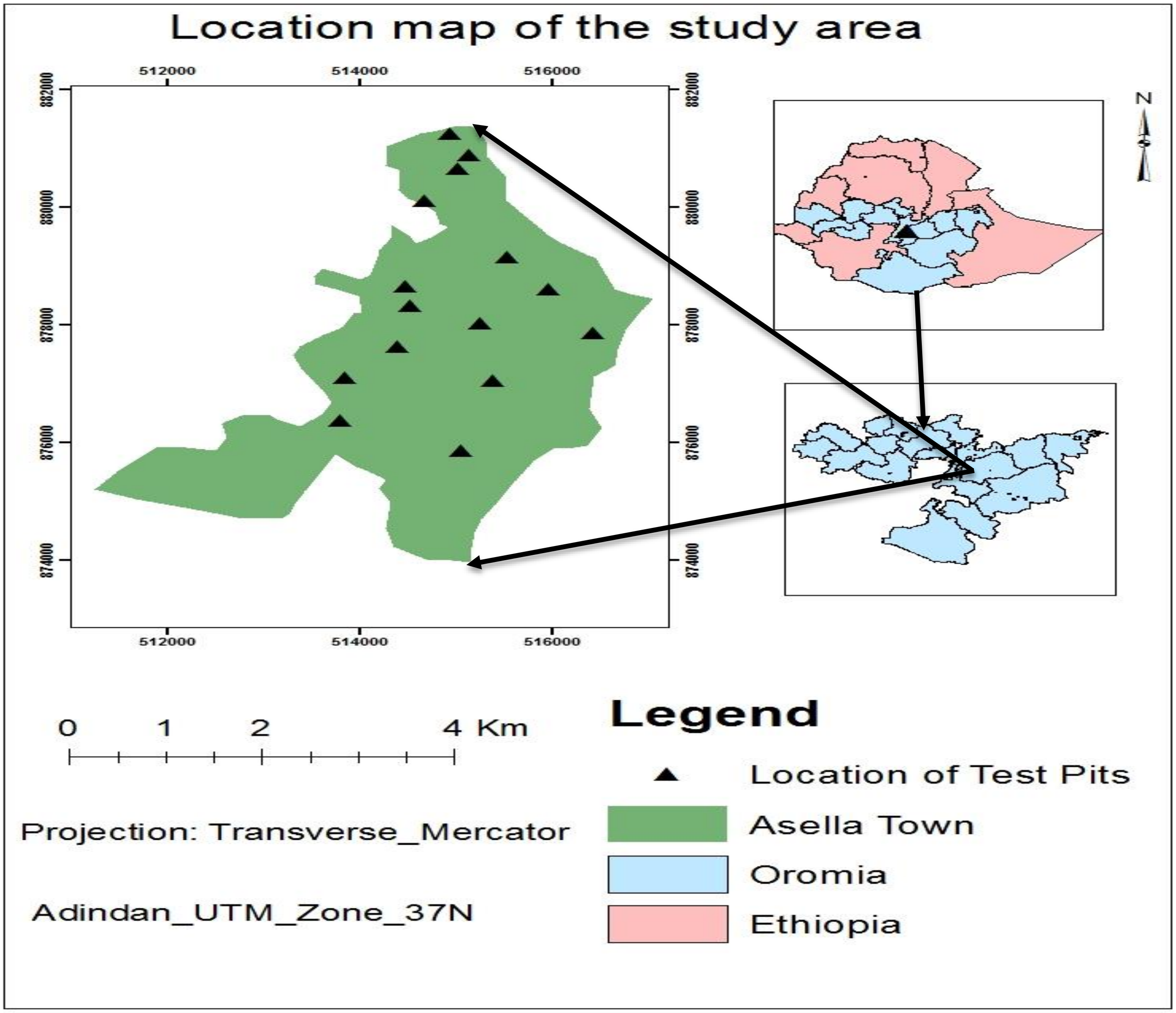

Figure 1.1: Location map of the study area and test pits location

1.5. Thesis Outline

The thesis is composed of five chapters. Chapter 1 provides an introduction of the research topic. It also discuss the need of the work and the overall objectives of the thesis. The theoretical background of the present study and a review of the literature about geotechnical parameters required for predicting the behavior of expansive soils and empirical relation between bearing capacity and DCP are given in Chapter 2. In Chapter 3, the experimental methods are explained by presenting the procedures of samples preparation followed by testing program. The interpretation of test results obtained in each experiment and, parametric studies to correlate ultimate bearing capacity of shallow foundation with field DCP test results are presented in Chapter 4. Finally, the conclusions obtained from the present study and recommendations for future work are given in Chapter 5. This is followed by a list of references and an appendix.

CHAPTER TWO

2. LITRATURE REVIEW

2.1. Distribution of expansive soils

Expansive soils are found in various parts of the globe including: Argentina, Australia, Brazil, Canada, China, Cuba, Ethiopia, Ghana, India, Israel, Iran, Japan, Mexico, Morocco, Myanmar, Oman, Peru, Saudi Arabia, South Africa, Spain, Sudan, Turkey, United States of America, Venezuela, and Zimbabwe (Chen, 1988). They are formed in areas where the annual evapo-transpiration exceeds the Precipitation (Chen, 1988)**.** The relationship between the climatic similarity of the regions and the existence of expansive soils in the areas is evident. Slater (1983) described that the distribution of expansive soils is generally the result of geologic history, sedimentation, and local climatic conditions. This type of soil has been characterized by the presence of high amounts of expansive clay minerals. Expansive soils are typically consists of 2:1 expansive clay minerals such as montmorillonite. These minerals evolved in geologic time under an arid and semi-arid climate that, in turn, governs the volume change behavior, that affects the shear strength property.

2.2. Identification and classification of expansive soil.

The key to all expansive soil classification systems is the method of measuring swelling potential, since soils are rated by their measured swelling potential. Swelling potential may be measured directly in swelling test or indirectly determined by correlation with other test results of swelling test data.

2.2.1. Field Identification

It is easy to recognize expansive soils in the field during either dry or wet seasons. Their color varies from dark grey to black. During dry seasons, shrinkage cracks are visible on the ground surface with the maximum width of these cracks reaching up to 20mm or more and deeper in depth. Lump of dry black cotton soil requires a hammer to break. A shiny surface is easily obtained when a partially dry piece of the soil is polished with a smooth object such as the top of a finger nail.

During rainy seasons, these soils become very sticky and very difficult to walk on. Appearance of cracking in the nearby structures is also indicative (Murthy, 2007; Teklu, 2003)

2.2.2. Laboratory identification

Generally, there are three different method of identifying expansive soil in the laboratory.

i. Mineralogical identification

This method is used for identifying the mineralogy of clay particles such as characteristic crystal dimensions, characteristic reaction to heat treatment, size and shape of clay particles and charge deficiency and surface activity of clay particle. These properties are a fundamental factor controlling expansive soil behavior (Chen, 1988)**.** The various techniques under these methods are:

-X-ray diffraction

-Differential thermal analysis

-Dye absorption

-Electron microscope

-Base ex-change capacity, etc.

But these methods are not suitable for routine tests because of the following reason; they are time consuming, require expensive test equipment and, the results are interpreted by specially trained technicians.

ii. Indirect methods

These methods include simple soil property test that a practicing engineer resort to use for identifying expansive soil. The commonly used test is the Atterberg limit and yields an excellent indices of expansive soil properties. In this method, measurement of the plasticity and the shrinkage characteristics of the soil are conducted for identification of soils and provide a wide acceptable means of rating by using liquid limit, plastic limit, shrinkage limit, free swell tests, colloid content test, etc.

iii. Direct measurement

The direct method provides the actual physical measurement of swelling that the soil undergoes as the moisture content changes and hence a convenient and dependable method for a practicing Engineer. It can be done by the use of a conventional one-dimensional consolidometer which is available in most soil mechanics laboratories.

2.3. Classification of expansive soils

Soil classification is an important aspect of laboratory test, which tells the characteristic of the soil under interest. There are a number of classification systems based on identification tests. Among these, the Unified Soil Classification System (USCS) and the American Association of State Highway Transport Officials (AASHTO) method make use the liquid limit and plasticity index of the soil.

A. Classification according to USCS

This practice describes a system for classifying soils for engineering purpose based on laboratory determination of particle size characteristics, liquid limit and plasticity index and used when precise classification of soil is required. The USCS uses symbols for the particle size groups. These symbols and their representations are G—gravel, S—sand, M—silt, and C—clay. These are combined with other symbols expressing gradation characteristics: W for well graded and P for poorly graded and plasticity characteristics: H for high and L for low, and a symbol, O, indicating the presence of organic material. The flow charts shown in Figures 2.1 provide systematic means of classifying a fine grained soil according to the USCS (Budhu, 2007)

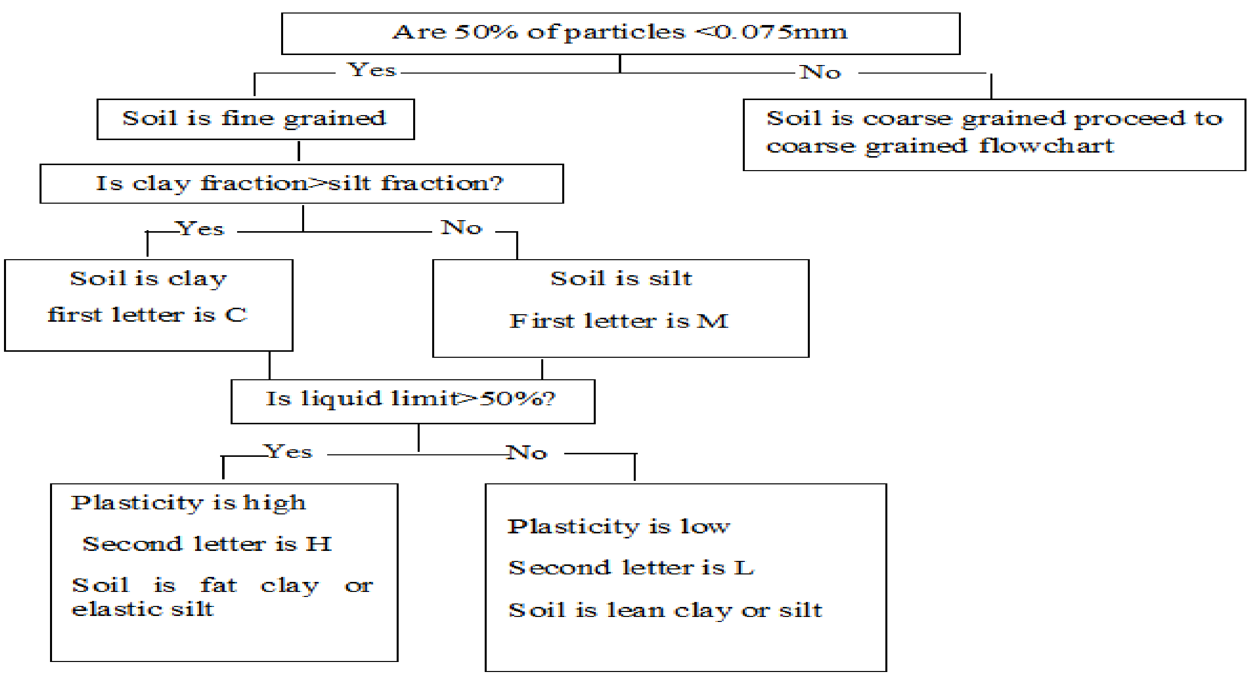

Figure 2.1: Unified soil classification flowchart for inorganic fine-grained soils (Budhu, 2007)

A high numerical value of plasticity index is an indication of the presence of high percentage of clay in the soil sample which implies that the plasticity values increase with the corresponding increase in clay contents. This was done by means of a plasticity chart (Figure 2.2) developed from soils tested from different parts of the world (Budhu, 2007). Clays, silts and organic soils lie in distinct region on the chart. The A-line separates clays from silts. The U-line defines the upper limit of the correlation between plasticity index and liquid limit. If the results of the soil tests fall above the U-line, one should be doubtful on the quality of the tests and should be repeated.

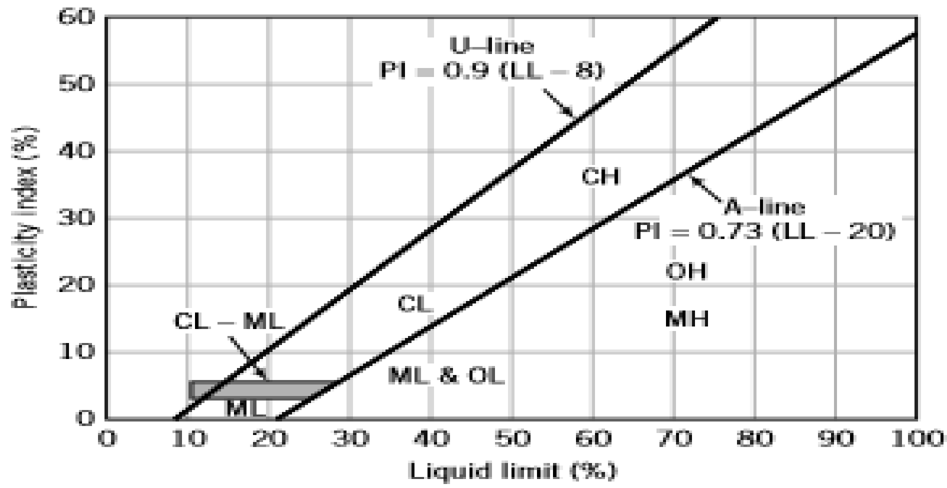

Figure 2.2: USCS according to plasticity chart (Budhu, 2007).

B. Classification according to AASHTO

According to this system, soil is classified into seven major groups: A-1 through A-7. Soils classified under groups A-1, A-2, and A-3 are granular materials of which 35% or less of the particles pass through the No. 200 (0.075mm) sieve. Soils with more than 35% pass through the No. 200 (0.075mm) sieve are classified under groups A-4, A-5, A-6 and A-7. These soils are mostly silt and clay-type materials.

Geotechnical engineers generally prefer the USCS as it is general and can be used for different engineering application, while the AASHTO classification is widely used by highway and transportation engineers for selection of sub grade materials (Das, 2002). There are also other classification methods specifically proposed for expansive soils, one of them is the single index method. However, the use of single index method of classification alone may lead to wrong conclusion (Chen, 1988; Teklu, 2003). But, combining of index property, swell and physical indicators can develop a better indirect classification system of expansive soils.

2.4. Bearing capacity of shallow foundation

The ultimate bearing capacity of soil Q_{ult} is defined as value of bearing pressure that will cause large increment in settlement of foundation without further increase bearing pressure resulting in shear failure. The ultimate bearing capacity of shallow foundation is usually calculated from Terzaghi's bearing capacity equation by incorporating appropriate soil parameters (cohesion, internal friction and unit weight), footing details and foundation depth. The allowable bearing pressure (q_{all}) is the maximum bearing pressures that can safely be applied to foundation such that, it is safe against instability due to shear failure and maximum tolerable settlement. The allowable bearing pressure is normally calculated from ultimate bearing capacity by using appropriate factor of safety. Typical value of factor of safety for shallow foundation is 3.0. However, method of estimating these parameters is relatively become expensive and time consuming for small scale projects; because tri-axial or direct shear tests should be done to determine parameters such as Φ and C. Three types of laboratory tests are commonly used to determine shear characteristics of soils. These tests are the direct shear test, the tri-axial compression test and the unconfined compression test. It should be noted, however, that laboratory strength test are meaningful only if the laboratory conditions of loading and drainage are adequately represent the actual field conditions and also the soil sample being tested is representative of the in-situ soil. Out of the three types of tests mentioned above, the tri-axial compression test is more versatile and simulates the in situ conditions better. Therefore, it is used for this study. Various tri-axial test methods are defined on the bases of drainage conditions during the application of the confining pressure, σ_3, and the drainage condition upon the application of deviator stress, (σ_1-σ_3) through the loading ram in contact with the top of a cylindrical soil specimen enclosed in a rubber membrane placed in the tri-axial cell filled with water. The main advantages of this type of test includes the possibility to control drainage conditions, and procedures for measuring pore pressure during the test**.** So due to the difficulty to consolidate expansive clay soils and because of the fact that the consolidation swelling behavior is so complex and deserves special consideration and special laboratory arrangement, only UU test is performed in this study.

2.4.1. Factors affecting bearing capacity

Number of factors have been studied and found to affect bearing capacities of shallow foundations (Dzitse-Awuku, 2008). Some of these are;

- **a)** The unit weight, shear strength and deformation characteristics of soils.
- **b)** The size, shape, depth and roughness of the footing.
- **c)** Groundwater level and initial stress in the foundation soil

2.4.2. Terzaghi's ultimate bearing capacity (BC) equation

The Terzaghi's formula which is modified from Prandtl (1921) plastic failure theory is used for evaluation of ultimate bearing capacity of shallow foundations. Terzaghi's theory is based on the observation that the failure surface in the soil at ultimate load takes the form shown in fig 2.4, thus forming triangular elastic wedge zone directly under the footing and two bulges delineated by two log spiral curves extending to the ground surface. In the theory the angle α between footing base and sides of triangular zone were taken to be equal to the soil internal friction angle Φ.

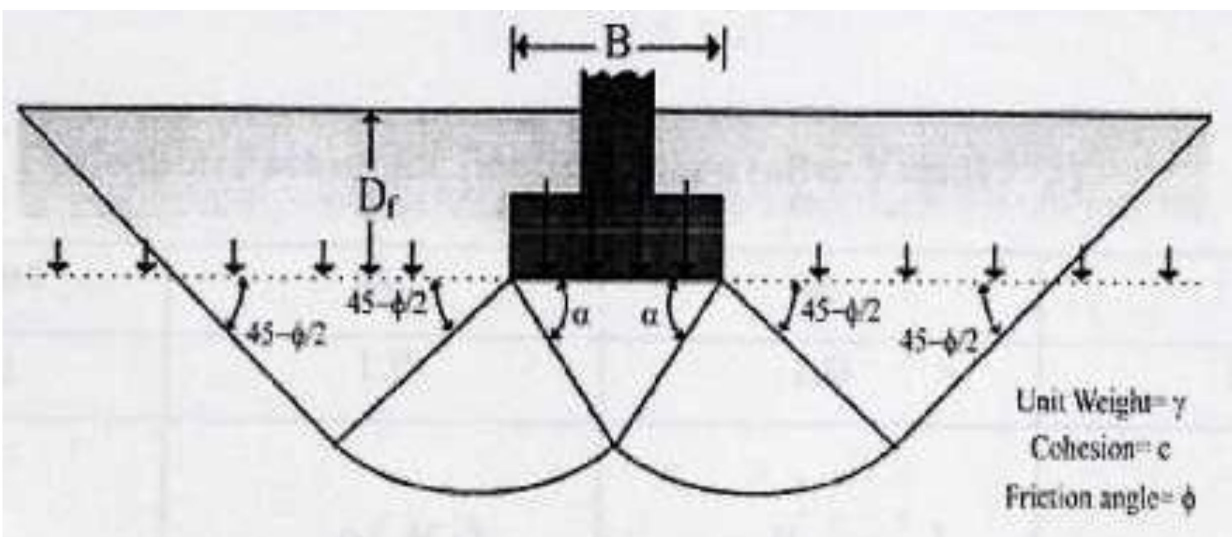

Figure 2.3: Shear failure surface after (Terzaghi, 1943)

Using equilibrium analysis, Terzaghi expressed the ultimate bearing capacity for shallow strip foundation in simplest form as:

$$Q_{ult}= C.N_C+\gamma D_f N_q+0.5\, \gamma B N_{\gamma} \text{..............} (2.1)$$

Where N_C, N_q, N_γ are Terzaghi's bearing capacity factors.

C= cohesion of soil, D_f =depth of footing, B= width of footing

The equation (2.1) is subjected to the following conditions

- **a)** General shear failure;
- **b)** Strip (continuous footing for which L > 5B
- **c)** Shallow foundation for ($Df \leq B$)

On the basis of comparative loading test on footing with different shapes equation 2.1 has been modified into equation 2.2 by incorporating correction factor for footing shapes configurations (Vesic, 1973)

$$Q_{ult} = C.N_C.S_C + \gamma.D_f.N_q.S_q + 0.5\gamma.B.N_\gamma.S_\gamma \quad \ldots\ldots\ldots\ldots\ldots\ldots\ldots\ldots \text{(2.2)}$$

Where S_c, N_q, N_γ are shape factors. Table 2.1 gives correction factors for footing shape configuration for shallow foundations.

Table 2.1: Correction factors for footing shapes

Shape factors	S_c	S_q	S_γ
Strip footing	1	1	1
Rectangular footing B≤L	$1+0.3\frac{B}{L}$	$1+\frac{B}{L}$	$1-0.2\frac{B}{L}$
Circular or square	1.3	1	0.6 or 0.8

For foundation that exhibit local shear failure equation, 2.2 is modified into

$$Q_{ult} = 0.67CN_c\,S_c + \gamma D_f N_q\,S_q + 0.5\gamma B N_\gamma S_\gamma \quad \ldots\ldots\ldots\ldots\ldots\ldots\ldots\ldots\ldots\ldots \text{(2.3)}$$

Where the value of N_c, N_q, N_γ are bearing capacity factors obtained after modifying Φ by $\Phi 1=\tan^{-1}(0.67\tan\Phi)$.

2.5. Dynamic cone penetration (DCP)

DCP is equipment that is applied to determine bearing capacity of foundation soils. Different types of penetrometers are used for site investigation in response to varying needs. Usually during initial exploration stage penetration test are employed to determine stratigraphy, thickness, soil types in terms of consistency, and lateral extent of lithologies. At detailed site investigation stage, penetration test are employed to determine some geotechnical parameters (Mayne et al., 1995)

Some of many version of the DCP used by various peoples are tabulated in table 2.2

Table 2.2: Some version of DCP adapted from (Ampadu, 2005)

Type	Cone diameter (mm)	Mass of hammer kg	Height of fall (mm)	Energy per blow per cone area kN- m/m^2
Sowers and hedges (1966)	38	6.8	508	30
Kleyn (1975)	20	8	575	144
Singh (1973)	35	10	500	51
Ampadu (2005)	20	10	460	144
Awuku (2008)	20	8	578	144
This study	20	8	575	143.7

Dynamic cone penetrometer in operation consists of drop weight, an anvil, rod and cone. It is used in testing of strength of subgrade soils for projects. It is also used during reconnaissance exploration of soils at shallow depth for other civil engineering projects.

2.6. Previous work on DCP test results and strength correlation

The dynamic cone Penetrometer (DCP) is the most versatile rapid, in situ evaluation device currently available. Its correlations to bearing capacity make it an attractive and alternative to more expensive and time consuming procedures for determination of bearing capacities. Many useful correlations had been proposed by various researchers for determination of bearing capacity of soils of their locality in which the DCP penetration index was used to develop these correlations.

The relationship between DCPI-value and other soil parameters also have been established by many researchers on empirical bases:

Relationship between D (mm/blow)-value and unconfined compressive strength (UCS) kN/m^3 has been studied in laboratory for lime stabilized soil and relation below have been established:

$$\text{Log (UCS)} = 3.21 - 0.809 \log D \qquad \text{(McElvaney et al., 1991)}$$

The relationship between n-value and allowable bearing pressure shown below has been derived from ultimate bearing capacity calculated using Terzaghi’s bearing capacity equation for sandy to silt clay soil materials.

$$Q_{all}\ (\text{KN/m}^2) = 164n - 504 \qquad \text{for n-value (blows/100mm)} > 6. \text{ (Ampadu, 2005)}$$

Q_{all} =46.2n+ 222, R^2=0.921 (Dzitse-Awuku, 2008)

Q_{all}=1030-439.1log (D), R^2= 0.953 (Dzitse-Awuku, 2008)

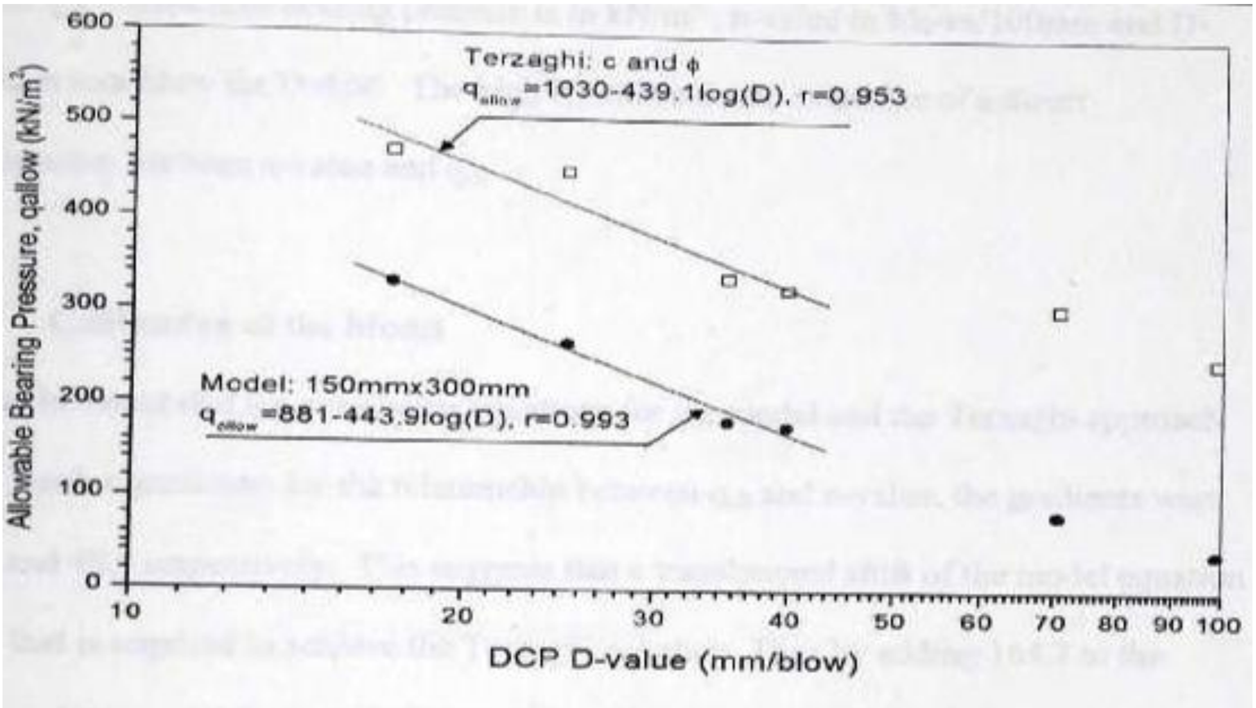

Figure 2.4: correlation between allowable bearing pressure and D-value for model footing and Terzaghi's approach (Dzitse-Awuku, 2008).

The relationship between D-Value and resilient modulus (MR) of subgrade soils depends on grain size of the soil (George et al., 2000)

MR (MN/m^2)=235.3$D^{-0.475}$ for Coarse grained soil

MR (MN/m^2)=532.1$D^{-0.492}$ for fine grained soil

The correlation between D value and CBR that have been investigated by different researcher using various materials is presented in table 2.3.

Table 2.3: Some relationship between D-value and CBR after (Amini, 2003)

No	Correlation	Materials	Investigators
1	LogCBR=2.45-1.12logD	granular and cohesive	Livneh et al. (1992)
2	LogCBR=2.46-1.12logD	various types of soil	Webster et al. (1992)
3	LogCBR=2.62-1.27logD	Unknown	Lleyn (1975)
4	LogCBR=2.44-1.107logD	aggregate base coarse	Ese et al. (1995)
5	LogCBR=2.06-1.107logD	aggregate base coarse and cohesive	NCDOT (Pavement 1998)

In Ethiopia also correlations have been made between DCPI and CBR for locally used sub grade materials, and DCPI with un-drained strength (UCS) of soils of Addis Ababa and established the following relations.

$UCS = 895.8*DCPI^{-0.56}$, R^2=52.4% and N=17, for clayey soils of Addis Ababa (Getachew, 2012)

$UCS = 397.23–4.05*DCPI–46.82*\gamma b+ 39.3*\gamma d+ 3.75*NMC + 83.1*LI + 0.74*PI– 1.06*LL–7.22*d$, R^2=52.0% (Getachew, 2012)

$UCS = -197*\ln (DCPI) +735.5$, R^2=71.1% and N=12, for red clay soils of Addis Ababa

$UCS = -5.84–10.87*DCPI–717*\gamma b+ 968.4*\gamma d +171.6*NMC + 1701.1*LI + 91.47*PI– 63.5*LL-16.62*d$, R^2=86% (Getachew, 2012)

$\log (CBR) = 2.954 – 1.496\log (DCPI)$ with $R^2 = 94.3\%$ (Desalegn, 2012)

As the above previous works suggest, the relationship between different engineering parameters with DCP is highly material dependent. In addition, the behavior of expansive soils varies from place to place depending upon the type of parent material, climate and topography, thus the applicability of the results mentioned above limited to the particular study areas. In the present work, the expansive soil from Asella area is studied to find the correlation between dynamic cone penetration index (DCPI) and Ultimate bearing capacity of shallow foundations.

CHAPTER THREE

3. METHODOLOGY

3.1. General

The research methodology used in this study was divided into two parts:

- The field work for DCP test and representative sample collection.
- The laboratory testing program which was focused on determination of geotechnical index properties, compaction test and tri-axial UU test for determination of shear strength parameters.

Each of the test procedures is described in this section with examples of calculation whereas the detail test data are given in the Appendix B.

3.2. Field work

Field work was carried out in the town at different location where expansive soils are found after visual identification. The work involves field DCP test on test pit and manual excavation to recover sample from test pit for laboratory tests. Fifteen samples were collected from depth of 1.5m to 3.0m.

3.2.1. DCP test

The DCP test device used in this study consists of two 16mm diameter rods. The lower rod contains anvil and replaceable 60^0 apex cone. The upper rod contains 8kg slide hammer with 575mm drop height. The cone diameter (20mm) is made wider than rod diameter (16mm) so that penetration resistance is provided by cone alone and not side friction of the rods.

As the drop weight hits the anvil kinetic energy is imparted into DCP system and the cone is driven into the ground. The depth of penetration in each blow is measured and recorded as D-value. The soil layering profile and strength are interpreted from this D-value.

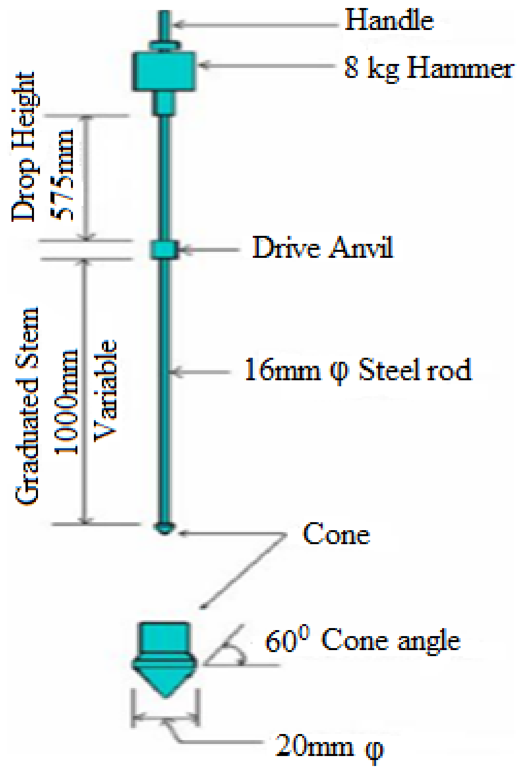

Figure 3.1: Field DCP equipment used for this study (Getachew, 2012)

Test procedures

1. The DCP set up was held vertically position at desired test location.
2. The hammer was lifted and dropped from specified height to initiate the test
3. Following each blows of hammer, the depth of penetration was measured and recorded as D-value(mm/blow)
4. Steps 2 and 3 were repeated until desired depth of testing was reached.
5. After testing was completed the device was extracted safely.

Sample DCP test result and calculation of DCPI is shown in Table 3.1 and Figure 3.2 and details are presented in appendix B.

Table 3.1: Typical illustration of DCP test on pit 4

pit 4: at 1.5m Silingo		
zero error =7cm		
No. blow	**depth of penetration (mm)**	**eff. Depth**
0	0	0
2	134	64
4	190	120
6	240	170
8	290	220
10	346	276
12	416	346
14	484	414
16	550	480
18	609	539
20	672	602
22	731	661
24	796	726
26	876	806
28	967	897
29	995	925
		DCPI =31.66mm/blow

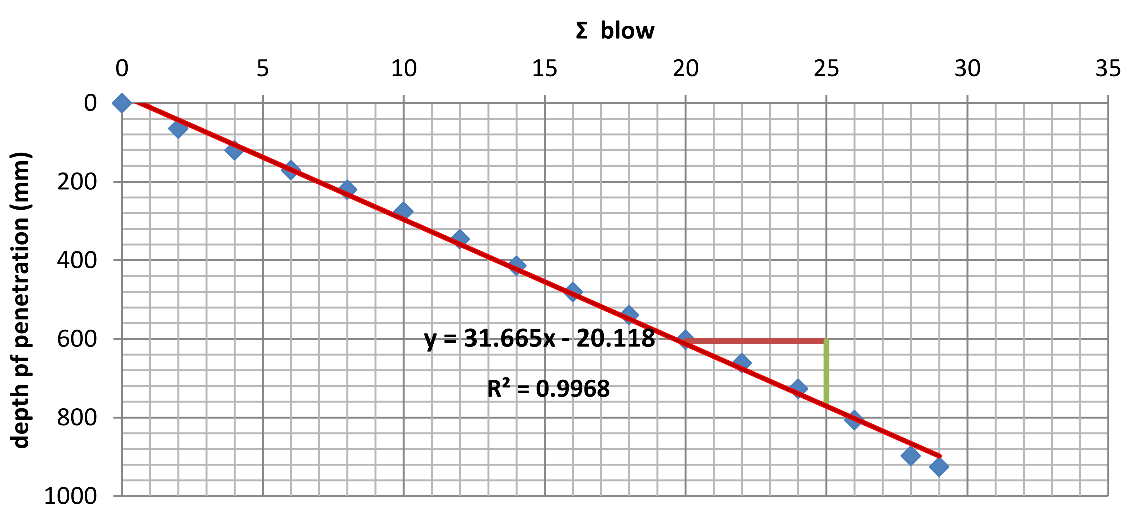

Figure 3.2: Typical illustration of DCP Vs. no. blow for pit 4

3.3. The laboratory tests

3.3.1. Sample preparation and characterization

The bulk sample was air dried to almost constant moisture content. Then laboratory test were performed on representative samples.

3.3.2. Natural moisture content

Water content of a material is the ratio expressed as a percent of the mass of "pore" or "free" water in a given mass of material to the mass of the solid material.

Sample for natural moisture content was taken directly from test pit in air tight plastic bags. ASTM D 2216 - Standard Test Method for Laboratory Determination of Water (Moisture) Content of Soil was used to carry out the test. Typical illustration is tabulated in Table 3.3 and detail is presented in appendix B.

Table 3.3: Typical illustration of natural moisture content for pit 10

pit10: at 2.5m prep school		
specimen number-	**1**	**2**
Mc=mass of empty, clean + lid (g)	96	96
Mcms=mass of can, lid ,and moist soil(g)	185	179
Mcds=mass of can, lid and dry soil (g)	161	158
Ms =mass of soil solids (g) =Mcds-Mc	65	62
Mw= mass of pore water (g) =Mcms-Mcds	24	21
w=water content ,w%=($\frac{Mw}{Ms}$)*100	37	34
Average	35.50	

3.3.3. Grain size analysis test

Grain size analysis provides the grain size distribution of soil mass, and it is required in classifying the soil. The distribution of particle sizes larger than 75 µm (retained on the No. 200 sieve) is determined by sieving, while the distribution of particle sizes smaller than 75 µm is determined by a sedimentation process, using a hydrometer test. ASTM -D422- 63 was followed to carry out the test and percent finer against size of soil particle in millimeter on a semi-log scale is plotted as shown in fig.3.3 and table 3.4 below. The details are presented in appendix B.

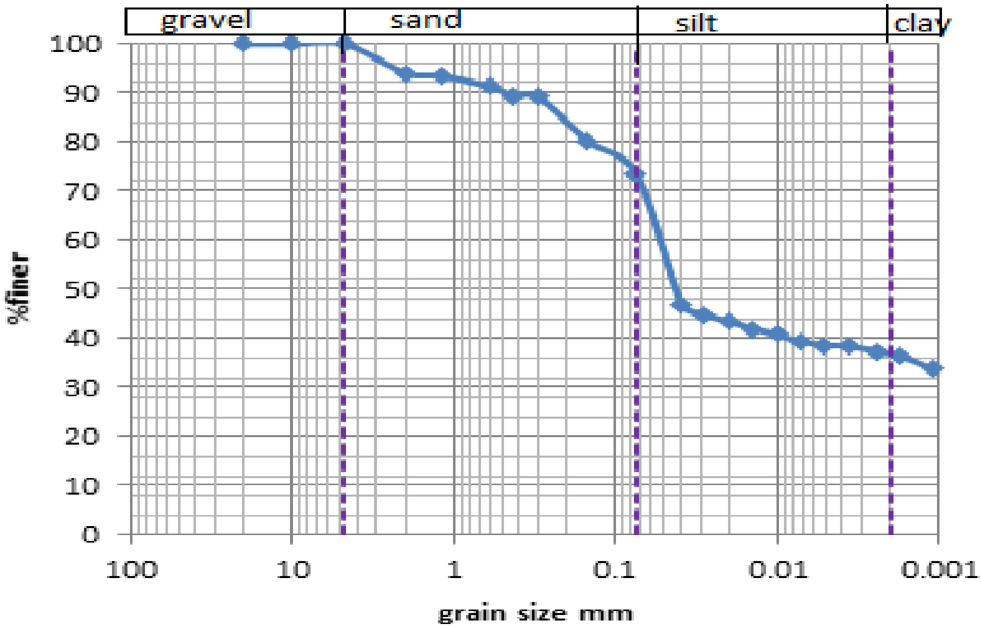

Figure 3.3: Grain size distribution curve for pit 1 (Asella hospital)

Table 3.4: Classification according to grain size for pit 1

%gravel (> 4.75mm)	%sand (4.75 to 0.075mm	%silt (0.075 to 0.002mm)	%clayey (< 0.002mm)
-	26.4	36.5	37.1

3.3.4. Consistency (Atterberg) Limit Tests

Atterberg developed Liquid Limit, Plastic Limit and Shrinkage Limit to describe the consistency (Das, 2002). Casagrande method was used for determination of liquid limit according to ASTM D 4318 - Standard Test Method for Liquid Limit, Plastic Limit, and Plasticity Index of Soil. The plot is drawn as the moisture content as ordinate (natural scale) and number of blows as abscissa (log scale) (Figure 3.4). From the plot, the liquid limit was determined by locating the water content at 25 blows.

Table 3.5: Typical procedures for computation of LL and PL are illustrated below.

testing date						
sample location	**Pit2:Asela stadium at 2.5m depth**					
sample description	**black soil**					
method of testing used	**ASTM D 4318**					
-	**LL**				**PL**	
sample no.	**1**	**2**	**3**	**4**	**1**	**2**
MC=mass of empty, clean can +lid(grams)	61	61	61	61	61	61
MCMS=mass of Can, lid and moist soil (grams)	81	78	78	81	70	71
MCDS=mass of can, lid and dry soils(grams)	72	71	72	75	68	69
MS=mass of soil solids(g)= MCDS-MC	11	10	11	14	7	8
MW= mass of pore water (g)=MCMS-MCDS	9	7	6	6	2	2
W=water content, w%=(MW/MS)*100	81.82	70	54.55	42.86	28.57	25
No. of drops (N)	19	24	29	34	26.79	
LL=64 at blow =25, PI=LL-PL=64-26.79=37.21						

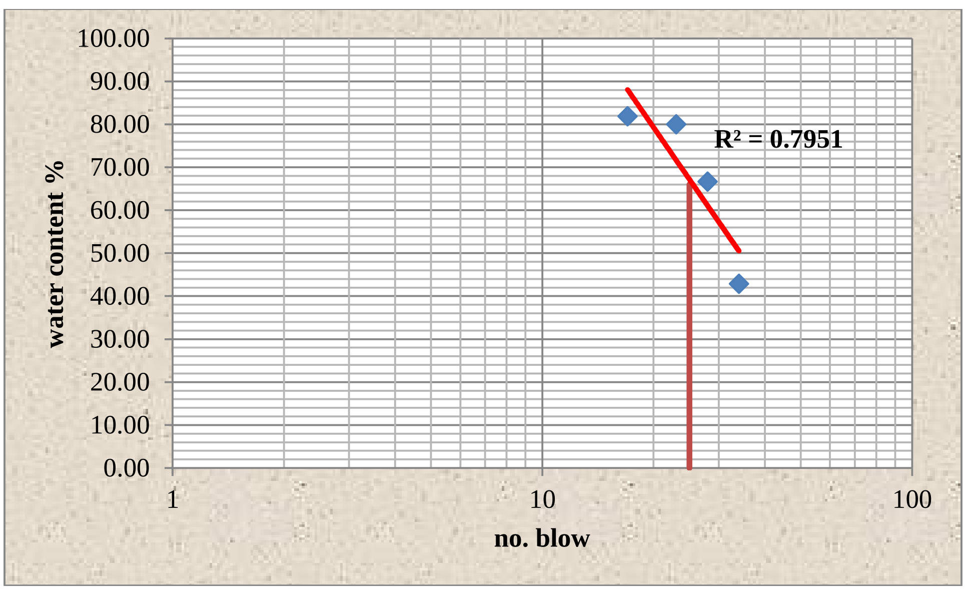

Figure 3.4: Flow chart LL determination (test pit 1)

3.3.5. Specific Gravity Test

Specific gravity of soil is the ratio of the unit weight of solids in the soil to the unit weight of water. It is determined using ASTM D854-83 and shown as table 3.6 below. Details are presented in appendix part.

Table 3.6: Typical illustration of Gs for pit 2.

sample location	**Asella stadium at 2.5m depth**	
sample description	**black soil**	
specimen number	**1**	**2**
Wp=mass of empty, clean pycnometer (g)	52	52
WPS=mass of empty pycnometer+dry soil (g)	62	61.5
WB=mass of pycnometer+dry soil+ water (g)	164.5	164
WA=mass of pycnometer +water (g)	158	158
Wo=wps-wp	10	9.5
Temperature T^0C	23	23
Conversion factor	0.9993	0.9993
specific gravity (Gs)= $\frac{w_o}{(w_o+(w_a-w_b))}$ at 20^0c	2.86	2.71
Average	**2.79**	

3.3.6. Free Swell Test

This test has not been standardized by ASTM. The method was suggested, in 1956, by Holtz and Gibbs to measure the expansive potential of cohesive soils, and it gives fair approximation of the degree of expansiveness of the soil sample. Soils having a free swell of 100% or more damage lightly loaded structures while those having free swell of less than 50% don't pose serious problems to structures. A $10cm^3$(V_i) dry soil passing thorough a No.40 (425micron) sieve is poured into a $100cm^3$ graduated cylinders filled with water. The volume of settled soil is measured after 24 hours which gives the value of V_f; the ratio of the increase in volume to its initial, $\frac{V_f-V_i}{V_i}$*100 expressed in %, is taken as the free swell and the results are indicated inTable3.7 while details are presented in appendix.

Table 3.7: Typical illustration of FS test for pit 3 at Maikel, kebele 9

sample location	**Maikel at 2.0m depth**	
sample description	**Black-gray soil**	
sample number	**1**	**2**
initial volume =V_i (cm^3)	10	10
final volume =V_f(cm^3)	15	17.5
%free swell(FS)=($\frac{V_f - V_i}{V_i}$*100)	50	75
average FS	**62.5**	

3.3.7. Compaction test

Laboratory compaction tests provide the basis for determining the percent compaction and water content needed to achieve the required engineering properties, and for controlling construction to assure the required compaction and water contents. The standard proctor compaction tests were done on the investigated soil according to ASTM D698-98 method A. The procedure for computation is illustrated in table 3.8 and the details are presented in appendix part.

Table 3.8: Typical illustration of MDD and OMC of pit 2.

sample location	**Asella stadium ,at 2.5m depth**					
sample description	**black soil**					
method of test used	**ASTM D 698**					
compacted soil- sample no	1	2	3	4	5	6
MC = Mass of empty, clean can + lid (grams)	60	60	8	8	7	7
MCMS = Mass of can, lid, and moist soil (grams)	134	112	56	70	83	67
MCDS = Mass of can, lid, and dry soil (grams)	121	101	44	53	59	45
MS = Mass of soil solids (grams)	61	41	36	45	52	38
MW = Mass of pore water (grams)	13	11	12	17	24	22
W = Water content, w%	13.31	18.83	25.33	29.78	38.15	49.9
density determination	**volume of mold=944cm^3**					
Compacted Soil - Sample no.	1	2	3	4	5	6
w = Assumed water content, w%	8	12	16	20	24	28
Actual average water content, w%	13.31	18.83	25.33	29.78	38.15	49.9
Mass of compacted soil and mold	5658	5739	5861	5948	6007	5981
Mass of mold (grams)	4405	4405	4405	4405	4405	4405
Wet mass of soil in mold (grams)	1253	1334	1456	1543	1602	1576
Wet density, ρ , (g/cm^3)	1.33	1.42	1.54	1.64	1.70	1.67
Dry density, ρd , (g/cm^3)	1.17	1.19	1.23	1.26	1.23	1.12
dry unit weight ɤd (KN/m^3)	11.71	11.90	12.32	12.61	12.30	11.15

For drawing saturation line (zero air void line (S=100%)	**Wsat= (ɤw/ɤd-1/Gs)100**				**Gs=2.79**	
ɤd	11.71	11.90	12.32	12.61	12.30	11.15
Water content (%)	49.53	48.16	45.33	43.47	45.48	53.85
		MDD=12.6		**OMC=30**		

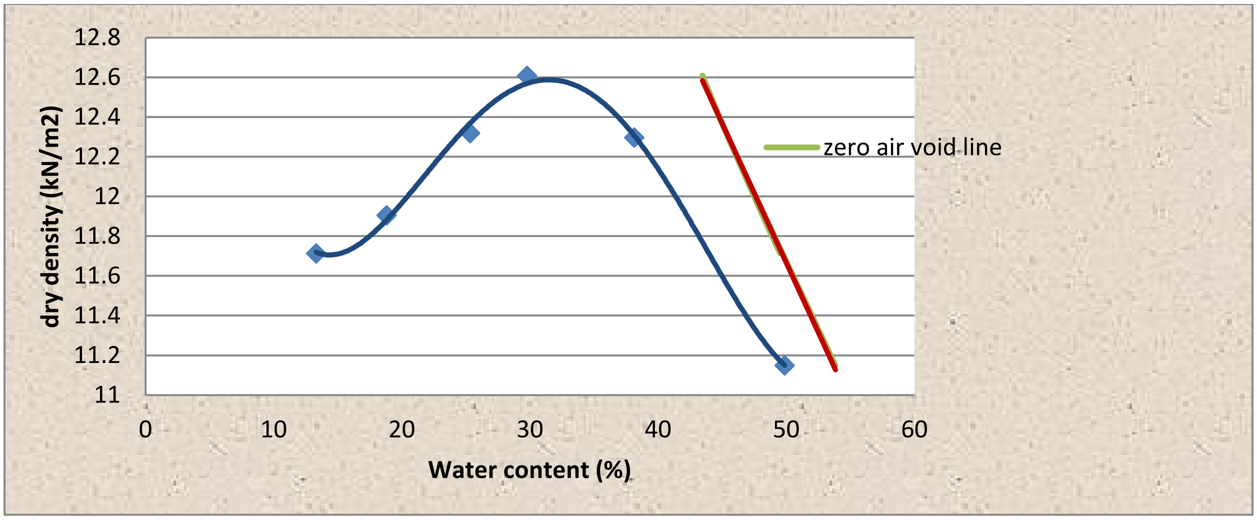

Figure 3.5: Compaction curve for pit2

3.3.8. Tri-axial Shear Strength test

The drainage conditions of the sample is generally the deciding factor in choosing a particular type of the test in the laboratory since the test specimen should conform as closely as possible to the conditions under which the soil will be stressed in the field. Since consolidation of expansive soils take long period of time, UU tri-axial test have been selected and ASTM D 2850- 95 is used for determination of strength parameters and stress-strain relationships for the soils of the study area.

In tri-axial compression tests used in this study a cylindrical soil sample of Standard size (dia. =38mm and height=76mm) is encased by a thin rubber membrane and placed inside a chamber. For conducting the test, the chamber is filled with water and the sample is subjected to a confining pressure by application of pressure to the water in the chamber. Axial (or deviator) stress is applied through a vertical loading ram. No drainage is permitted during the test and specimen is sheared in compression without drainage at constant rate of axial deformation (strain controlled) of 1mm/min. The tri-axial machine used for this study is shown in fig 3.6 below. From stress-strain graphs of tri-axial test deviator stress at failure and confining pressure were used to plot Mohr circles. From Mohr circles, the un-drained cohesion intercept, C_u and angle of internal friction Φ_u were deduced and used to calculate bearing pressure. Sample calculation of this test are given in table 3.9 below and details are presented in appendix B.

Figure 3.6: Tri-axial machine used for this study

Table 3.9: Typical illustration of strength parameter determination for pit12

sample A at Cell pressure ,σ_3 = 150kpa, strain rate :Δε/Δt= 1mm/min					**sample B, Cell pressure ,σ_3 = 300kpa, strain rate := 1mm/min**				
axial deformation (ΔL) mm	**Axial load P (N)**	**axial strain (εa)=ΔL/L0**	**corrected area (A)=A0/(1-εa)(mm^2)**	**Deviator stress (σd)=P/A(kPa)**	**axial deformation (ΔL) mm**	**Axial load P (N)**	**axial strain (εa)=ΔL/L0**	**corrected area (A)=A0/(1-εa)**	**Deviator stress (σd)=P/A(kPa)**
0	0	0	1133.54	0	0	0	0	1133.54	0
0.051	2	0.0671	1134.30	1.76	0.051	14	0.0671	1134.30	12.34
1.023	15	1.3461	1149.01	13.05	1.023	56	1.3461	1149.01	48.74
1.543	21	2.0303	1157.03	18.15	1.543	102	2.0303	1157.03	88.16
1.957	28	2.5750	1163.50	24.07	1.957	178	2.5750	1163.50	152.99
2.201	46	2.8961	1167.35	39.41	2.201	254	2.8961	1167.35	217.59
2.354	56	3.0974	1169.77	47.87	2.354	321	3.0974	1169.77	274.41
2.569	95	3.3803	1173.20	80.98	2.569	369	3.3803	1173.20	314.53
2.802	164	3.6868	1176.93	139.35	2.802	402	3.6868	1176.93	341.57
2.909	213	3.8276	1178.65	180.71	2.909	431	3.8276	1178.65	365.67
3.216	267	4.2316	1183.63	225.58	3.216	465	4.2316	1183.63	392.86
3.534	289	4.6500	1188.82	243.10	3.534	498	4.6500	1188.82	418.90
3.798	321	4.9974	1193.17	269.03	3.798	512	4.9974	1193.17	429.11
4.002	345	5.2658	1196.55	288.33	**4.002**	**523**	**5.2658**	**1196.55**	**437.09**
4.235	363	5.5724	1200.43	302.39	4.235	521	5.5724	1200.43	434.01
4.403	**371**	**5.7934**	**1203.25**	**308.33**	4.403	512	5.7934	1203.25	425.51
4.602	368	6.0553	1206.60	304.99	4.602	508	6.0553	1206.60	421.02
4.821	356	6.3434	1210.32	294.14	4.821	498	6.3434	1210.32	411.46
4.941	321	6.5013	1212.36	264.77	4.941	476	6.5013	1212.36	392.62
5.216	298	6.8632	1217.07	244.85	5.216	456	6.8632	1217.07	374.67
5.412	278	7.1211	1220.45	227.79	5.412	432	7.1211	1220.45	353.97
5.712	265	7.5158	1225.66	216.21	5.712	421	7.5158	1225.66	343.49
5.865	256	7.7171	1228.33	208.41	5.865	412	7.7171	1228.33	335.41

Cell pressure,σ_3 kPa	σ_d (σ_1-σ_3)kPa	σ_1 kPa
150	308.3	458.3
300	437.1	737.1

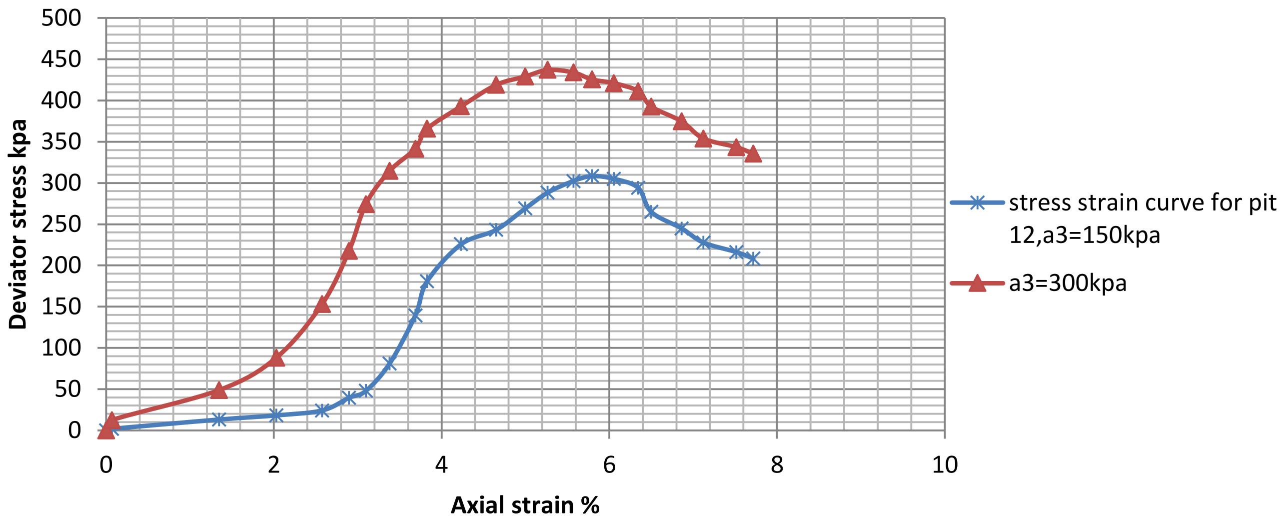

Figure 3.7: Stress-strain curve for pit 12 at 150kPa and 300kPa confining stress

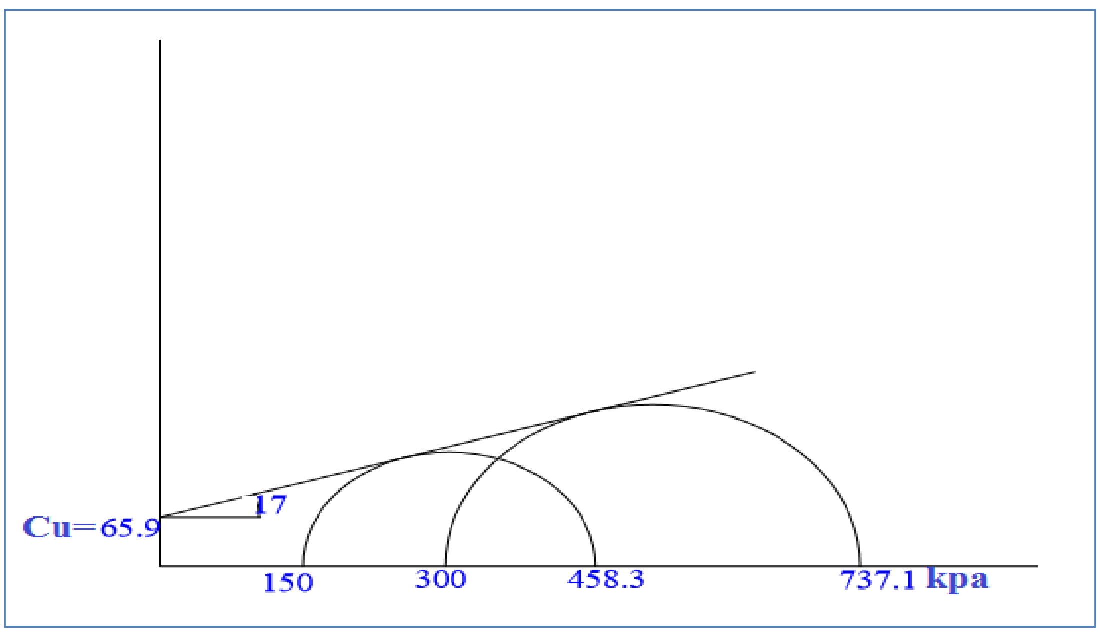

Figure 3.8: Mohr circle for pit 12

CHAPTER FOUR

4. RESULT ANALYSIS AND DISCUSSION

4.1. Discussion of soil properties

The primary purpose of this sub-section is to review all the tests results obtained in this research and compare them with previous similar results.

The formation from which the samples were obtained for this investigation was seen to be dark gray to black clayey soils. The specific gravity of most of the soil was found to be in range of 2.67 to 2.83 which is typical black cotton expansive soils, that is, between 2.7 and 2.9 (Murthy, 2007). From gradation curve materials finer than 0.075 mm and finer than 0.002 mm were respectively found to be in between 73% - 91% and 35-53%, thereby, confirming the fine grained nature of the soil. Figure 4.1 below shows the summary of gradation curve of the soils under study area.

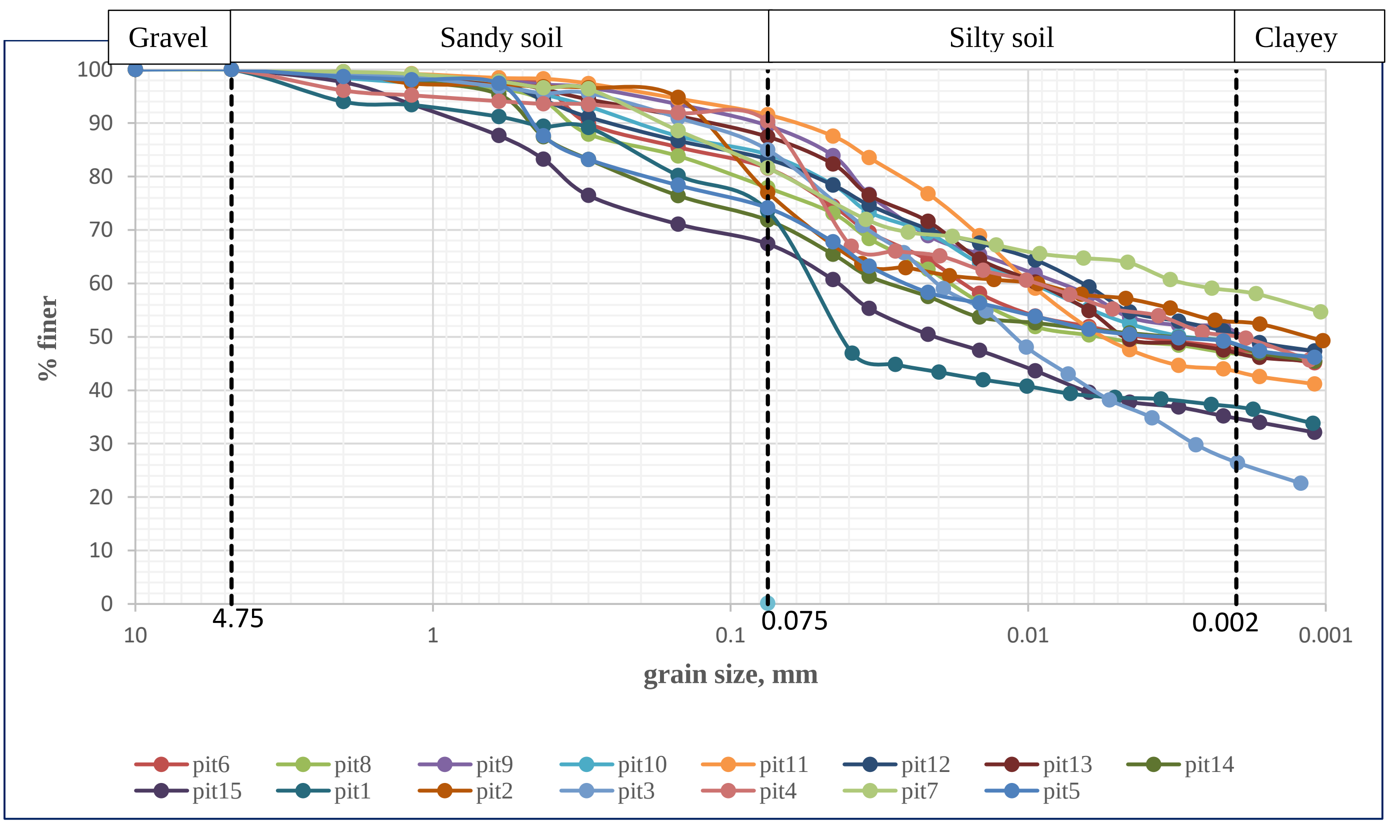

Figure 4.1: Gradation curve for soil of study area

The liquid limit (LL) ranges between 56% and70% and plastic limit (PL) ranges between 23% and 40% indicating the soils under investigation possess significant water adsorption and retention capacity. The free swell value varied between 62% and 135% which typical characteristics of expansive soils and can cause significant damage on light weight structures. Table 4.1 below shows summary of liquid limit, plastic limit and other test results.

From compaction test results the maximum dry density was found to be 1.21-1.32 g/cm^3 at the optimum water content of 24-29% which is close to plastic limit. This closely matches with the model (OMC = 0.92 PL) used by (Chowdhury, 2013) for cohesive soils. The increase in γ_d with an increase in water content on dry side of optimum is due to expulsion of air from the pore space and re-arrangement of particles that decreases the pore space. Conversely, an increase in water content on wet side of optimum results in an increased volume of water (γ_w = 1 g/cm^3) which replaces the soil particles and decrease dry density.

According to unified soil classification plasticity chart, most of the soils of the study area lies above A-line which means the soils are clay with high plasticity (CH) and conforms to gradation test results. Classification of soils of study area according to USCS is shown in figure 4.2.

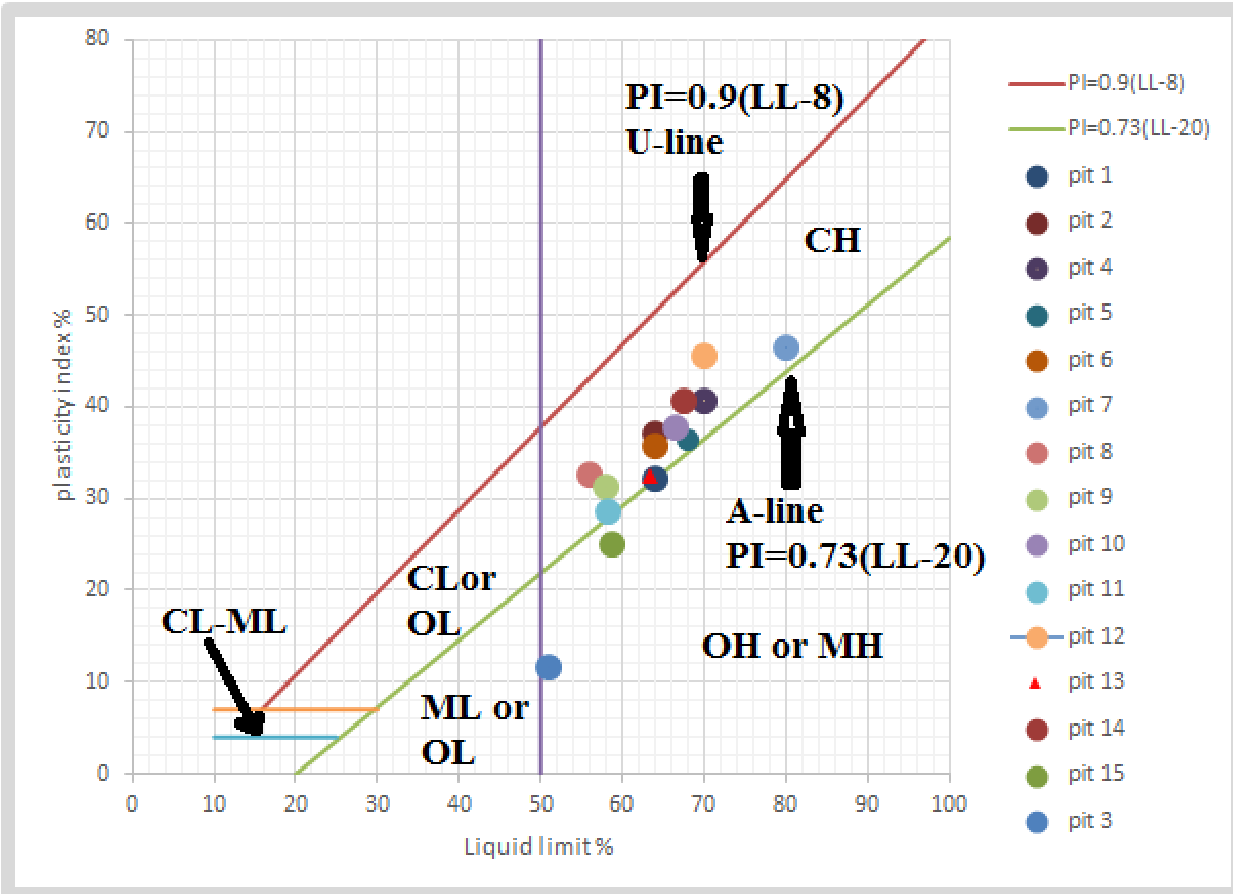

Figure 4.2: Plasticity chart of the soils of study area according to USCS

According to AASTHO classification system the soil of the study area falls in the region of A-2-7, A-7-5 and A-7-6. Since more than 35% of soil mass passes through no.200 sieve soils under study is not classified as A-2-7 which contains granular materials. So, these soils categorized under A-7-5 and A-7-6 which belongs to clayey soils. This means the soil under interest is plastic clay which has a high volume change capacity when moisture varies. A-7 materials are generally considered the least suitable as a highway material or subgrade. AASHTO classification system of soils of study area is shown in figure 4.3.

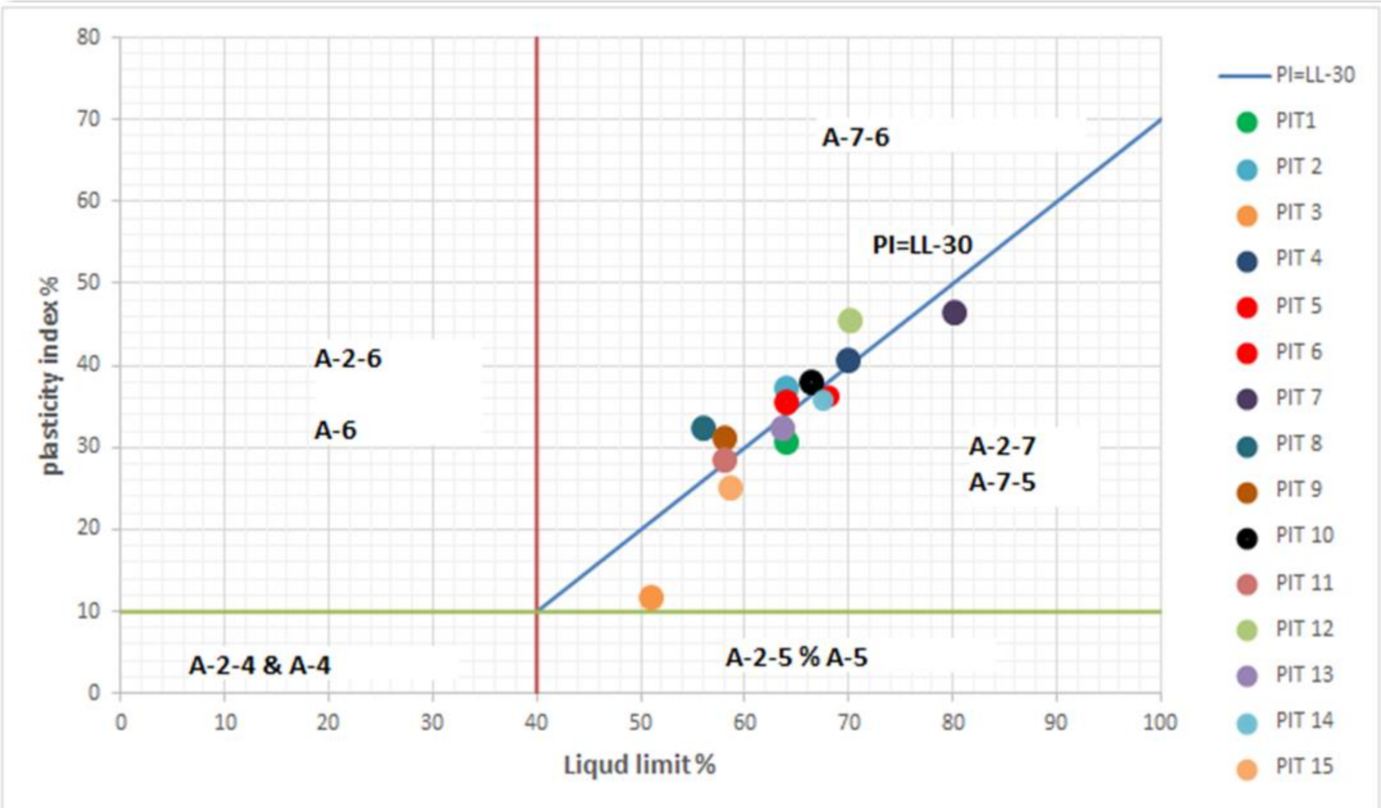

Figure 4.3: Plasticity chart of the soils of study area according to AASHTO classification system.

Table 4.1: Summary of all test results.

site designation	depth (m)	NMC %	specific gravity Gs	clay fraction%	liquid limit%	plastic limit%	plasticity index	liquidity index(Li) = (Wn-Wp)/pI	consistency index (ci) = (wl-wn)PI = 1-Li	free swell %	bulk density (kN/m^3)	DCPI (mm/blow	consistency of soil from ci	USCS classification	AASHTO classification
pit1:Asella hospital	1.5	48.8	2.83	37.1	65.5	33.33	32.17	0.48	0.52	130	17.95	43.6	Stiff	CH	A-7-5
pit2:stadium	2.5	46.95	2.79	52.5	64	26.79	37.21	0.54	0.46	105	17.65	65	Stiff	CH	A-7-6
pit 3: kebele 9 Maikel	2	42.45	2.69	28.2	61	39.39	11.61	0.26	0.74	62.5	17.9	20.67	Stiff	MH	A-7-5
pit4: kebele10 Silingo	1.5	44.61	2.67	50	70	29.29	40.71	0.38	0.62	107.5	17.6	31.66	Stiff	CH	A-7-6
pit5:Arsi university	2.5	43.25	2.71	48.5	68	31.67	36.33	0.32	0.68	82.5	17.9	29.52	Stiff	CH	A-7-5
pit6:kebele 2	2	41.56	2.69	47.8	64	28.34	35.66	0.37	0.63	102.5	17.6	35.87	Stiff	CH	A-7-6
pit7:Boseta meda	1.5	35.27	2.71	58.5	80	33.33	46.67	0.04	0.96	132.5	17.4	41.97	Stiff	CH	A-7-5
pit8:keb.1; Chilalo college	1.5	32.94	2.77	47.4	56	23.44	32.56	0.29	0.71	112.5	17.65	37.88	Stiff	CH	A-7-6
pit9:keble 4,mosque	2	37.3	2.75	49.7	58	26.79	31.21	0.34	0.66	125	17.65	36.62	Stiff	CH	A-7-6
pit10:Behind,prep.school	2.5	35.4	2.82	48.3	66	28.64	37.86	0.18	0.82	135	17.9	38.2	Stiff	CH	A-7-6
pit11:welkesa river area	2	30.53	2.69	43.4	60	31.37	28.63	-0.03	1.03	117.5	17.85	31.72	v. stiff	CH	A-7-6
pit12:keb.10,TTC	1.5	40.12	2.75	49.5	70	24.41	45.59	0.34	0.66	115	17.85	32.25	Stiff	CH	A-7-6
pit13:keb.9,mosque area	1.5	33.8	2.69	46.7	63.5	30.95	32.55	0.09	0.91	122.5	17.9	32.98	Stiff	CH	A-7-5
pit14: keb.10 condominium	1.5	39.3	2.74	47.4	67.5	31.67	35.83	0.21	0.79	97.5	17.6	33.7	Stiff	CH	A-7-5
pit15;keb.4, behind OPDO bldg.	2	37.45	2.69	34.3	58.5	33.33	25.17	0.16	0.84	85	17.7	38.54	Stiff	MH	A-7-5

4.2. Prediction of ultimate bearing capacity from DCPI

From stress-strain curve of tri-axial test the deviator stress at failure and confining pressure were used to plot Mohr circle. From Mohr circle un-drained cohesion C_u (intercept) and internal angle of friction ϕ_u (slope) were deduced (Figure 3.7) and the result summarized in Table 4.2. The results were then used to calculate ultimate bearing pressure using Terzaghi's bearing capacity equation.

Table 4.2: Summary of tri-axial test results of study area.

test pit no.	sample no.	moisture content%	dry density g/cm^3	σ3 kPa	(σ1-σ3) kPa	C_u (kPa)	ϕ_u
1	A	39.64	1.29	150	226.78	98.75	3
	B	40.45	1.28	300	232.86		
2	A	45.28	1.22	150	216.23	94.15	3
	B	44.76	1.21	300	227.2		
3	A	36.28	1.31	150	495.6	181.93	10
	B	38.74	1.31	150	555.54		
4	A	40	1.28	150	441.2	197.77	4
	B	43.27	1.21	300	454.37		
5	A	40.9	1.28	150	338.34	58.53	21
	B	43	1.24	300	505.72		
6	A	42.7	1.28	150	329.3	152.45	4
	B	43.27	1.21	300	340.9		
7	A	39.8	1.25	150	205.33	57.42	11
	B	41.9	1.22	300	274.63		
8	A	37.42	1.29	150	264.5	86.33	10
	B	38.53	1.27	300	323.93		
9	A	39.28	1.27	150	271.64	72.43	13
	B	40.4	1.23	300	355.59		
10	A	40.37	1.265	150	275.23	120.41	3
	B	41.28	1.265	300	325.33		
11	A	39.1	1.277	150	363.47	101.6	15
	B	40	1.277	300	466.36		
12	A	37.5	1.29	150	308.33	65.9	17
	B	39.2	1.27	300	437.1		
13	A	39.3	1.3	150	259.3	56.5	19
	B	37.84	1.29	300	420.74		
14	A	40	1.278	150	328.74	110	10
	B	37.98	1.254	300	394.1		
15	A	39	1.27	150	262.3	45	19
	B	41	1.24	300	408.4		

From consistency index, physical state of the soils of study areas is stiff. For stiff cohesive soils and soils that show peak value stress-strain curve at strain about 5%, types of bearing capacity failures are mostly general shear failure. For such kind of failure, Terzaghi's bearing capacity equation is given by:

$$Q_{ult}=CNc\ (1+0.3\frac{B}{L}) +\boldsymbol{\gamma}D_f\ N_q\ (1+\frac{B}{L}) +1/2\boldsymbol{\gamma}BN\gamma\ (1\text{-}0.2\frac{B}{L})$$

Where the values of N_C, N_q and $N_{\boldsymbol{\gamma}}$ are obtained by reading bearing capacity factor from Terzaghi's bearing capacity chart for given Φ values.

Sample rectangular footing of dimension B=1.5m and L=4m and depth of foundation is at proposed pit depth was used for ultimate bearing capacity determination. The results at different test pits are summarized in Table 4.3.

Table 4.3: Computation of ultimate bearing capacity of study area

Test pit no.	**depth (m)**	**Cu (kPa)**	**Φ(^{0})**	**Nc**	**Nq**	**Nγ**	**γbulk (kN/m^3)**	**Q_{ult} (kN/m^2), B=1.5m,L=4m**
1	1.5	98.75	3	6.8	1.4	0.3	17.95	802.61
2	2.5	94.15	3	6.8	1.4	0.3	17.65	800.86
3	2	181.93	10	9.6	2.7	1.2	17.9	2090.82
4	1.5	197.77	4	7	1.5	0.4	17.6	1599.47
5	2.5	58.53	21	19	8.4	6	17.9	1931.92
6	2	152.45	4	7	1.5	0.4	17.6	1264.69
7	1.5	57.42	11	10.6	3.2	1.3	17.4	807.66
8	1.5	86.33	10	9.6	2.7	1.2	17.65	1034.99
9	2	72.43	13	12	3.6	1.8	17.65	1163.72
10	2.5	120.41	3	6.8	1.4	0.3	17.9	1000.77
11	2	101.6	15	12.9	4.4	2.5	17.85	1705.03
12	1.5	65.9	17	14.6	5.8	3.7	17.85	1404.45
13	1.5	56.5	19	16.7	6.6	4.4	17.9	1348.00
14	1.5	110	10	9.6	2.7	1.2	17.6	1287.46
15	2	45	19	16.7	6.6	4.4	17.7	1211.33

4.3. Regression analysis for prediction of Q_{ult}.

In order to establish relevant correlations, ultimate bearing pressure have been plotted against DCPI –values and the regression analysis have been done. Regression analysis is concerned with how the values of Y depend on the corresponding values of X. Y, whose value is to be predicted, is known as dependent variable or response and X, which is used in predicting the value of dependent variable, is called independent variable. A regression model that contains more than one independent variable is called multiple regression models. Alternatively, regression model containing one independent variable is termed as single regression model. During regression analysis, a regression model with higher value of coefficient of determination (R^2), is usually accepted.

To carry out statistical analysis, Microsoft® excel was used for single regression with both linear and non-linear functions. Different models are used and those models with a higher value of coefficient of determination are accepted. The parameters considered as component of analysis include ultimate bearing capacity, dynamic cone penetration index, bulk unit weight, dry unit weight, natural water content, liquidity index, plasticity index, liquid limit and foundation depth. But to see the effect of width of foundation on bearing capacity, ultimate bearing capacity of foundation is determined at different width of sample footing and the variation in correlation equation due to different width of footing have been determined. Table 4.4 presents summary of parameters used for these analysis.

Table 4.4: Summary of parameters used for these analysis

site designation	**depth (m)**	**NMC %**	**liquid limit%**	**plasticity index**	**Consistency index (ci) = (wl-wn)PI =1-Li**	**bulk density(kN/m^3)**	**Dry density (kN/m^3)**	**DCPI (mm/blow)**	**Qult kN/m^2 B=1.5m**
pit1:asela hospital	1.5	48.8	64	30.67	0.5	17.95	12.85	43.6	802.61
pit2:asela stadium	2.5	46.95	64	37.21	0.46	17.65	12.15	65	800.86
pit 3:aselakebele 9 Maikel	2	42.45	61	11.61	0.74	17.9	13.1	20.67	2090.82
pit4:aselakebele10 Silingo	1.5	44.61	70	40.71	0.62	17.6	12.45	31.66	1599.47
pit5:aArsi university	2.5	43.25	68	36.33	0.68	17.9	12.6	29.52	1931.92
pit6:kebele 2	2	41.56	64	35.66	0.63	17.6	12.45	35.87	1264.69
pit7:boseta meda	1.5	35.27	80	46.67	0.96	17.4	12.35	41.97	807.66
pit8:kebele1;chilalo college	1.5	32.94	56	32.56	0.71	17.65	12.8	37.88	1034.99
pit9:keble 4,mosque	2	37.3	58	31.21	0.66	17.65	12.5	36.62	1163.72
pit10:kebele 10,prep.school	2.5	35.4	66	37.86	0.82	17.9	12.65	38.2	1000.77
pit11:welkesa river area	2	30.53	60	28.63	1.03	17.85	12.77	31.72	1705.03
pit12:kebl 10,TTC	1.5	40.12	70	45.59	0.66	17.85	12.8	32.25	1404.45
pit13:keb.9,mosque area	1.5	33.8	63.5	32.55	0.91	17.9	12.95	32.98	1348
pit14:keb.10 condominium	1.5	39.3	67.5	35.83	0.79	17.6	12.66	33.7	1287.46
pit15:keb4, behind OPDO bldg.	2	37.45	58.5	25.17	0.84	17.7	12.3	38.54	1211.33

4.3.1. Single regression

In developing correlation, first the relation of Q_{ult} with DCPI, γdry, γbulk, NMC, LI, PI, LL and depth of foundation have been checked using single regression with Microsoft excel 2013 and shown in figure 4.4 to 4.11.

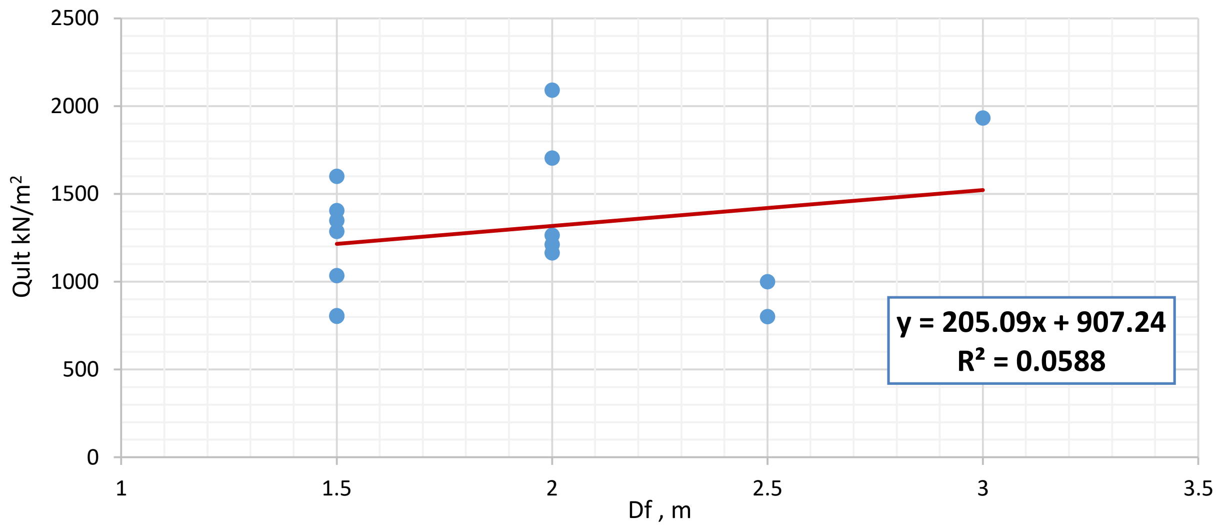

Figure 4.4: Plot of Q_{ult} vs. Depth of footing

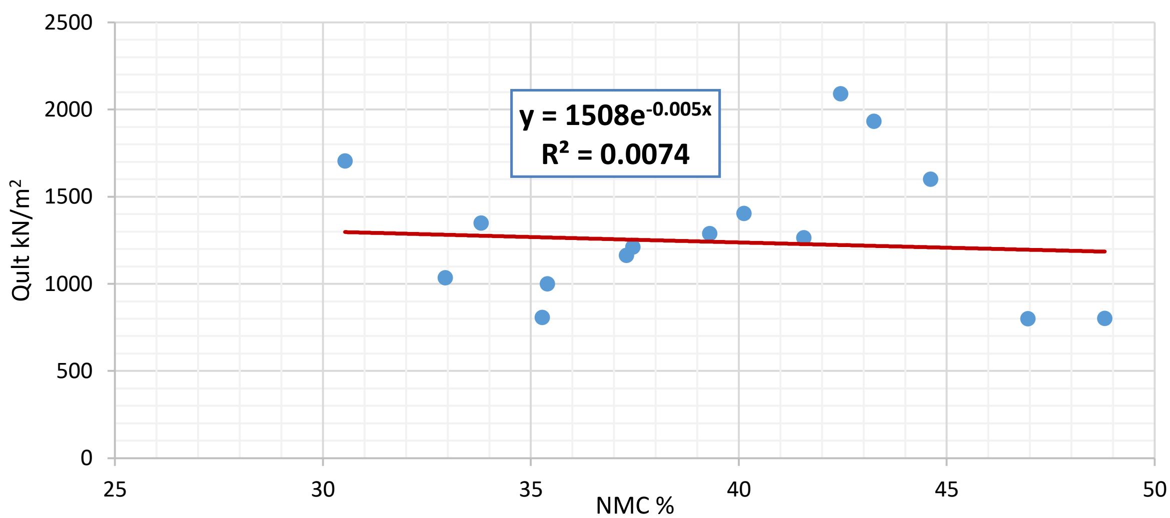

Figure 4.5: Plot of Q_{ult} vs. Natural moisture content

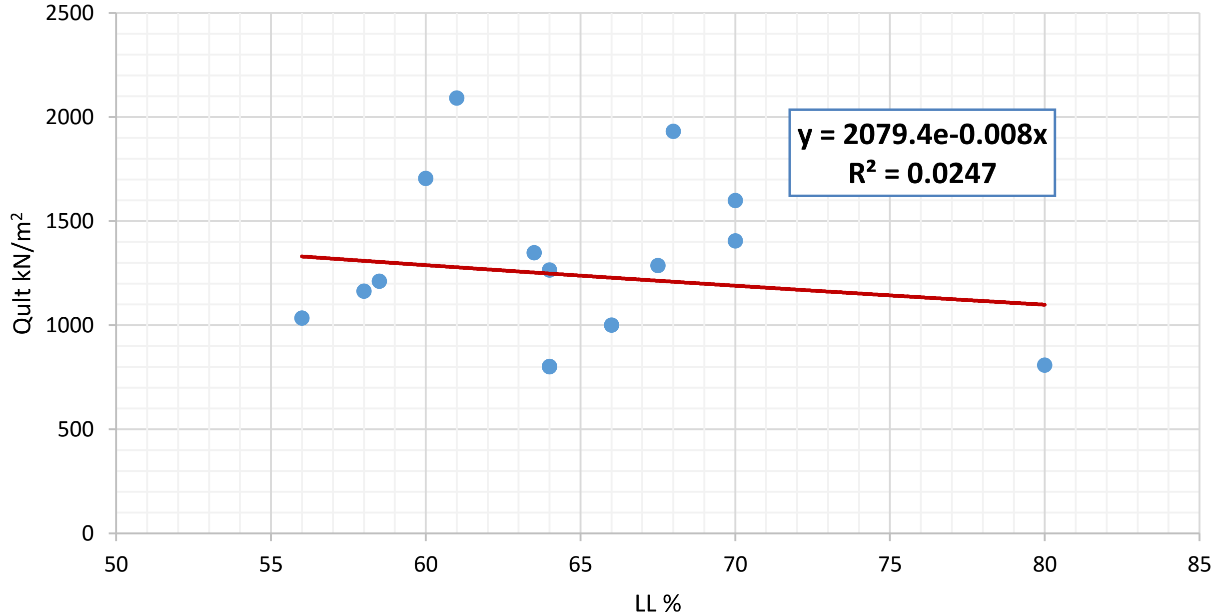

Figure 4.6: Plot of Q_{ult} vs. liquid limit

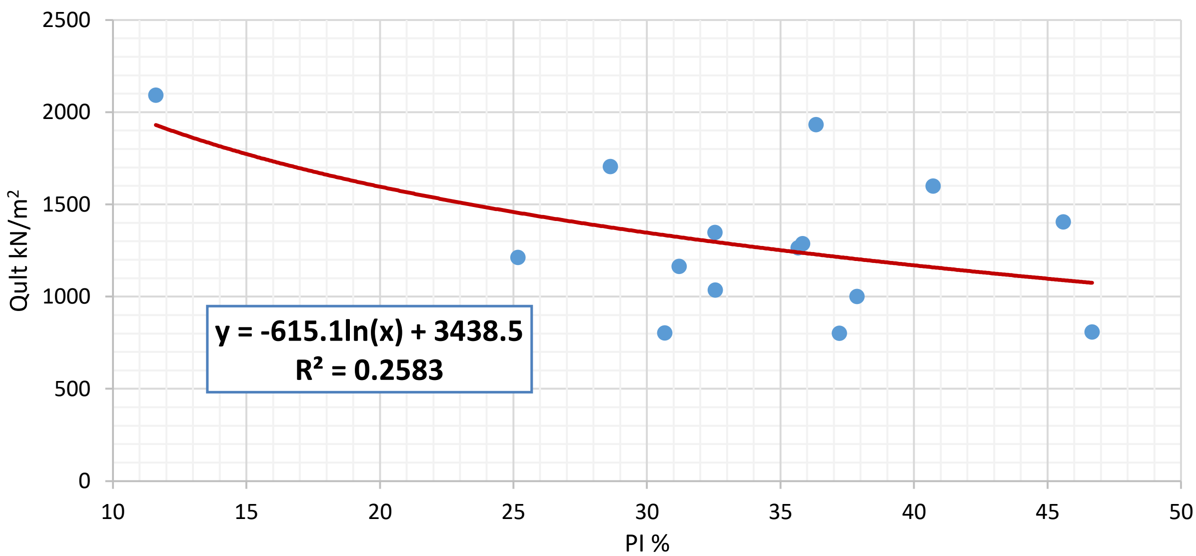

Figure 4.7: Plot of Q_{ult} vs. plasticity index

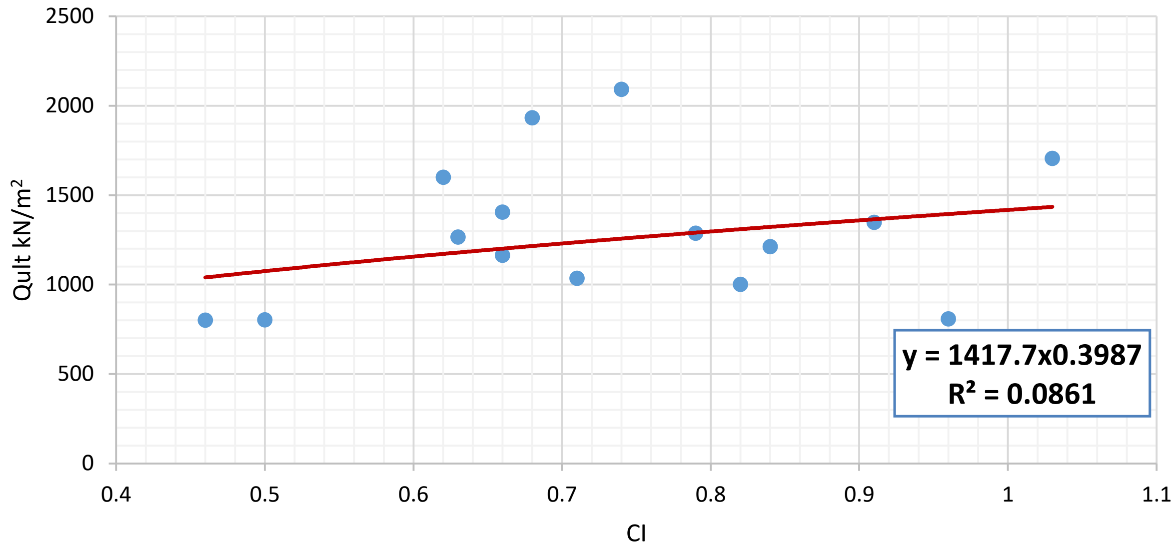

Figure 4.8: Plot of Q_{ult} vs. consistency index

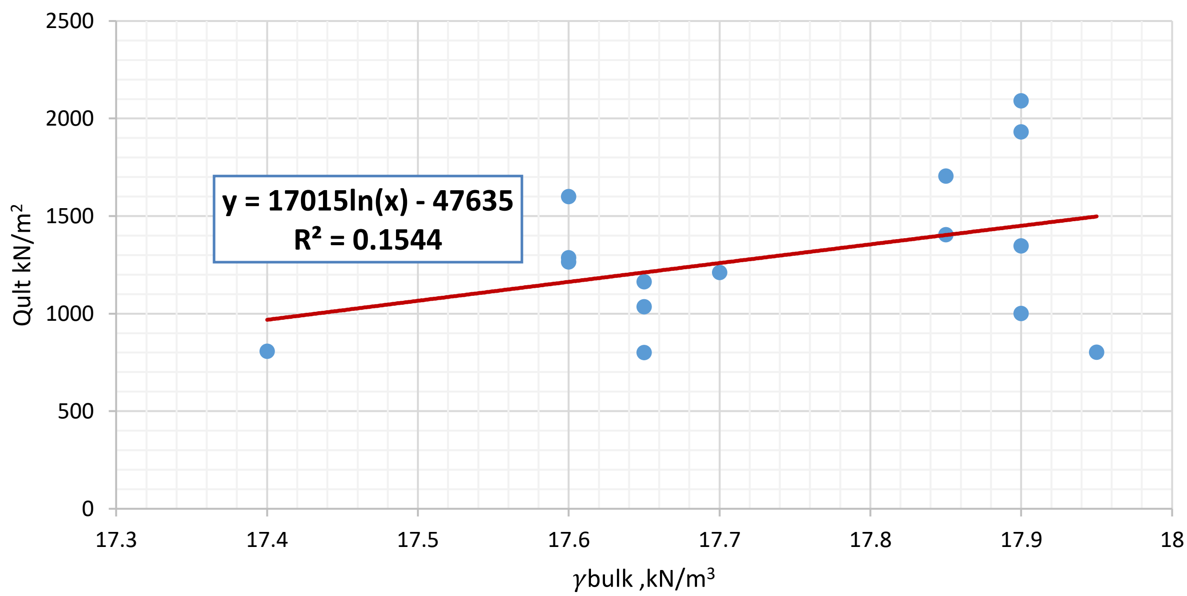

Figure 4.9: Plot of Q_{ult} vs. γbulk

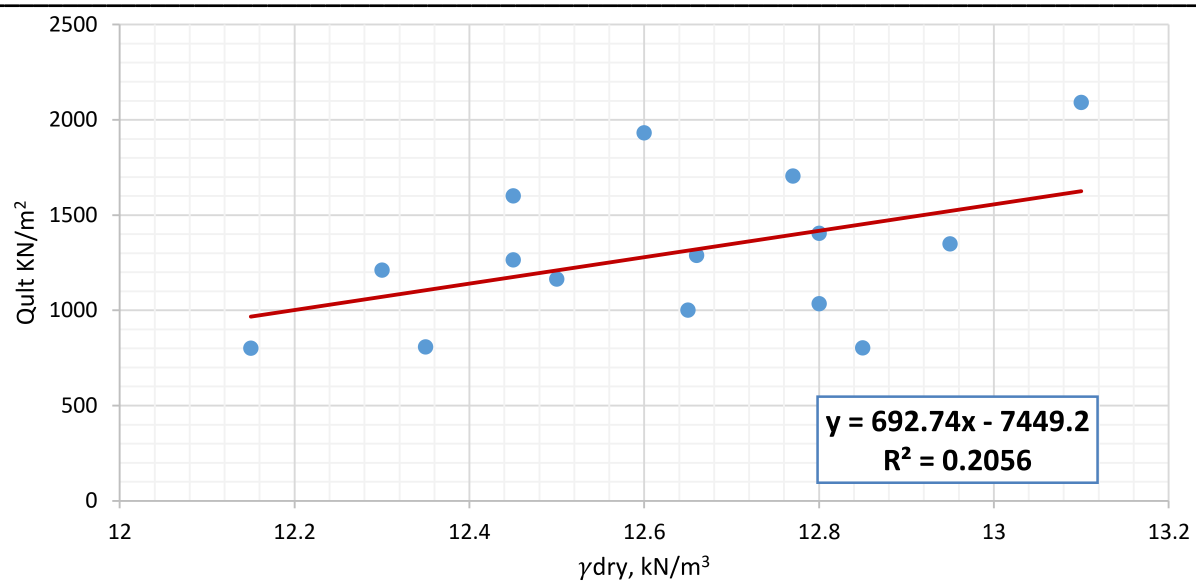

Figure 4.10: Plot of Q_{ult} vs. γdry

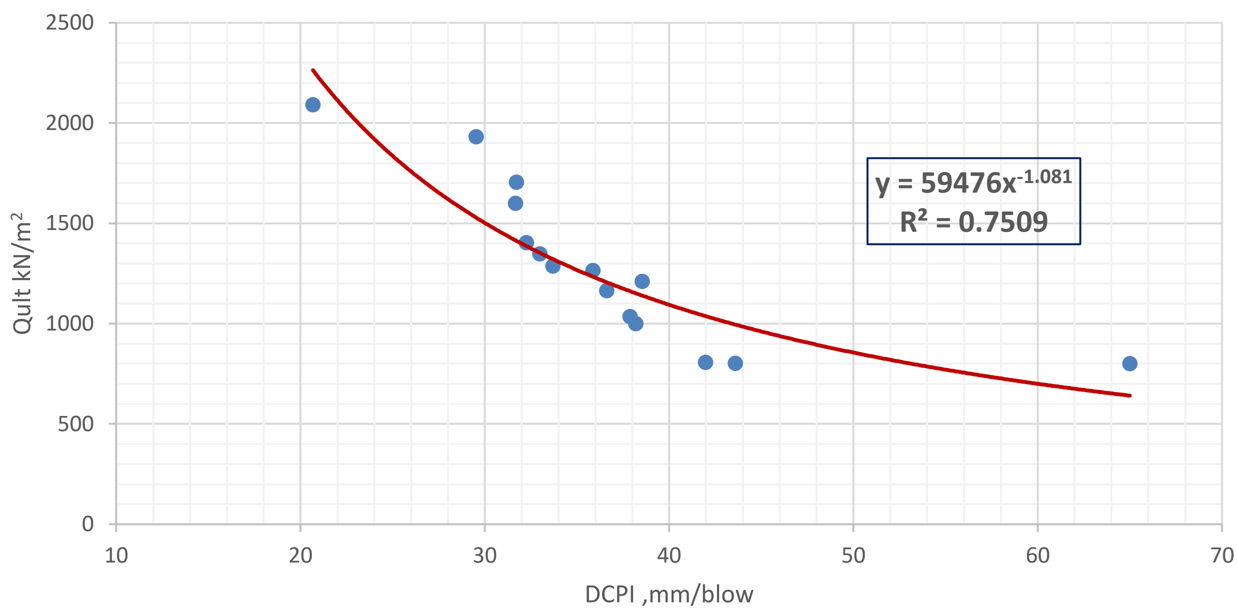

Figure 4.11: Plot of Q_{ult} vs. DCPI

The above scatter diagrams provide a visual method of displaying a relationship between variables as plotted in a two dimensional coordinate system. After carefully studying the data trend on the scatter plot from Figure 4.4 to Figure 4.11 and applying different models, correlations were developed for this category. The summary of the correlations is presented in Tables 4.5.

Table 4.5: Summary of single correlation

Reg. type	model	equation	R^2	α	Sample no.
Single regression type	1	$Q_{ult}=205.09*Df+907.24$	0.059	>0.05	15
	2	$Q_{ult}=150e^{-0.005NMC}$	0.0074	>0.05	15
	3	$Q_{ult}=2079.24e^{-0.008LL}$	0.025	>0.05	15
	4	$Q_{ult}=-615.1\ln(PI)+3438.5$	0.26	>0.05	15
	5	$Q_{ult}=1417.7CI^{0.4}$	0.086	>0.05	15
	6	$Q_{ult}=17015\ln(\gamma bulk)-47635$	0.154	>0.05	15
	7	$Q_{ult}=692.74\gamma dry-449.2$	0.206	>0.05	15
	8	$Q_{ult}=59476DCPI^{-1.08}$	0.751	<0.05	15

From the above developed single linear regression models, based on the coefficient of determination (R^2) and significance (α) it was noted that the Q_{ult} value correlates relatively better with dynamic cone penetration index, plasticity index, maximum dry density and bulk density which is an indication for these variables to form the multiple regression variables that could yield a better correlation result. While the remaining parameters showed a weak relationship with Q_{ult}.

4.3.2 Discussion of the regression analysis results

After carefully studying the data trend on the scatter plot and applying different models of single regression, it is clear that Q_{ult} is relatively more influenced by dynamic cone penetration index, plasticity index and dry density with coefficient of determination of 75.1%, 26% and 20.5%, respectively. The correlation of Q_{ult} with bulk unit weight, natural moisture content, consistency index and liquid limit gave weaker correlation coefficient. The relatively strong correlation between Q_{ult} and DCPI (given below) indicates the potential of DCP test in complementing the conventional geotechnical testing methods to determine the ultimate bearing capacity. The model is able to explain over seventy five percent of the variation in bearing capacity of soil.

$$Q_{ult}=59476DCPI^{-1.08} \text{ with } R^2= 75.1\%,$$

4.4. Evaluation and validation of developed equation.

Prior to considering the models for practical application to predict the bearing capacity of the soil, the model should be validated. Hence, the suitability of developed models have been examined by calculating ultimate bearing capacity using developed equation and comparing it with the actual value and also comparing developed equation with previous works. The comparison of the actual and predicted ultimate bearing capacity compared in Table 4.6.

$$Q_{ult}=59476DCPI^{-1.08}$$

Table 4.6: Comparison of actual value of Q_{ult} with predicted value.

sample no.	actual Q_{ult} kN/m^2	Predicted Q_{ult} kN/m^2, (from single reg.)	variation %
	A	a	$\lvert(A-a)/A*100\rvert$
1	802.61	1004.75	-25.18
2	800.86	652.50	18.52
3	2090.82	2251.43	-7.68
4	1599.47	1420.00	11.22
5	1931.92	1531.60	20.72
6	1264.69	1240.73	1.89
7	807.66	1046.99	-29.63
8	1034.99	1169.72	-13.02
9	1163.72	1213.28	-4.26
10	1000.77	1159.13	-15.82
11	1705.03	1417.10	16.89
12	1404.45	1391.94	0.89
13	1348	1358.67	-0.79
14	1287.46	1327.31	-3.09
15	1211.33	1148.08	5.22
average	**1296.92**	**1288.88**	**±11.7**

As shown in table 4.6 the correlation result has average variation of about ±11.7% from actual values of Q_{ult}. This means that determining ultimate bearing capacity of expansive soil of study area using developed correlation has valid results.

The model is again compared with previous work of Dzitse-Awuku (2008) and Getachew (2012). It can deduced that the developed correlation predict higher values at lower DCPI than that of Dzitse-Awuku (2008) and the work of Getachew (2012) shows lower values than that of this study.

But generally the gradient of the lines are almost the same for all studies as DCPI increases the bearing capacity decreases.

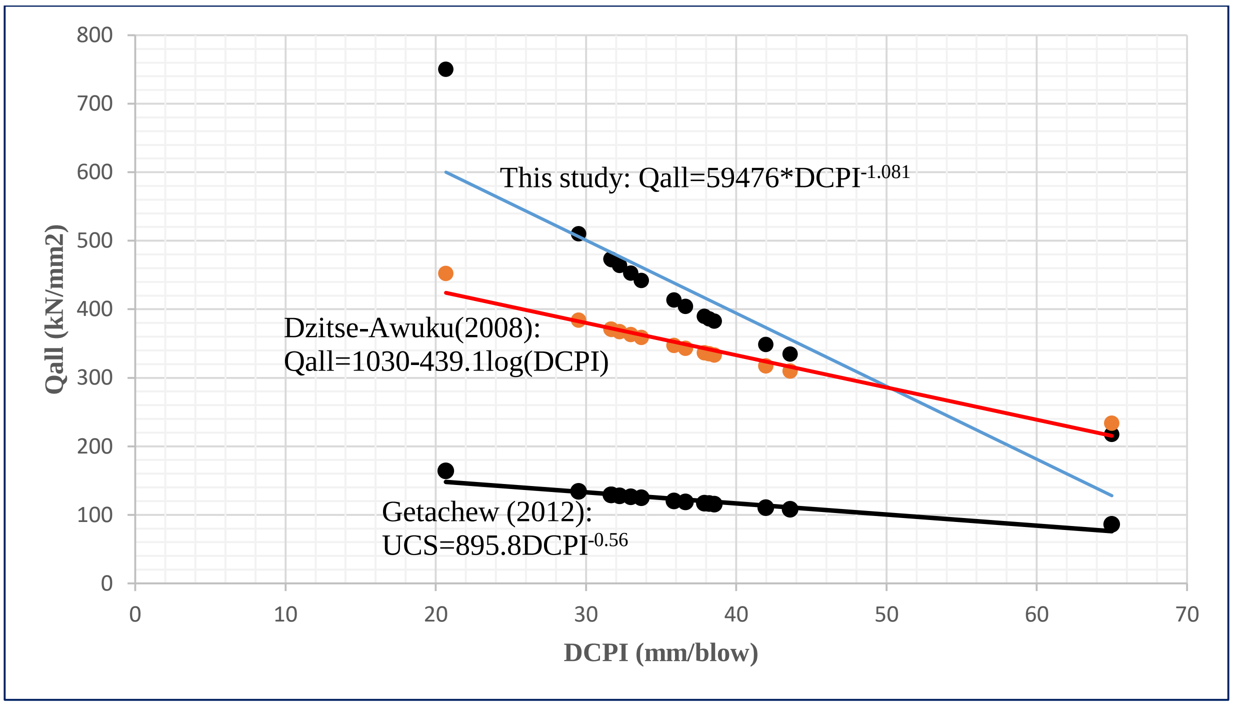

Figure 4.12: comparison developed correlation with work of Dzitse-Awuku (2008) and Getachew (2012)

To examine the effect of width of footing on ultimate bearing capacity, Q_{ult} for different width of footing have been calculated from Terzaghi's bearing capacity equation and correlated with only DCPI. Table 4.7 shows developed equations of Q_{ult} at different footing width. The coefficient of correlation remained almost the same for different width of footing, suggesting the width of footing has less effect on the prediction of bearing capacity.

Table 4.7: Values of Q_{ult} for different width of footing.

Reg. type	**Width of footing B (m)**	**Equation**	**R^2**	**Sample**
Single regression	B=1.5m	$Q_{ult}=59476DCPI^{-1.081}$	0.751	15
	B=2m	$Q_{ult}=67302DCPI^{-1.105}$	0.758	15
	B=2.5m	$Q_{ult}=70948DCPI^{-1.108}$	0.753	15

Then, the variation of Q_{ult} equations with width of footing have been seen and tabulated as table 4.8 below.

Table 4.8: Variation of Q_{ult} with width of footing.

sample no.	Predicted Q_{ult} kN/m^2, (from single reg.)			variation %	
	A	B	C		
	B=1.5m	B=2m	B=2.5m	$\lvert(B-A)/B*100\rvert$	$\lvert(C-B)/C*100\rvert$
1	1004.75	1038.47	1082.40	3.25	4.06
2	652.50	667.97	695.40	2.32	3.94
3	2251.43	2369.06	2474.82	4.97	4.27
4	1420.00	1478.98	1543.03	3.99	4.15
5	1531.60	1597.90	1667.44	4.15	4.17
6	1240.73	1288.40	1343.69	3.70	4.11
7	1047.00	1083.13	1129.08	3.34	4.07
8	1169.72	1213.07	1264.92	3.57	4.10
9	1213.28	1259.27	1313.23	3.65	4.11
10	1159.13	1201.84	1253.18	3.55	4.10
11	1417.10	1475.89	1539.80	3.98	4.15
12	1391.94	1449.11	1511.78	3.95	4.15
13	1358.67	1413.71	1474.75	3.89	4.14
14	1327.31	1380.37	1439.88	3.84	4.13
15	1148.08	1190.13	1240.94	3.53	4.09
average	**1288.88**	**1340.49**	**1398.29**	**3.71**	**4.12**

As seen from table 4.8 the variation of equation of Q_{ult} from equation of model footing used with width of footing is on average about 3.9%, when the width B increased form 1.5m to 2.0m and 2.0 to 2.5m and so on. So width of foundation has less effect on bearing capacity compared to other parameters. Thus, one can use equation developed for model footing of b=1.5m and account the variation for specific footing under consideration.

CHAPTER FIVE

5. CONCLUSION AND RECOMMENDATION

5.1. Conclusion

The aim of this study was to establish relationship between ultimate bearing capacity and DCPI (mm/blow) of expansive soil. For this study, fifteen soil samples were collected from different part of Asella.

Accordingly, the required laboratory tests (i.e. Atterberg limits, compaction, tri-axial shear strength test, etc.) were conducted on samples retrieved from different areas of the town. Using the obtained test results of fifteen soil sample, a single regressions analysis were made and a relationship was developed between Q_{ult} value and index properties (DCPI, LL, NMC, PI, CI ,γ_{bulk},γ_{dry} and depth of foundation) to construct empirical prediction models. The suitability of developed models have been examined by calculating ultimate bearing capacity using developed equation and comparing it with the actual value.

From the results of this study the following conclusions are drawn:

The correlation of Q_{ult} with DCPI has better relation than relation of Q_{ult} with other index properties. DCPI can be able to express the ultimate bearing capacity about 75%.

The comparison between the predicted ultimate bearing capacity (from developed equation) and actual ultimate bearing capacity is relatively good with average percentage variation of ±11.7%.

This means that the predicting ultimate bearing capacity of expansive soil of study area using developed correlation is reliable.

Footing dimension has little effect on bearing capacities since the variation in bearing capacities with width of footing is very small.

The results in general confirm that DCP has a great potential in contributing to the geotechnical investigation of expansive soil for preliminary assessment of the bearing capacity of soil and thus, in shallow foundation design.

5.2. Recommendation

The experience encountered in trying to conduct the current research has shown areas where further efforts may be required in the future. Following are some of the recommendations in relation to the subject study:

1. Additional works should be done with large number of samples from similar materials so as to validate the established correlation over the wide range.
2. Another mechanisms of correlating Q_{ult} with DCPI should tried to overcome the effect of footing shape and size to make the equation more general for all types of footing.

REFERENCES

Amini, F., 2003. Potential application of dynamic and static cone penetrometers in Mississippi department of transportation pavement design and construction, s.l.: final report, Mississippi department of transportation –USA.

Ampadu, S., 2005. A correlation between the dynamic cone penetrometer and bearing capacity of local soil formation, s.l.: 16th ICSMGE, Osaka, japan.

ASTM-D, 1998. Standard test methods for soil and rock, New York.: American Standard for Testing and Materials.

Budhu, M., 2007. Soil Mechanics and Foundations. 2nd ed., New York.: John Wiley & Sons Inc.

Burnham,T.,and Johnson,D., 1993. In-situ foundation characterization using the dynamic cone penetrometer, ,Minnesota department of transportation –USA.: s.n.

Chen, F., 1988. Foundation on Expansive Soils, s.l.: Elsevier scientific publishing company..

Chowdhury, M. R. H., 2013. shear strength properties of compacted expansive soils", s.l.: a thesis submitted to the faculty of graduate studies and research in partial fulfillment of the requirements for the degree of master of applied science in civil engineering.

Das, B. M., 2002. Principles of Geotechnical Engineering. 5th ed ., Thomson Learning, , U.S.A.

Desalegn, Y., 2012. developing correlation between DCP and CBR for locally used subgrade materials, s.l.: a thesis submitted to the school of graduate studies in the partial fulfillment of a master's degree in civil engineering, Addis Ababa university..

Dzitse-Awuku, D., 2008. correlation between dynamic cone penetrometer and allowable bearing pressure of shallow foundation using model footing, s.l.: Thesis submitted to department of civil engineering, Kwame Nkrumah University of science and technology, Ku.

George ,K.P., and Uddin,W.,2000. Subgrade characterization for highway pavement design, s.l.: Mississippi department of transportation, Jackson, MS..

Getachew, A., 2012. Correlating Dynamic Cone Penetration Index (DCPI) with Un-drained Shear Strength for Clayey Soils, addis ababa: thesis submitted to school of graduate studies of Addis Ababa University in partial fulfillment of the requirement for degree of masters of science.

Mayne,P.,W.,Auxt,J.,A.,Mitchell,J.,K.,and Yilmaz,R.,1995. Proceedings of international symposium on cone penetration testing. Linköping, Sweden vol.1.

McElvaney,J.,and Djatnika,I.,1991. Strength evaluation of lime-stabilized pavement foundation using the dynamic cone penetrometer, s.l.: Australian road res., volume 21..

Murthy, V., 2007. Geotechnical Engineering, Principles and Practice of Soil Mechanics and Foundation Engineering. In: Geotechnical Engineering, Principles and Practice of Soil Mechanics and Foundation Engineering. New York: Marcel Dekker, INC..

Prandtl, L., 1921. study on penetrating strength of plastic construction materials and shear strength of cutting edges, s.l.: zeit.Angew.maths.mechanics 1..

Sanglerat, G., 1972. The penetrometer and soil exploration, New york: Elsevier publishing.

Slater, D., 1983. Potential expansive soils in Arabian Peninsula. Journal of Geotechnical Engineering, ASCE, 109: A744–746.

T.G. Sitharam , 2013. Advanced Foundation Engineering , Bangalore : s.n.

Teklu, D., 2003. Examining the Swelling Pressure of Addis Ababa Expansive Soil, Addis Ababa: A Thesis presented to School of Graduate Studies, Addis Ababa University..

Terzaghi, K., 1943. Theoretical soil mechanics, New York.: Wiley Publications.

Vesic, A., 1973. Analysis of ultimate loads of shallow foundations. journal of soil mechanics and foundation division, ASCE vol.99.

Yilma, B., 2013. Study some of the Engineering properties of soil found in Asela Town, Addis Ababa: A thesis submitted to the school of graduate studies, Addis Ababa University, in partial fulfillment of the requirements for the Degree of Masters of Science in civil engineering.

APPENDIX A: Details of the SPSS Regression Analysis Outputs

Model 1: correlation between Qult and DCPI, LL, D_f, PI, NMC, CI, γbulk, γdry

Model Summary				
Model	R	R Square	Adjusted R Square	Std. Error of the Estimate
1	0.905[a]	0.819	0.577	259.00812
a. Predictors: (Constant), DCPI, LL, Df, NMC, bulkd, PI, dryd, CI				

Coefficients[a]						
Model		Unstandardized Coefficients		Standardized Coefficients	t	Sig.
		B	Std. Error	Beta		
1	(Constant)	6893.152	11138.006		0.619	0.559
	Df	398.549	277.205	0.471	1.438	0.201
	NMC	78.094	79.788	1.042	0.979	0.365
	LL	-39.978	51.858	-0.605	-0.771	0.470
	PI	18.895	32.813	0.403	0.576	0.586
	CI	2080.739	2465.847	0.838	0.844	0.431
	Bulkd	-823.763	1304.857	-0.337	-0.631	0.551
	Dryd	539.688	993.594	0.353	0.543	0.607
	DCPI	-32.850	11.606	-0.791	-2.830	0.030
a. Dependent Variable: Qult						

Model 2: correlation between Qult and DCPI, PI, γbulk, γdry

Model Summary				
Model	R	R Square	Adjusted R Square	Std. Error of the Estimate
1	0.859[a]	0.738	0.633	241.28469
a. Predictors: (Constant), DCPI, bulkd, PI, dryd				

Coefficients[a]						
Model		Unstandardized Coefficients		Standardized Coefficients	t	Sig.
		B	Std. Error	Beta		
1	(Constant)	-2401.932	8068.821		-0.298	0.772
	PI	-8.827	8.736	-0.188	-1.010	0.336
	Bulkd	800.372	560.197	0.327	1.429	0.184
	Dryd	-696.691	433.674	-0.456	-1.606	0.139
	DCPI	-38.298	9.216	-0.922	-4.155	0.002
a. Dependent Variable: Qult						

Model 3: correlation between Qult and DCPI and PI

Model Summary				
Model	R	R Square	Adjusted R Square	Std. Error of the Estimate
1	0.813[a]	0.661	0.605	250.24120
a. Predictors: (Constant), PI, DCPI				

Coefficients[a]						
Model		Unstandardized Coefficients		Standardized Coefficients	t	Sig.
		B	Std. Error	Beta		
1	(Constant)	2704.172	324.360		8.337	0.000
	DCPI	-30.186	7.468	-0.727	-4.042	0.002
	PI	-8.855	8.435	-0.189	-1.050	0.314
a. Dependent Variable: Qult						

Model 4: correlation between Qult and NMC, D_f, DCPI

Model Summary				
Model	R	R Square	Adjusted R Square	Std. Error of the Estimate
1	0.887[a]	0.787	0.729	207.29906
a. Predictors: (Constant), NMC, Df, DCPI				

Coefficients[a]						
Model		Unstandardized Coefficients		Standardized Coefficients	t	Sig.
		B	Std. Error	Beta		
1	(Constant)	1600.041	450.555		3.551	0.005
	DCPI	-36.994	6.049	-0.891	-6.116	0.000
	Df	289.167	120.130	0.342	2.407	0.035
	NMC	12.829	10.962	0.171	1.170	0.267
a. Dependent Variable: Qult						

Model 5: correlation between Qult and CI, LL, D_f, DCPI, NMC

Model Summary				
Model	R	R Square	Adjusted R Square	Std. Error of the Estimate
1	0.897[a]	0.805	0.697	219.24775
a. Predictors: (Constant), CI, LL, Df, DCPI, NMC				

Coefficients[a]						
Model		Unstandardized Coefficients		Standardized Coefficients	t	Sig.
		B	Std. Error	Beta		
1	(Constant)	888.846	1417.131		0.627	0.546
	DCPI	-34.536	7.057	-0.831	-4.894	0.001
	Df	263.022	130.657	0.311	2.013	0.075
	NMC	32.320	25.767	0.431	1.254	0.241
	LL	-9.594	12.009	-0.145	-0.799	0.445
	CI	715.423	885.723	0.288	0.808	0.440
a. Dependent Variable: Qult						

Model 6: correlation between Qult and NMC, LL, PI, CI, D_f, γdry, γbulk

Model Summary				
Model	R	R Square	Adjusted R Square	Std. Error of the Estimate
1	0.759[a]	0.576	0.152	366.43965
a. Predictors: (Constant), dryd, NMC, LL, Df, PI, bulkd, CI				

Coefficients[a]						
Model		Unstandardized Coefficients		Standardized Coefficients	t	Sig.
		B	Std. Error	Beta		
1	(Constant)	7585.222	15754.037		.481	0.645
	Df	675.413	366.956	.798	1.841	0.108
	NMC	145.301	107.768	1.938	1.348	0.220
	LL	-72.364	71.559	-1.096	-1.011	0.346
	CI	4517.433	3269.109	1.819	1.382	0.210
	PI	37.725	45.459	.804	.830	0.434
	Bulkd	-2249.915	1702.899	-.920	-1.321	0.228
	Dryd	2116.157	1164.088	1.385	1.818	0.112
a. Dependent Variable: Qult						

APPENDIX B: Details of the Laboratory Test Results

1. DCP test results

pit 1:@ 1.5m Asella hospital		latitude:
zero error =6cm		longitude:
cumulative no. of blow	depth of penetration (mm)	eff. Depth (mm)
0	0	0
2	150	90
4	250	190
6	272	212
8	322	262
10	371	311
12	442	382
14	556	496
16	731	671
18	860	800
20	957	897
22	1000	940
	slope=DCPI=43.6mm/blow	

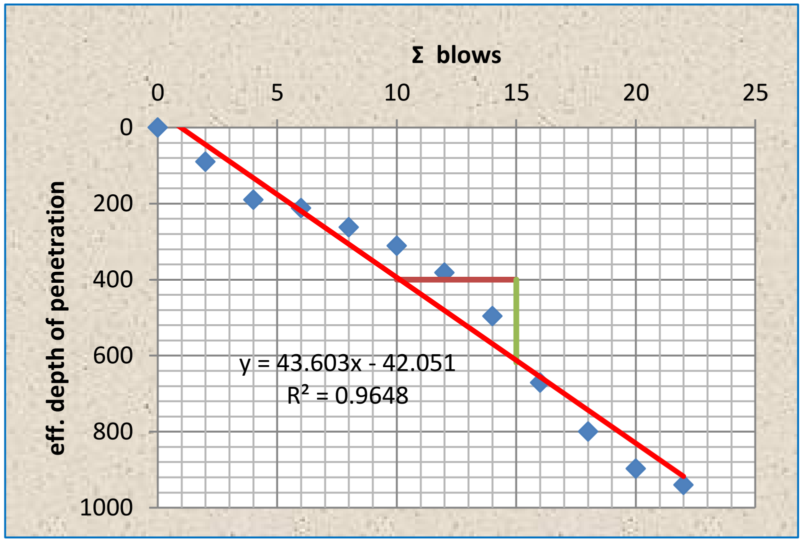

pit2 @2.5m stadium		latitude: 7.59.34
zero error=7.3cm		longitude: 39.7.45
No. Blow	depth of penetration (mm)	eff. Depth
0	0	0
2	132	59
4	238	165
6	378	305
8	522	449
10	647	574
12	817	744
14	939	866

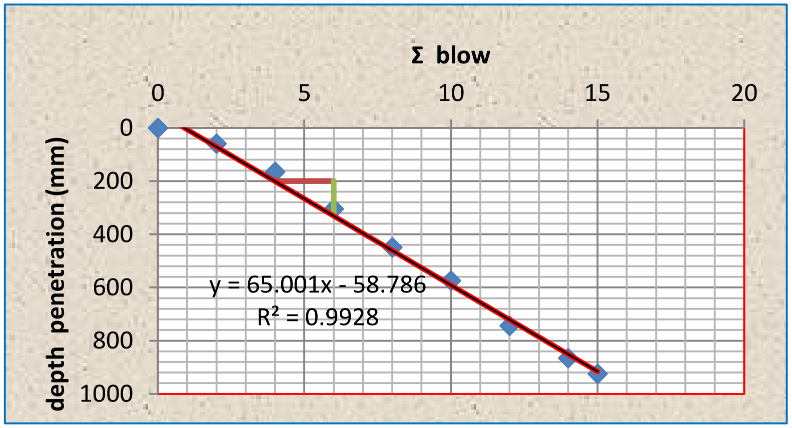

15	997	924
	DPI =slope =(330-200)/(6-4)=65mm/blow	

pit3 @ 2.0m kebele 9		Latitude
zero error= 5.8cm		Longitude
no blow	depth of penetration (mm)	eff. Depth
0	0	0
2	85	27
4	125	67
6	166	108
8	234	176
10	285	227
12	326	268
14	359	301
16	393	335
18	426	368
20	467	409
22	507	449
24	543	485
26	577	519
28	612	554
30	648	590
32	691	633
34	736	678
36	787	729
38	844	786
40	895	837
42	944	886
44	996	938
	slope=DPI=20.67mm/blow	

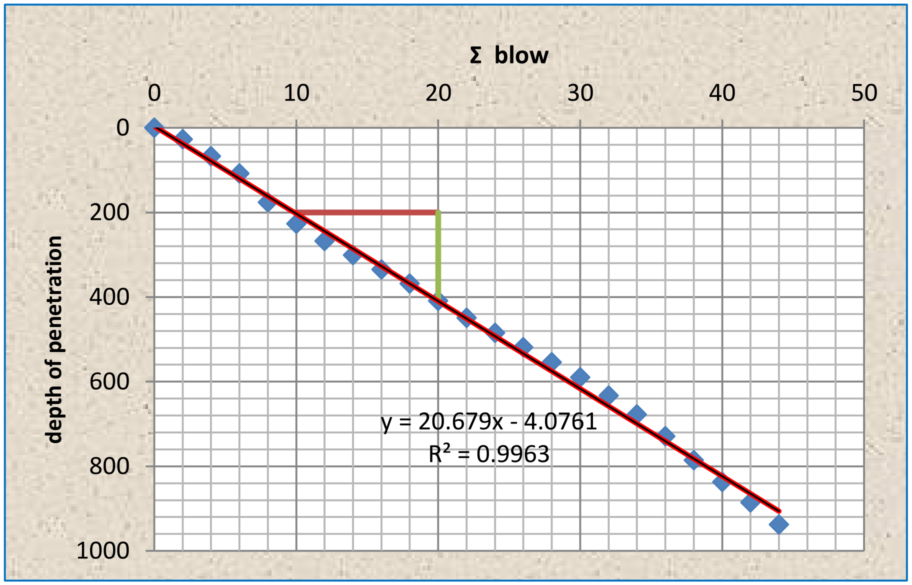

pit 4:@ 1.5m silingo		latitude:
zero error =7cm		longitude:
no blow	depth of penetration (mm)	eff.depth
0	0	0
2	134	64
4	190	120
6	240	170
8	290	220
10	346	276
12	416	346
14	484	414
16	550	480
18	609	539
20	672	602
22	731	661
24	796	726
26	876	806
28	967	897
29	995	925
	slope=DPI =31.66mm/blow	

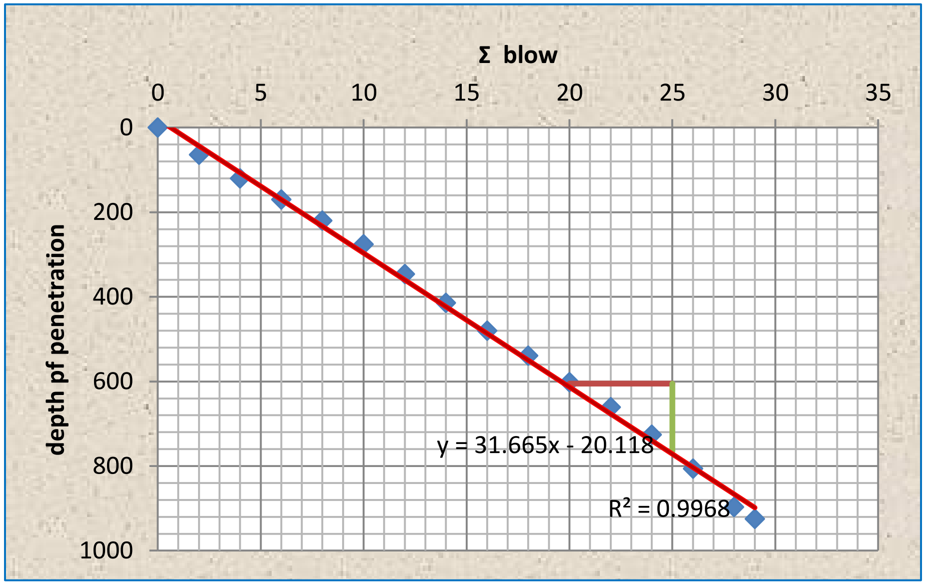

pit 5:@ 2.5m ;Arsi university		latitude:
zero error =7cm		longitude:
no blow	depth of penetration (mm)	eff.depth
0	0	0
2	141	71
4	187	117
6	234	164
8	302	232
10	336	266
12	416	346

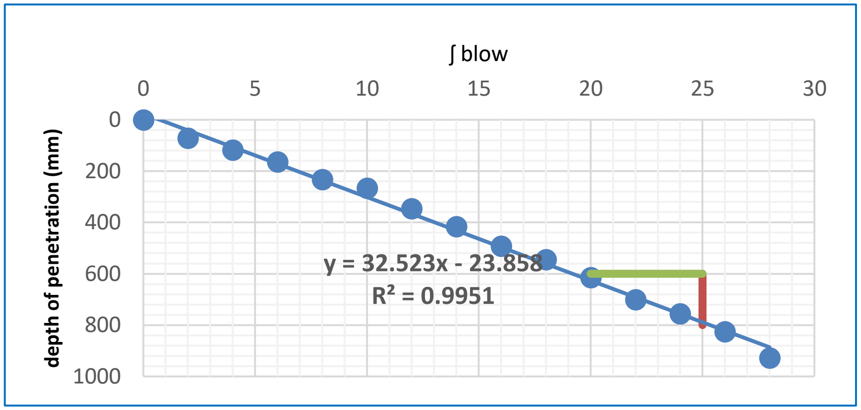

14	486	416
16	562	492
18	614	544
20	684	614
22	770	700
24	826	756
26	896	826
28	998	928
	slope=DPI =32.523mm/blow	

pit 6:@ 2.0m kebele 2		latitude:
zero error =7cm		longitude:
no blow	depth of penetration (mm)	eff.depth
0	0	0
2	78	8
4	134	64
6	168	98
8	213	143
10	247	177
12	289	219
14	323	253
16	379	309
18	446	376
20	531	461
22	592	522
24	633	563
26	687	617
28	736	666
30	796	726
32	841	771
34	882	812
36	953	883

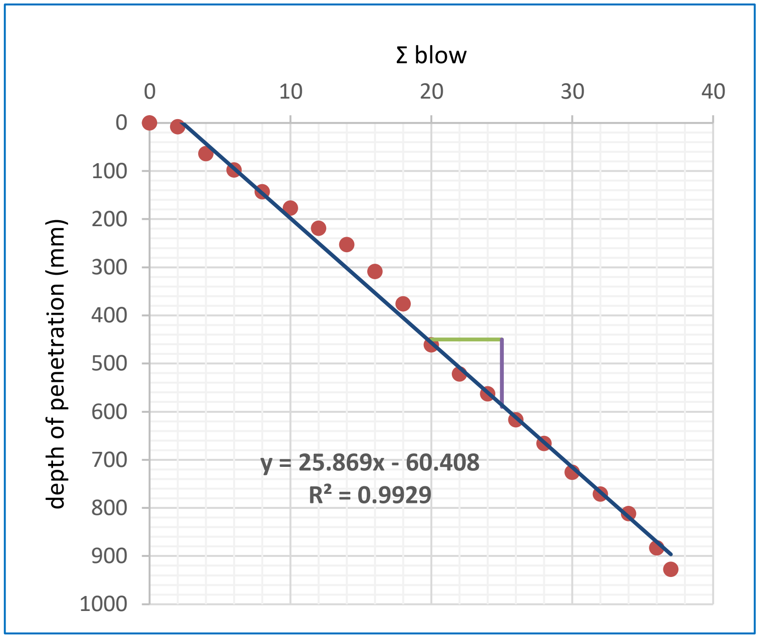

37	998	928
	slope=DPI =25.87mm/blow	

pit 7:@ 1.5m ,boseta meda		latitude:
zero error =7cm		longitude:
no blow	depth of penetration (mm)	eff.depth
0	0	0
2	169	99
4	280	210
6	368	298
8	461	391
10	508	438
12	599	529
14	682	612
16	776	706
18	853	783
20	947	877
22	997	927
	slope=DPI =41.97mm/blow	

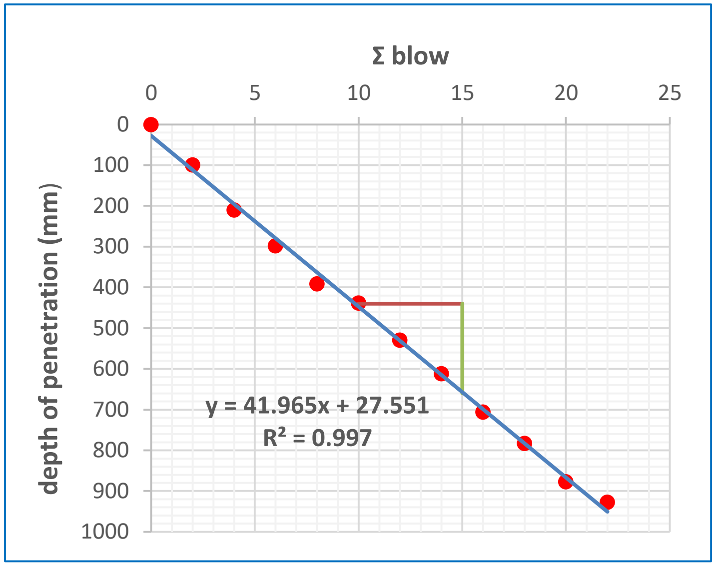

pit 8:@ 1.5m ,chilalo college		latitude:
zero error =7cm		longitude:
no blow	depth of penetration (mm)	eff.depth
0	0	0
2	141	71
4	190	120
6	226	156
8	284	214
10	348	278
12	422	352
14	488	418
16	548	478
18	612	542
20	678	608

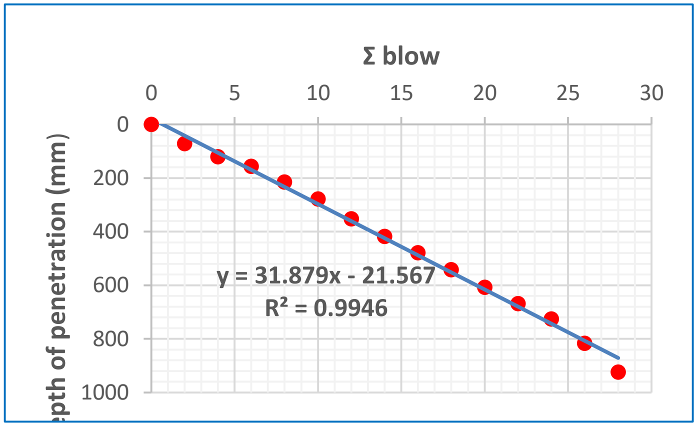

22	738	668
24	796	726
26	886	816
28	994	924
	slope=DPI =31.88mm/blow	

2. Natural moisture content

Pit 1 @:1.5m ,Asella hospital		
specimen number	1	2
Mc=mass of empty,clean+llid(g)	61	62
Mcms=mass of can,lid,and moist soil(g)	121	124
Mcds=mass of can, lid and dry soil (g)	101	104
Ms =mass of soil solids (g) =Mcds-Mc	40	42
Mw= mass of pore water (g) =Mcms-Mcds	20	20
w=water content ,w%= (mw/ms)*100	50	47.62
Average	48.81	

Pit 2 @ :2.5m Asella stadium		
specimen number	1	2
Mc=mass of empty,clean+llid(g)	61	61
Mcms=mass of can,lid,and moist soil(g)	120	115
Mcds=mass of can, lid and dry soil (g)	102	97
Ms =mass of soil solids (g) =Mcds-Mc	41	36
Mw= mass of pore water (g) =Mcms-Mcds	18	18
w=water content ,w%= (mw/ms)*100	43.90	50.00
Average	46.95	

Pit 3 @:2.0m keb.9		
specimen number	1	2
Mc=mass of empty,clean+llid(g)	62	62
Mcms=mass of can,lid,and moist soil(g)	138	137
Mcds=mass of can, lid and dry soil (g)	115	115
Ms =mass of soil solids (g) =Mcds-Mc	53	53
Mw= mass of pore water (g) =Mcms-Mcds	23	22
w=water content ,w%= (mw/ms)*100	43.40	41.51
Average	42.45	

Pit 4 @: 1.5m keb.10 ,Silingo		
specimen number	1	2
Mc=mass of empty,clean+llid(g)	97	96
Mcms=mass of can,lid,and moist soil(g)	201	193
Mcds=mass of can, lid and dry soil (g)	169	163
Ms =mass of soil solids (g) =Mcds-Mc	72	67
Mw= mass of pore water (g) =Mcms-Mcds	32	30
w=water content ,w%= (mw/ms)*100	44.44	44.78
Average	44.61	

Pit 5 @:2.5m Arsi university		
specimen number	1	2
Mc=mass of empty,clean+llid(g)	96	96
Mcms=mass of can,lid,and moist soil(g)	203	201
Mcds=mass of can, lid and dry soil (g)	171	169
Ms =mass of soil solids (g) =Mcds-Mc	75	73
Mw= mass of pore water (g) =Mcms-Mcds	32	32
w=water content ,w%= (mw/ms)*100	42.67	43.84
Average	43.25	

Pit 6 @: 2.0m keb. 2		
specimen number	1	2
Mc=mass of empty,clean+llid(g)	96	96
Mcms=mass of can,lid,and moist soil(g)	195	179
Mcds=mass of can, lid and dry soil (g)	168	153
Ms =mass of soil solids (g) =Mcds-Mc	72	57
Mw= mass of pore water (g) =Mcms-Mcds	27	26
w=water content ,w%= (mw/ms)*100	37.5	45.61
Average	41.56	

3. Specific gravity

Pit 1 @ 1.5m, hospital		
specimen number	1	2
Wp=mass of empty, clean pycnometer (g)	52	52
WPS=mass of empty pycnometer+dry soil (g)	60	61
WB=mass of pycnometer+dry soil +water (g)	158	159
WA=mass of pycnometer +water (g)	153	153
WO=wps-wp	8	9
specific gravity (Gs)= wo/(wo+(Wa-wb))	2.67	3.00
Average	2.83	

Pit 2 @:2.5m stadium		
specimen number	1	2
Wp=mass of empty, clean pycnometer (g)	52	52
WPS=mass of empty pycnometer+dry soil (g)	62	61.5
WB=mass of pycnometer+dry soil+water (g)	164.5	164
WA=mass of pycnometer +water (g)	158	158
WO=wps-wp	10	9.5
specific gravity (Gs)= wo/(wo+(Wa-wb))	2.86	2.71
average	2.79	

Pit 3 @ :2.0m keb.9		
specimen number	1	2
Wp=mass of empty, clean pycnometer (g)	52	52
WPS=mass of empty pycnometer+dry soil (g)	61	61.5
WB=mass of pycnometer+dry soil+water (g)	164.5	164
WA=mass of pycnometer +water (g)	158.5	158.5
WO=wps-wp	9	9.5
specific gravity (Gs)= wo/(wo+(Wa-wb))	3.00	2.38
average	2.69	

Pit 4 @:1.5m keb.10 Silingo		
specimen number	1	2
Wp=mass of empty, clean pycnometer (g)	46	46
WPS=mass of empty pycnometer+dry soil (g)	56.5	55.5
WB=mass of pycnometer+dry soil+water (g)	160	159.5
WA=mass of pycnometer +water (g)	153.5	153.5
WO=wps-wp	10.5	9.5
specific gravity (Gs)= wo/(wo+(Wa-wb))	2.63	2.71
average	2.67	

Pit 5 @:2.5m Arsi university		
specimen number	1	2
Wp=mass of empty, clean pycnometer (g)	46	46
WPS=mass of empty pycnometer+dry soil (g)	58	57
WB=mass of pycnometer+dry soil+water (g)	161	160.5
WA=mass of pycnometer +water (g)	153.5	153.5
WO=wps-wp	12	11
specific gravity (Gs)= wo/(wo+(Wa-wb))	2.67	2.75
Average	2.71	

Pit 6 @:2.0m keb .2		
specimen number	1	2
Wp=mass of empty, clean pycnometer (g)	46	46
WPS=mass of empty pycnometer+dry soil (g)	57	56.5
WB=mass of pycnometer+dry soil+water (g)	160.5	160
WA=mass of pycnometer +water (g)	153.5	153.5
WO=wps-wp	11	10.5
specific gravity (Gs)= wo/(wo+(Wa-wb))	2.75	2.63
Average	2.69	

4. Atterberg limit

testing date						
sample location	pit1:asela hospital ,@ 1.5m depth					
sample description	black soil					
method of testing used	ASTM D 4318					
	LL				PL	
sample no.	1	2	3	4	1	2
MC=mass of empty, clean can+lid(grams)	61	61	61	61	61	61
MCMS=mass of Can, lid and moist soil (grams)	81	79	76	71	69	73
MCDS=mass of can, lid and dry soils(grams)	72	71	70	68	67	70
MS=mass of soil solids(g)= MCDS-MC	11	10	9	7	6	9
MW= mass of pore water (g)=MCMS-MCDS	9	8	6	3	2	3
W=water content%=(MW/MS)*100	81.82	80	66.67	42.86	33.33	33.33
No. of drops (N)	17	23	28	34	33.33	
LL=64@ Blow =25,PI=LL-PL=64-33.33=30.67						

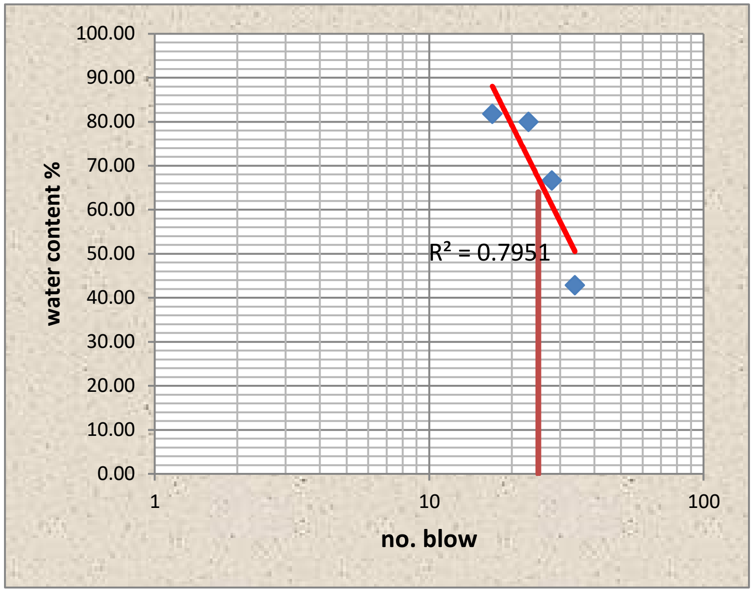

testing date	1.					
sample location	pit2:asela stadium @ 2.5m depth					
sample description	black soil					
method of testing used	ASTM D 4318					
	LL				PL	
sample no.	1	2	3	4	1	2
MC=mass of empty, clean can+lid(grams)	61	61	61	61	61	61
MCMS=mass of Can, lid and moist soil (grams)	81	78	78	81	70	71
MCDS=mass of can, lid and dry soils(grams)	72	71	72	75	68	69
MS=mass of soil solids(g)= MCDS-MC	11	10	11	14	7	8

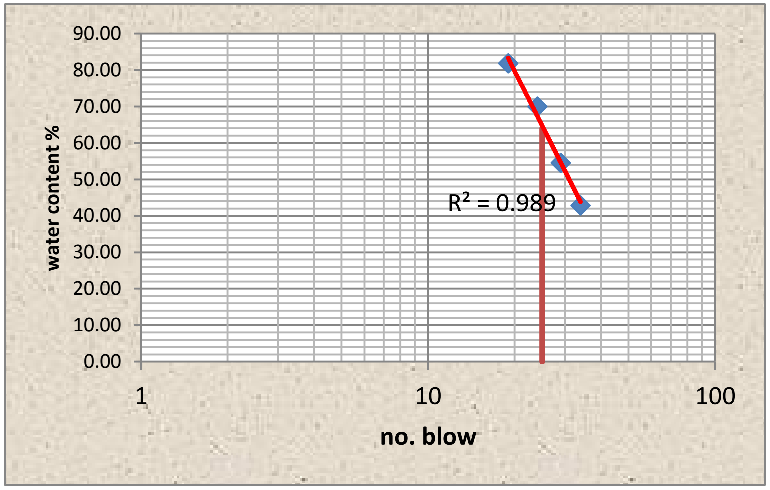

MW= mass of pore water (g)=MCMS-MCDS	9	7	6	6	2	2
W=water content%=(MW/MS)*100	81.82	70	54.55	42.86	28.57	25
No. of drops (N)	19	24	29	34	26.79	
LL=64@ Blow =25,PI=LL-PL=64-26.79=37.21						

testing date						
sample location	pit 3:asela kebele 9,@ 2m depth					
sample description	grayey soil					
method of testing used	ASTM D 4318					
	LL				PL	
sample no.	1	2	3	4	1	2
MC=mass of empty, clean can+lid(grams)	62	62	62	62	96	96
MCMS=mass of Can, lid and moist soil (grams)	72	81	78	74	118	109
MCDS=mass of can, lid and dry soils(grams)	68	74	73	71	111.5	105.5
MS=mass of soil solids(g)= MCDS-MC	6	12	11	9	15.5	9.5
MW= mass of pore water (g)=MCMS-MCDS	4	7	5	3	6.5	3.5
W=water content%=(MW/MS)*100	66.67	58.33	45.45	33.33	41.94	36.84
No. of drops (N)	18	23	28	34	39.40	
LL=51@ Blow =25,PI=LL-PL=50-45.56=11.61						

testing date						
sample location	pit4:asela kebele10 Silingo; @ 1.5m depth					
sample description	black soil					
method of testing used	ASTM D 4318					
	LL				PL	
sample no.	1	2	3	4	1	2
MC=mass of empty, clean can+lid(grams)	61	61	61	61	61	61
MCMS=mass of Can, lid and moist soil (grams)	76	77	79	77	70	74
MCDS=mass of can, lid and dry soils(grams)	69	70	72	71	68	71
MS=mass of soil solids(g)= MCDS-MC	8	9	11	10	7	10
MW= mass of pore water (g)=MCMS-MCDS	7	7	7	6	2	3
W=water content%=(MW/MS)*100	87.5	77.78	63.64	60	28.57	30
No. of drops (N)	16	24	29	34	29.29	
LL=70@ Blow =25 , PI=LL-PL=70-47.33=40.71						

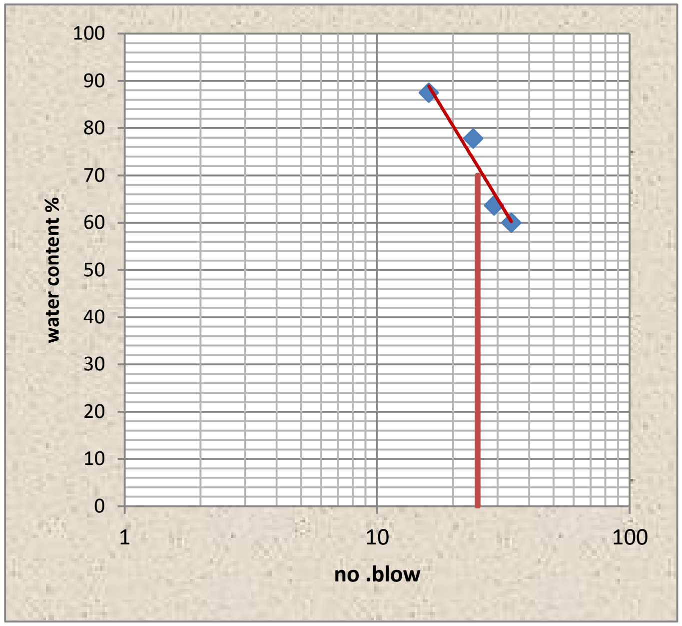

testing date						
sample location	pit5:arsi university; @ 2.5m depth					
sample description	black soil					
method of testing used	ASTM D 4318					
	LL				PL	
sample no.	1	2	3	4	1	2
MC=mass of empty, clean can+lid(grams)	61	61	61	61	61	61
MCMS=mass of Can, lid and moist soil (grams)	78	79	79	77	69	74
MCDS=mass of can, lid and dry soils(grams)	70	71	72	72	67	71
MS=mass of soil solids(g)= MCDS-MC	9	10	11	11	6	10

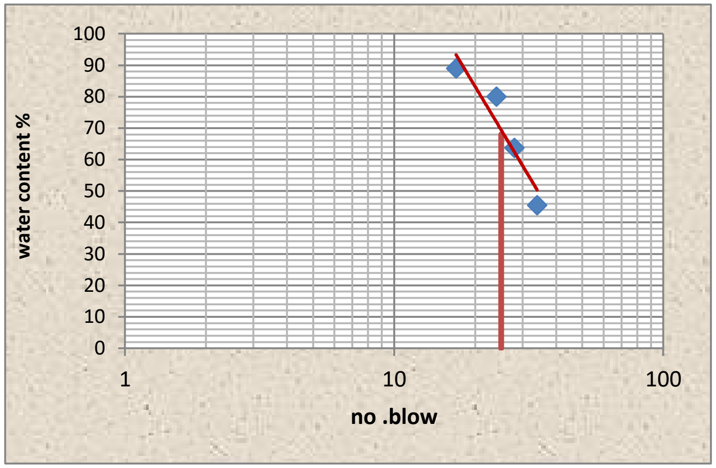

MW= mass of pore water (g)=MCMS-MCDS	8	8	7	5	2	3
W=water content%=(MW/MS)*100	88.89	80	63.64	45.45	33.33	30
No. of drops (N)	17	24	28	34	31.67	
LL=68@ Blow =25 , PI=LL-PL=68-38.89=36.33						

5. Free swell test results

Pit 1 @:1.5m		
sample number	1	2
initial volume =Vi (cm3)	10	10
final volume =Vf(cm3)	24	22
%free swell(FS)=((Vf-Vi)/Vi)*100	140	120
average FS	130	

Pit 2 @: 2.5m		
sample number	1	2
initial volume =Vi (cm3)	10	10
final volume =Vf(cm3)	21	20
%free swell(FS)=((Vf-Vi)/Vi)*100	110	100
average FS	105	

Pit 3 @ 2.0m		
sample number	1	2
initial volume =Vi (cm3)	10	10
final volume =Vf(cm3)	15	17.5
%free swell(FS)=((Vf-Vi)/Vi)*100	50	75
average FS	62.5	

Pit 4 @:1.5m		
sample number	1	2
initial volume =Vi (cm3)	10	10
final volume =Vf(cm3)	20.5	21
%free swell(FS)=((Vf-Vi)/Vi)*100	105	110
average FS	107.5	

Pit 11 @: 2m		
sample number	1	2
initial volume =Vi (cm3)	10	10
final volume =Vf(cm3)	21	22.5
%free swell(FS)=((Vf-Vi)/Vi)*100	110	125
average FS	117.5	

Pit 15 @: 2m		
sample number	1	2
initial volume =Vi (cm3)	10	10
final volume =Vf(cm3)	19	18
%free swell(FS)=((Vf-Vi)/Vi)*100	90	80
average FS	85	

6. Grain size distribution test results

sieve no	diameter(mm)	mass of empty sieve(g)	mass of sieve+retained soil(g)	mass of soil retained(g)	%retained	cum. Retained	% passing
	20			0			100
	10			0			100
	4.75			0		0	100
	2	466	496	30	6	6	94
	1.18	434	437	3	0.6	6.6	93.4
	0.6	406	417	11	2.2	8.8	91.2
	0.425	366	375	9	1.8	10.6	89.4
	0.3	373	374	1	0.2	10.8	89.2
	0.15	343	388	45	9	19.8	80.2
	0.075	252	285	33	6.6	26.4	73.6
	pan	253		368	73.6	100	0
%gravel=0,retained on 4.75			**%sand=26.4,retained on 0.075**			**%fine=73.6,pass 0,075**	
hydrometer test results							
Tested By:		K EMAL A.	Test Date:		27/02/017		
boring no.	pit 1@ Asella hospital		depth of sample		1.5m		
Specific Gravity of Solids:		2.83	Soil description		black clay soil		
Hydrometer Number (if known):		152H	Zero Correction: 8		Meniscus Correction:		1
Dispersing Agent:		sodium hexametaphosphate	amount used: 4%		and		125ml
Weight of Soil Sample:		50.gm	% finer	73.6	control sieve no.		200(75micron)

date	time of reading	elapsed time (min.)	Temp. °C	Actual Hyd.reading Ra	hyd.corr. For meniscus R.	L from table 1	K from table 2	D (mm)	CT From table 3	a from table 4	corr. Hyd. Reading RC	% Finer P	% Adjusted finer PA
27/02/017	9.33 am	0	22.5	41	42	9.6	0.01256	0	0.55	0.965	-	-	-
"	9:34	1	22.5	40.5	41.5	9.65	0.01256	0.03902	0.55	0.965	33.05	63.79	46.95
	9:35	2	22.5	39	40	9.9	0.01256	0.02794	0.55	0.965	31.55	60.89	44.82
	9:37	4	22.5	38	39	10.1	0.01256	0.01996	0.55	0.965	30.55	58.96	43.40
	9:41	8	22.5	37	38	10.2	0.01256	0.01418	0.55	0.965	29.55	57.03	41.98
	9:49	16	23	36	37	10.4	0.01252	0.01009	0.7	0.965	28.7	55.39	40.77
	10:05	32	23	35	36	10.6	0.01252	0.00721	0.7	0.965	27.7	53.46	39.35
	10:37	64	23	34.5	35.5	10.65	0.01252	0.00511	0.7	0.965	27.2	52.50	38.64
	11:41	128	24	34	35	10.7	0.012375	0.00358	1	0.965	27	52.11	38.35
	2:10	277	25	33	34	10.9	0.01223	0.00243	1.3	0.965	26.3	50.76	37.36
	6:20	527	26	32	33	11.1	0.01209	0.00175	1.65	0.965	25.65	49.50	36.44
28/02/017	9:30	1487	21.5	31.5	32.5	11.15	0.01275	0.00110	0.3	0.965	23.8	45.93	33.81

%gravel	% sandy	% silty	% clayey
0	**26.4**	**36.5**	**37.1**

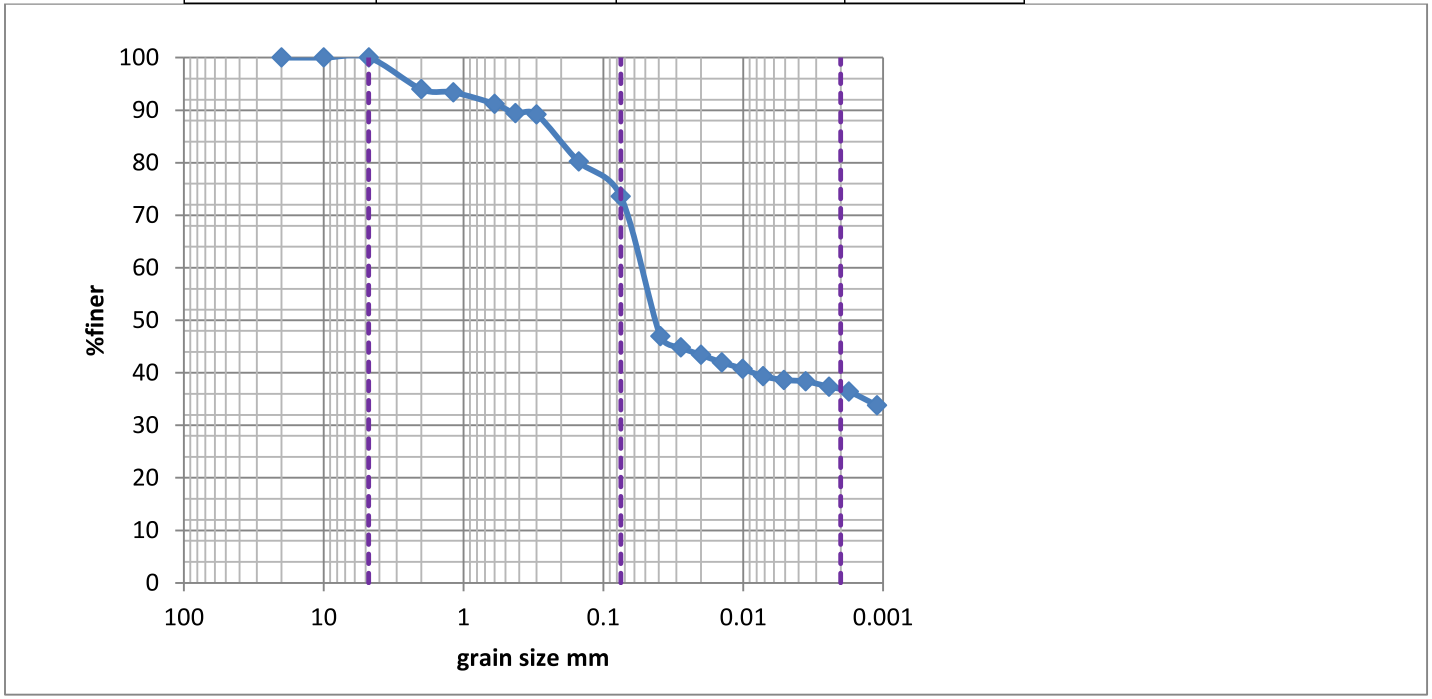

sieve no.	**diameter(mm)**	**mass of empty sieve(g)**	**mass of sieve+retained soil(g)**	**mass of soil retained(g)**	**%retained**	**cum. Retained**	**% passing**
	20						100
	10						100
	4.75					0	100
	2	466	468	2	0.4	0.4	99.6
	1.18	434	445	11	2.2	2.6	97.4
	0.6	406	407	1	0.2	2.8	97.2
	0.425	366	368	2	0.4	3.2	96.8
	0.3	373	374	1	0.2	3.4	96.6
	0.15	343	352	9	1.8	5.2	94.8
	0.075	252	341	89	17.8	23	77
	pan	253		385	77	100	0
	%gravel=0,retained on 4.75			**%sand=23,retained on 0.075**		**%finer=77,pass 0.075**	
hydrometer test results							
Tested By:		K EMAL A.	Test Date:		28/02/017		
boring no.		pit 2@ Asella stadium	depth of sample		2.5m		
Specific Gravity of Solids:		2.79	Soil description		black clay soil		
Hydrometer Number (if known):		152H	Zero Correction:	8	Meniscus Correction:		1
Dispersing Agent:		sodium hexametaphosphate	amount used:	4%	and		125ml
Weight of Soil Sample:		50.gm	% finer	77	control sieve no.		200(75micron)

date	time of reading	elapsed time (min.)	Temp. °C	Actual Hyd.reading Ra	hyd.corr. For meniscus R.	L from table 1	K from table 2	D (mm)	CT From table 3	a from table 4	corr. Hyd. Reading RC	% Finer P	% Adjusted finer PA
28/02/017	9:54	0	22.5	51	52	7.9	0.01273	0	0.55	0.972	-	-	
"	9:55	1	22.5	50	51	8.1	0.01273	0.03623	0.55	0.972	42.55	82.72	63.69
	9:56	2	22.5	49.5	50.5	8.2	0.01273	0.02578	0.55	0.972	42.05	81.75	62.94
	9:58	4	22.5	48.5	49.5	8.35	0.01273	0.01839	0.55	0.972	41.05	79.80	61.45
	10:02	8	22.5	48	49	8.4	0.01273	0.01304	0.55	0.972	40.55	78.83	60.70
	10:10	16	22.5	47.5	48.5	8.5	0.01273	0.00928	0.55	0.972	40.05	77.86	59.95
	10:26	32	23	46	47	8.8	0.01265	0.00663	0.7	0.972	38.7	75.23	57.93
	10:58	64	23	45.5	46.5	8.85	0.01265	0.00470	0.7	0.972	38.2	74.26	57.18
	12:02	128	24	44	45	9.1	0.01250	0.00333	1	0.972	37	71.93	55.38
	2:10	256	25.5	42	43	9.4	0.01229	0.00236	1.48	0.972	35.48	68.97	53.11
	6:20	506	27	41	42	9.6	0.01208	0.00166	2	0.972	35	68.04	52.39
29/02/017	10:00	1506	22	40.5	41.5	9.65	0.01279	0.00102	0.4	0.972	32.9	63.96	49.25

% gravel	%sandy	%silty	% clay
0	23	24.25	52.75

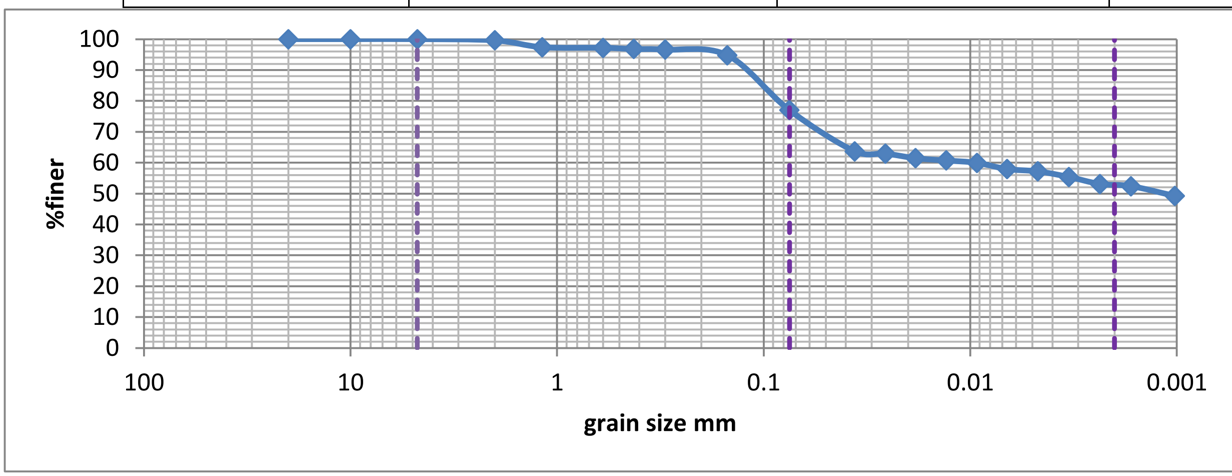

sieve no.	diameter(mm)	mass of empty sieve(g)	mass of sieve+retained soil(g)	mass of soil retained(g)	%retained	cum. Retained	% passing
	20					0	100
	10					0	100
	4.75					0	100
	2	466	470	4	0.8	0.8	99.2
	1.18	434	437	3	0.6	1.4	98.6
	0.6	406	415	9	1.8	3.2	96.8
	0.425	366	372	6	1.2	4.4	95.6
	0.3	373	373	0	0	4.4	95.6
	0.15	343	366	23	4.6	9	91
	0.075	252	282	30	6	15	85
	pan	253		425	85	100	0
	%gravel=0,retained on 4.75		**%sand=15,reatained on 0.075**			**%finer=85,pass 0.075**	
hydrometer test results							
Tested By:		K EMAL A.	Test Date:		28/02/017		
boring no.		pit 3@ maikel, kebele 9	depth of sample		2m		
Specific Gravity of Solids:		2.69	Soil description		gray clay soil		
Hydrometer Number (if known):		152H	Zero Correction:	8	Meniscus Correction:		1
Dispersing Agent:		sodium hexametaphosphate	amount used:	4%	and		125ml
Weight of Soil Sample:		50.gm	% finer	85	control sieve no.		200(75micron)

date	time of reading	elapsed time (min.)	Temp. °C	Actual Hyd.reading Ra	hyd.corr. For meniscus R.	L from table 1	K from table 2	D (mm)	CT From table 3	a from table 4	corr. Hyd. Reading RC	% Finer P	% Adjusted finer PA
27/02/017	10:20	0	27	50	51	8.1	0.01243	0	2	0.992	-	-	
"	10:21	1	27	48	49	8.4	0.01243	0.03603	2	0.992	42	83.33	70.83
	10:22	2	27	45	46	8.9	0.01243	0.02622	2	0.992	39	77.38	65.77
	10:24	4	27	41	42	9.6	0.01243	0.01926	2	0.992	35	69.44	59.02
	10:28	8	27	38.5	39.5	9.95	0.01243	0.01386	2	0.992	32.5	64.48	54.81
	10:36	16	27	34.5	35.5	10.65	0.01243	0.01014	2	0.992	28.5	56.54	48.06
	10:52	32	27	31.5	32.5	11.15	0.01243	0.00734	2	0.992	25.5	50.59	43.00
	11:24	64	26	29	30	11.5	0.01257	0.00533	1.65	0.992	22.65	44.94	38.20
	12:28	128	26	27	28	11.9	0.01257	0.00383	1.65	0.992	20.65	40.97	34.82
	2:40	260	26.5	24	25	12.4	0.0125	0.00273	1.68	0.992	17.68	35.08	29.82
	6:40	506	26.5	22	23	12.7	0.0125	0.00198	1.68	0.992	15.68	31.11	26.44

% gravel	% sand	% silty	%clay
0	**15**	**58**	**27**

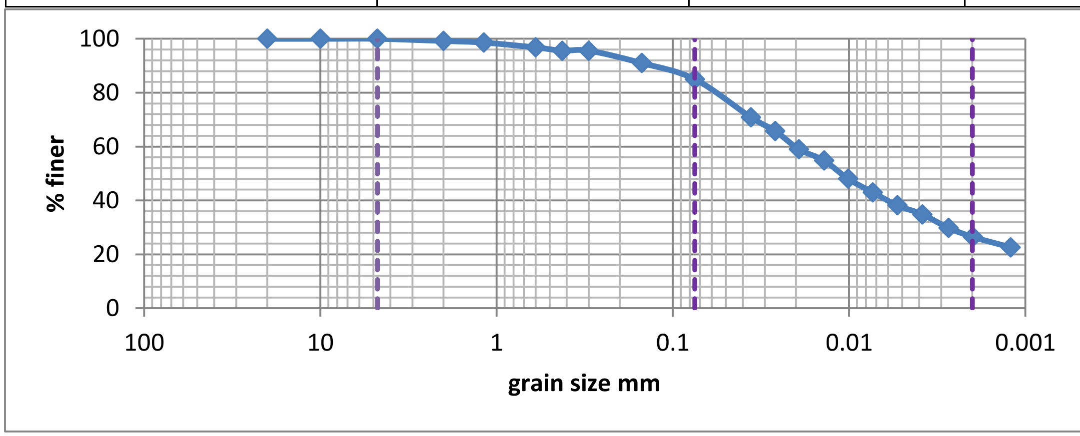

7. compaction test results

sample location	**asella stadium ,@ 2.5m depth**					
sample description	**black soil**					
method of test used	**ASTM D 698**					
compacted soil- sample no	**1**	**2**	**3**	**4**	**5**	**6**
MC = Mass of empty, clean can + lid (grams)	60	60	8	8	7	7
MCMS = Mass of can, lid, and moist soil (grams)	134	112	56	70	83	67
MCDS = Mass of can, lid, and dry soil (grams)	121	101	44	53	59	45
MS = Mass of soil solids (grams)	61	41	36	45	52	38
MW = Mass of pore water (grams)	13	11	12	17	24	22
W = Water content, w%	13.31148	18.82927	25.33333	29.77778	38.15385	49.89474
density determination	**volume of mold=944cm3**					
Compacted Soil - Sample no.	1	2	3	4	5	6
w = Assumed water content, w%	8	12	16	20	24	28
Actual average water content, w%	13.31148	18.82927	25.33333	29.77778	38.15385	49.89474
Mass of compacted soil and mold (grams)	5658	5739	5861	5948	6007	5981
Mass of mold (grams)	4405	4405	4405	4405	4405	4405
Wet mass of soil in mold (grams)	1253	1334	1456	1543	1602	1576
Wet density, ρ , (g/cm3)	1.327331	1.414634	1.544008	1.636267	1.698834	1.671262
Dry density, ρd , (g/cm3)	1.1714	1.190476	1.231922	1.260822	1.229668	1.114957
dry unit weight ɤd (KN/m3)	11.714	11.90476	12.31922	12.60822	12.29668	11.14957
for drawing saturation line(zero air void line S=100%	**Wsat= (ɤw/ɤd-1/Gs)100**				**Gs=2.79**	
ɤd	11.714	11.90476	12.31922	12.60822	12.29668	11.14957
Water content (%)	49.52565	48.15771	45.3317	43.47102	45.48048	53.84726
		MDD=12.5		OMC=31		

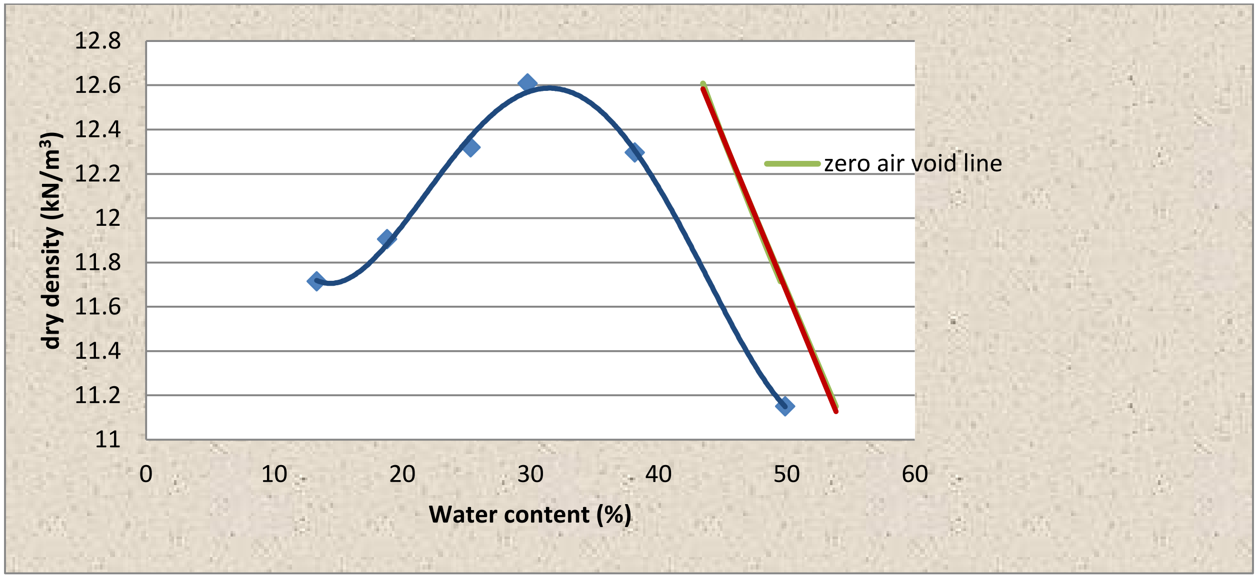

sample location	Asella maikel ,@ 2.0m depth					
sample description	**gray soil**					
method of test used	**ASTM D 698**					
compacted soil- sample no	**1**	**2**	**3**	**4**	**5**	**6**
MC = Mass of empty, clean can + lid (grams)	96	95	9	8	61	62
MCMS = Mass of can, lid, and moist soil (grams)	200	179	47	67	156	171
MCDS = Mass of can, lid, and dry soil (grams)	184	162	38	50	125	133
MS = Mass of soil solids (grams)	88	67	29	42	64	71
MW = Mass of pore water (grams)	16	17	9	17	31	38
W = Water content, w%	10.18182	17.37313	23.03448	32.47619	40.4375	45.52113

density determination	**volume of mold=944cm3**					
Compacted Soil - Sample no.	1	2	3	4	5	6
w = Assumed water content, w%	8	14	20	26	30	32
Actual average water content, w%	10.18182	17.37313	23.03448	32.47619	40.4375	45.52113
Mass of compacted soil and mold (grams)	5610	5784	5880	5983	6000	5961
Mass of mold (grams)	4405	4405	4405	4405	4405	4405
Wet mass of soil in mold (grams)	1205	1379	1475	1578	1595	1556
Wet density, ρ , (g/cm3)	1.276483	1.460805	1.5625	1.67161	1.689619	1.648305
Dry density, ρd , (g/cm3)	1.158524	1.244582	1.269969	1.261819	1.203111	1.132691
dry unit weight ɤd (KN/m3)	11.58524	12.44582	12.69969	12.61819	12.03111	11.32691
for drawing saturation line(zero air void line S=100%	Wsat= (ɤw/ɤd-1/Gs)100				Gs=2.69	
ɤd	11.58524	12.44582	12.69969	12.61819	12.03111	11.32691
Water content (%)	49.14199	43.17353	41.56735	42.07593	45.94315	51.11059
		OMC=27		MDD=12.8		

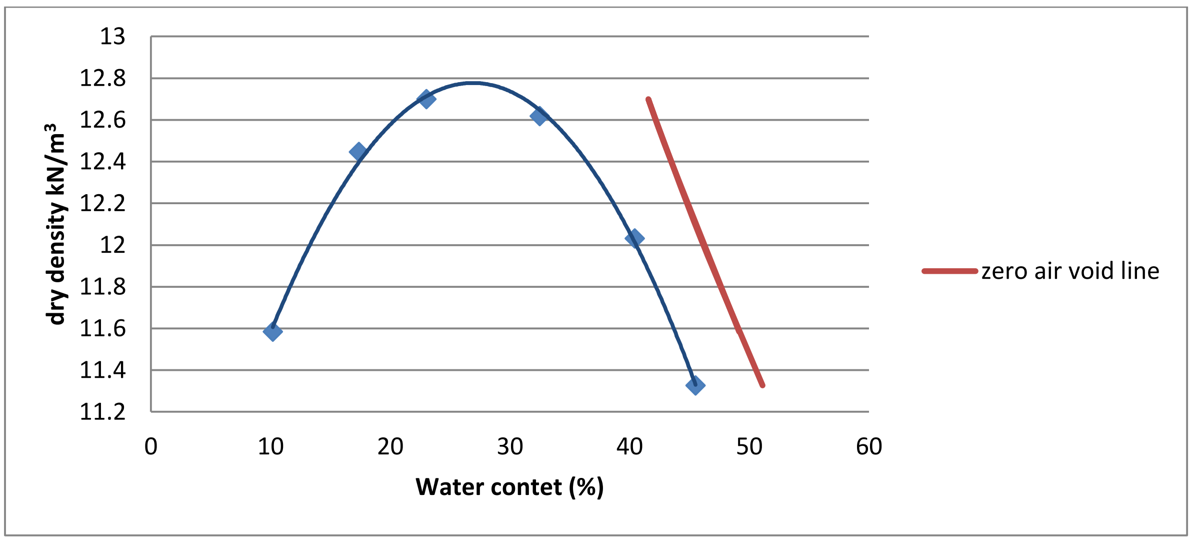

sample location	**Asella Maikel ,@ 1.5m depth**				
sample description	**black soil**				
method of test used	**ASTM D 698**				
compacted soil- sample no	**1**	**2**	**3**	**4**	**5**
Water content - Sample no.	8	12	18	22	26
Moisture can number - Lid number					
MC = Mass of empty, clean can + lid (grams)	61	61	61	61	61
MCMS = Mass of can, lid, and moist soil (grams)	127	111	122	120	126
MCDS = Mass of can, lid, and dry soil (grams)	118	103	109	104	106
MS = Mass of soil solids (grams)	57	42	48	43	45
MW = Mass of pore water (grams)	9	8	13	16	20
W = Water content, w%	10.78947	14.04762	22.08333	32.2093	39.44444
density determination	**volume of mold=944cm3**				
Compacted Soil - Sample no.	1	2	3	4	5
w = Assumed water content, w%	8	14	20	26	32
Actual average water content, w%	10.78947	14.04762	22.08333	32.2093	39.44444
Mass of compacted soil and mold (grams)	5689	5779	5926	6074	6056
Mass of mold (grams)	4405	4405	4405	4405	4405
Wet mass of soil in mold (grams)	1284	1374	1521	1669	1651
Wet density, ρ , (g/cm3)	1.360169	1.455508	1.611229	1.768008	1.748941
Dry density, ρd , (g/cm3)	1.227706	1.276229	1.319778	1.33728	1.25422
dry unit weight ɤd (KN/m3)	12.27706	12.76229	13.19778	13.3728	12.5422
for drawing saturation line(zero air void line S=100%	Wsat= (ɤw/ɤd-1/Gs)100			Gs=2.67	
ɤd	12.27706	12.76229	13.19778	13.3728	12.5422
Water content (%)	43.99951	40.90268	38.31714	37.32548	42.27762
	OMC=28		MDD=13.43		

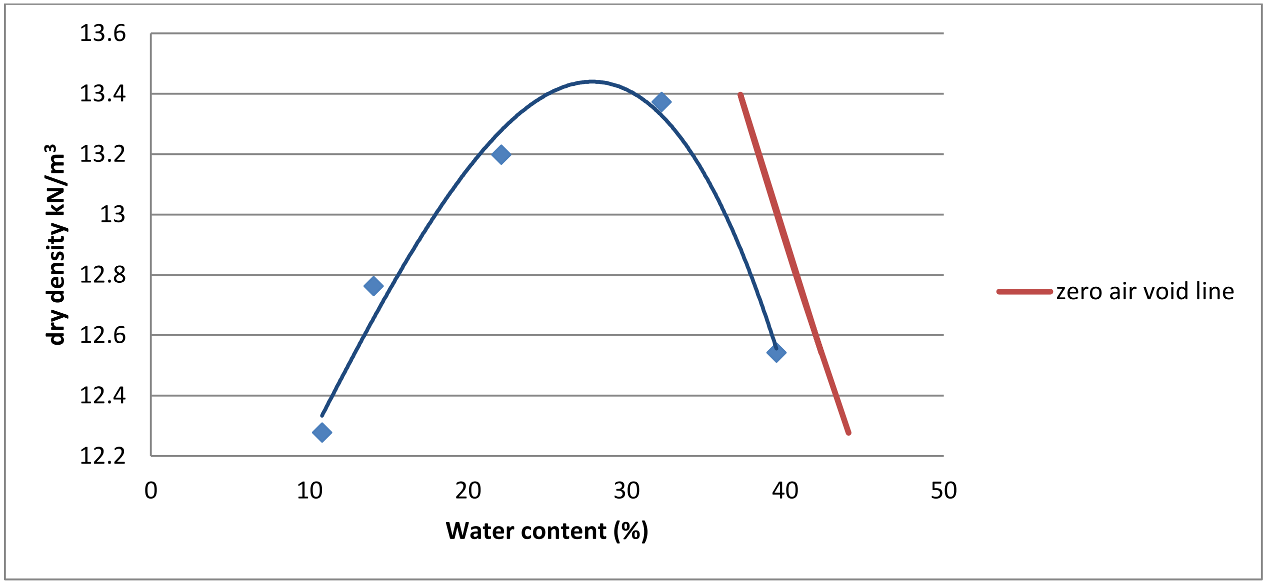
13.6
13.4
13.2
13
12.8
12.6
12.4
12.2
dry density kN/m³
0
10
20
30
40
50
Water content (%)
zero air void line

8. UU-Tri-axial test results

PIT3:sample A, Cell pressure ,σ3 = 150kpa, strain rate :Δε/Δt= 1mm/min					sample B, Cell pressure ,σ3 = 300kpa, strain rate :Δε/Δt= 1mm/min				
axial deformation (ΔL) mm	**Axial load P N**	**axial strain (εa)=ΔL/L0**	**corrected area (A)=A0/(1-εa)**	Deviator stress (σd)=P/A	**axial deformation (ΔL) mm**	**Axial load P N**	**axial strain (εa)=ΔL/L0**	**corrected area (A)=A0/(1-εa)**	**Deviator stress (σd)=P/A**
0	0	0	1133.54	0	0	0	0	1133.54	0
0.059	17	0.077631579	1134.420669	14.98562	0.059	3	0.07763158	1134.420669	2.644522
0.12	27	0.157894737	1135.33263	23.78158	0.12	6	0.15789474	1135.33263	5.284795
0.368	64	0.484210526	1139.055426	56.18691	0.368	12	0.48421053	1139.055426	10.53504
0.548	95	0.721052632	1141.772783	83.20395	0.548	17	0.72105263	1141.772783	14.88913
0.645	122	0.848684211	1143.242519	106.714	0.655	88	0.86184211	1143.394253	76.96383
0.761	153	1.001315789	1145.005117	133.6239	0.763	200	1.00394737	1145.035554	174.6671
0.863	183	1.135526316	1146.559485	159.6079	0.862	278	1.13421053	1146.544225	242.4678
0.981	222	1.290789474	1148.362948	193.3187	0.982	354	1.29210526	1148.378256	308.2608
1.074	243	1.413157895	1149.788324	211.3432	1.073	402	1.41184211	1149.772979	349.6342
1.16	282	1.526315789	1151.109567	244.981	1.163	439	1.53026316	1151.155712	381.3559
1.252	322	1.647368421	1152.526355	279.3862	1.254	470	1.65	1152.557194	407.7889
1.321	354	1.738157895	1153.591237	306.8678	1.319	494	1.73552632	1153.560343	428.2394
1.387	373	1.825	1154.611663	323.0523	1.388	512	1.82631579	1154.627138	443.4332
1.471	412	1.935526316	1155.913	356.4282	1.473	538	1.93815789	1155.94402	465.4205
1.553	443	2.043421053	1157.186186	382.8252	1.555	558	2.04605263	1157.217274	482.1912
1.641	473	2.159210526	1158.555656	408.267	1.643	575	2.16184211	1158.586818	496.2943
1.746	500	2.297368421	1160.193929	430.9624	1.779	600	2.34078947	1160.709772	516.9251
1.877	526	2.469736842	1162.244378	452.5726	1.876	614	2.46842105	1162.228698	528.2953
2.054	539	2.702631579	1165.026371	462.6505	2.056	636	2.70526316	1165.057882	545.8956
2.386	**580**	**3.139473684**	**1170.280653**	**495.6076**	**2.484**	**651**	**3.26842105**	**1171.840688**	**555.5363**
2.654	541	3.492105263	1174.556758	460.5993	2.721	631	3.58026316	1175.630672	536.7332
2.754	500	3.623684211	1176.160336	425.1121	2.753	626	3.62236842	1176.144279	532.2476

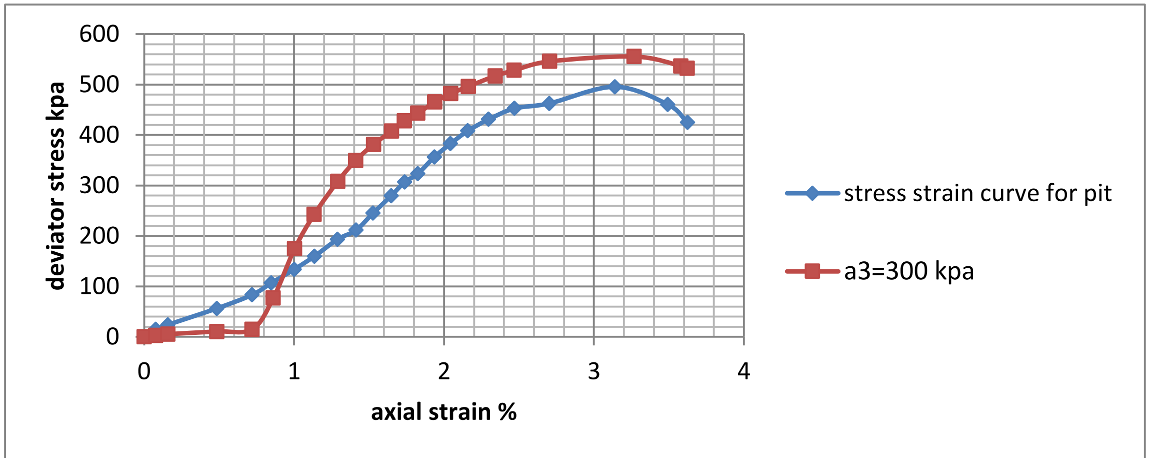

Cell pressure,σ_3 kpa	σ_d (σ_1-σ_3)kpa	σ_1 kpa
150	495.6	645.6
300	555.5	855.5

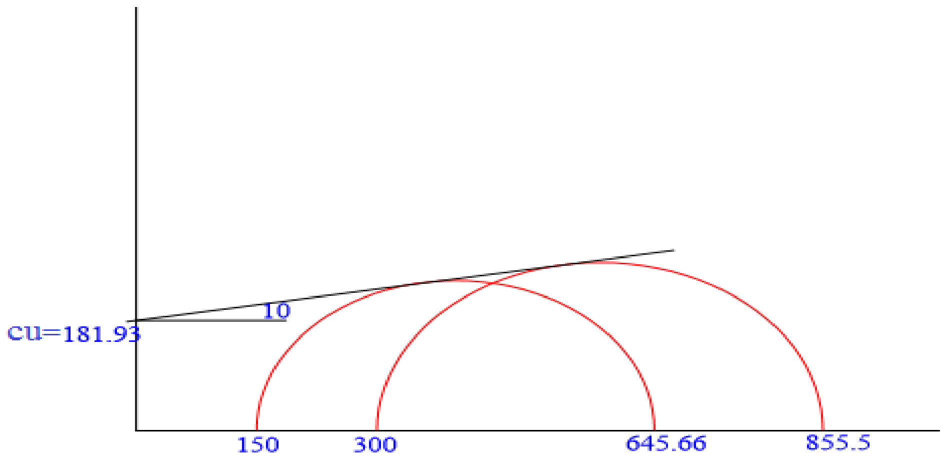

PIT6:sample A, Cell pressure ,σ3 = 150kpa, strain rate :Δε/Δt= 1mm/min					sample B, Cell pressure ,σ3 = 300kpa, strain rate :Δε/Δt= 1mm/min				
axial deformation (ΔL) mm	**Axial load P N**	**axial strain (εa)=ΔL/L0**	**corrected area (A)=A0/(1-εa)**	**Deviator stress (σd)=P/A**	**axial deformation (ΔL) mm**	**Axial load P N**	**axial strain (εa)=ΔL/L0**	**corrected area (A)=A0/(1-εa)**	**Deviator stress (σd)=P/A**
0	0	0	1133.54	0	0	0	0	1133.54	0
0.085	8	0.111842105	1134.809194	7.049643	0.085	18	0.11184211	1134.809194	15.8617
0.716	34	0.942105263	1144.320706	29.71195	0.716	59	0.94210526	1144.320706	51.55897
1.002	87	1.318421053	1148.684498	75.73881	1.002	103	1.31842105	1148.684498	89.66779
1.293	121	1.701315789	1153.158874	104.9292	1.293	197	1.70131579	1153.158874	170.8351
1.542	159	2.028947368	1157.01523	137.4226	1.542	231	2.02894737	1157.01523	199.6517
1.872	198	2.463157895	1162.165983	170.3715	1.872	269	2.46315789	1162.165983	231.4644
2.191	226	2.882894737	1167.188825	193.6276	2.191	304	2.88289474	1167.188825	260.4549
2.452	265	3.226315789	1171.330832	226.2384	2.452	354	3.22631579	1171.330832	302.2203
2.873	299	3.780263158	1178.074309	253.804	2.873	389	3.78026316	1178.074309	330.1999
3.123	331	4.109210526	1182.115619	280.0065	**3.123**	**403**	**4.10921053**	**1182.115619**	**340.9142**
3.543	356	4.661842105	1188.967802	299.4194	3.543	398	4.66184211	1188.967802	334.7441
3.923	375	5.161842105	1195.236206	313.7455	3.923	389	5.16184211	1195.236206	325.4587
4.211	387	5.540789474	1200.031203	322.4916	4.211	383	5.54078947	1200.031203	319.1584
4.512	394	5.936842105	1205.08393	326.9482	4.512	380	5.93684211	1205.08393	315.3307
4.897	**399**	**6.443421053**	**1211.609074**	**329.3141**	4.897	369	6.44342105	1211.609074	304.5537
5.001	394	6.580263158	1213.38385	324.7118	5.001	355	6.58026316	1213.38385	292.5702
5.542	386	7.292105263	1222.700616	315.6946	5.542	341	7.29210526	1222.700616	278.8908
5.783	376	7.609210526	1226.89719	306.4641	5.783	334	7.60921053	1226.89719	272.2314
6.123	362	8.056578947	1232.866895	293.6246	6.123	324	8.05657895	1232.866895	262.8021
6.543	342	8.609210526	1240.321926	275.7349	6.543	301	8.60921053	1240.321926	242.6789
6.983	321	9.188157895	1248.229277	257.1643	6.983	289	9.18815789	1248.229277	231.528
7.321	299	9.632894737	1254.37237	238.3662	7.321	276	9.63289474	1254.37237	220.0304

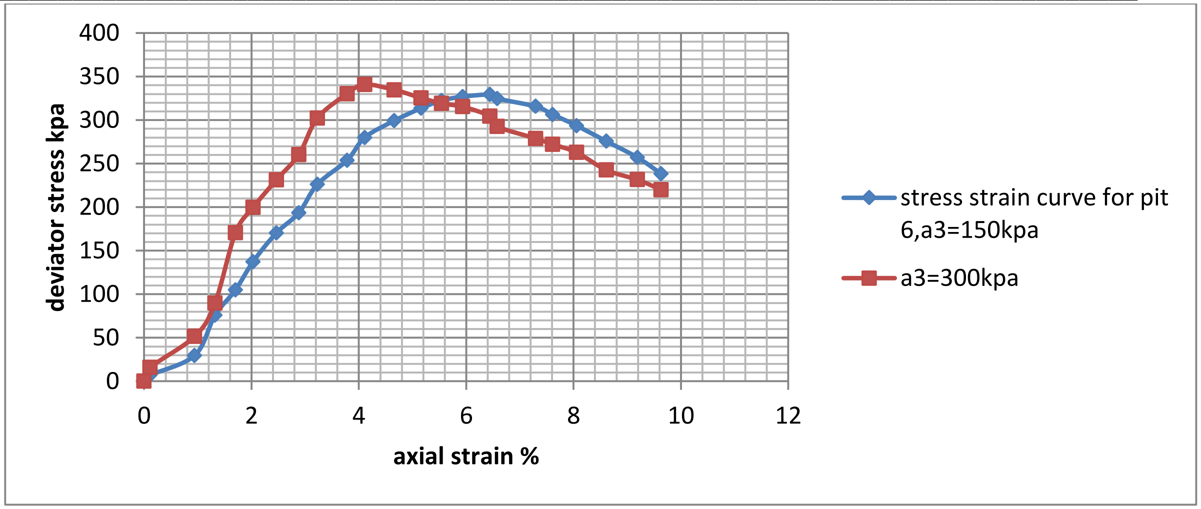

Cell pressure,σ_3 kpa	σ_d (σ_1-σ_3)kpa	σ_1 kpa
150	329.3	479.3
300	340.9	641

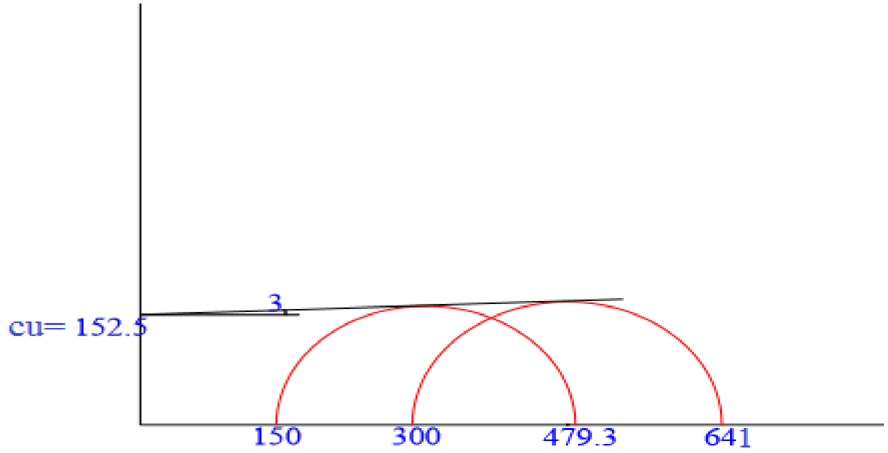

PIT7:sample A, Cell pressure ,σ3 = 150kpa, axial strain rate :Δε/Δt= 1mm/min					sample B, Cell pressure ,σ3 = 300kpa , strain rate :Δε/Δt= 1mm/min				
axial deformation (ΔL) mm	**Axial load P N**	**axial strain (εa)=ΔL/L0**	**corrected area (A)=A0/(1-εa)**	**Deviator stress (σd)=P/A**	**axial deformation (ΔL) mm**	**Axial load P N**	**axial strain (εa)=ΔL/L0**	**corrected area (A)=A0/(1-εa)**	**Deviator stress (σd)=P/A**
0	0	0	1133.54	0	0	0	0	1133.54	0
0.059	8	0.077631579	1134.420669	7.052058	0.059	20	0.07763158	1134.420669	17.63014
0.333	15	0.438157895	1138.528553	13.1749	0.333	22	0.43815789	1138.528553	19.32319
0.852	25	1.121052632	1146.391654	21.80756	0.852	56	1.12105263	1146.391654	48.84893
1.002	41	1.318421053	1148.684498	35.693	1.002	87	1.31842105	1148.684498	75.73881
1.228	64	1.615789474	1152.156422	55.54801	1.228	122	1.61578947	1152.156422	105.8884
1.336	80	1.757894737	1153.822994	69.33473	1.336	134	1.75789474	1153.822994	116.1357
1.559	100	2.051315789	1157.279456	86.40955	1.559	184	2.05131579	1157.279456	158.9936
1.73	127	2.276315789	1159.943988	109.488	1.73	216	2.27631579	1159.943988	186.2159
1.881	149	2.475	1162.307101	128.1933	1.881	230	2.475	1162.307101	197.8823
2.079	175	2.735526316	1165.420381	150.1604	2.079	262	2.73552632	1165.420381	224.8116
2.39	200	3.144736842	1170.344247	170.8899	2.39	293	3.14473684	1170.344247	250.3537
2.53	210	3.328947368	1172.574384	179.0931	2.53	312	3.32894737	1172.574384	266.0812
2.752	226	3.621052632	1176.128222	192.1559	2.752	318	3.62105263	1176.128222	270.3787
3	237	3.947368421	1180.123836	200.8264	3	321	3.94736842	1180.123836	272.0054
3.204	**243**	**4.215789474**	**1183.430958**	**205.3352**	**3.204**	**325**	**4.21578947**	**1183.430958**	**274.6252**
3.402	232	4.476315789	1186.658586	195.5069	3.402	319	4.47631579	1186.658586	268.8221
3.534	217	4.65	1188.820136	182.5339	3.534	289	4.65	1188.820136	243.0982
3.763	202	4.951315789	1192.58884	169.3794	3.763	267	4.95131579	1192.58884	223.8827
3.834	200	5.044736842	1193.762159	167.5376	3.834	253	5.04473684	1193.762159	211.935
3.953	192	5.201315789	1195.733896	160.5708	3.953	234	5.20131579	1195.733896	195.6957

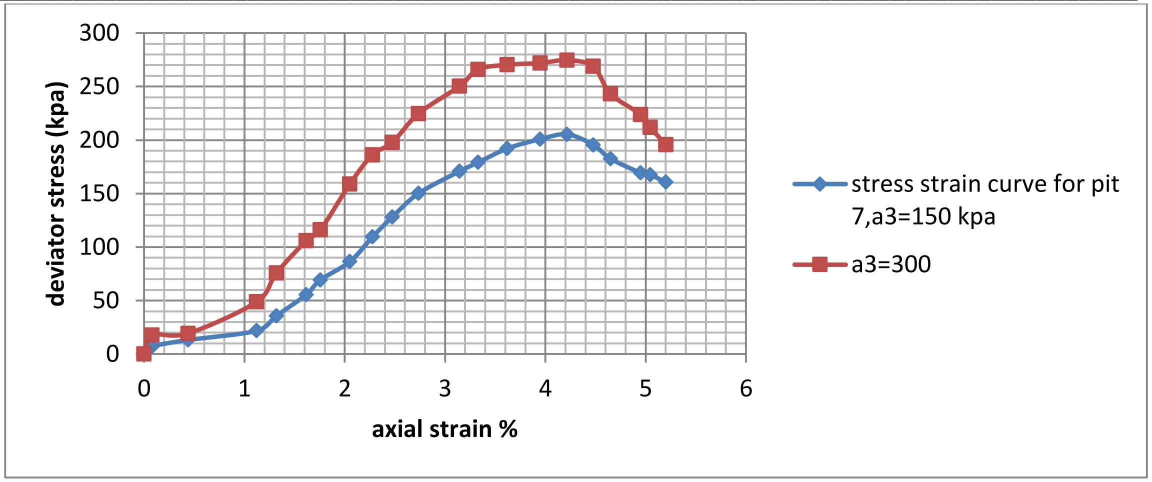

Cell pressure,σ_3 kpa	σ_d (σ_1-σ_3)kpa	σ_1 kpa
150	205.3	355.3
300	274.6	574.6

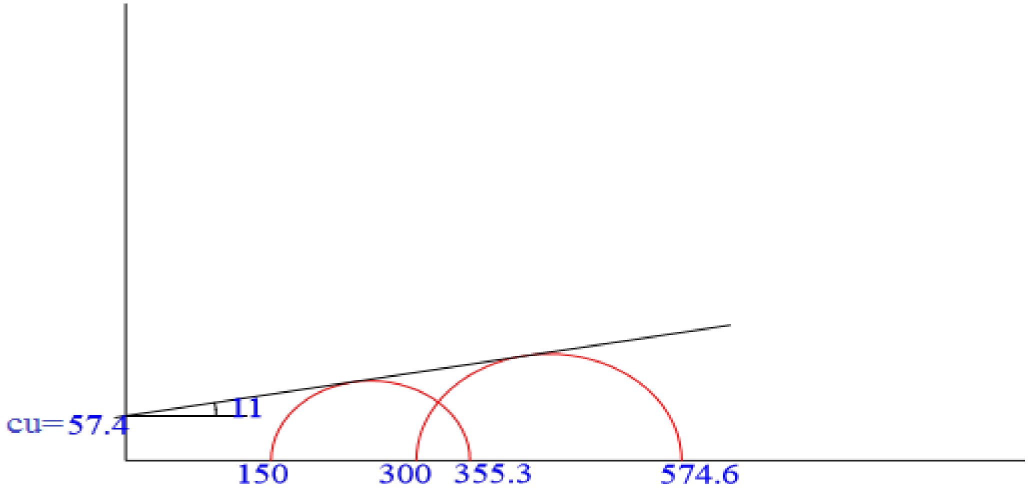

PIT10:sample A, Cell pressure ,σ3 = 150kpa, strain rate :Δε/Δt= 1mm/min					sample B, Cell pressure ,σ3 = 300kpa, strain rate :Δε/Δt= 1mm/min				
axial deformation (ΔL) mm	**Axial load P N**	**axial strain (εa)=ΔL/L0**	**corrected area (A)=A0/(1-εa)**	**Deviator stress (σd)=P/A**	**axial deformation (ΔL) mm**	**Axial load P N**	**axial strain (εa)=ΔL/L0**	**corrected area (A)=A0/(1-εa)**	**Deviator stress (σd)=P/A**
0	0	0	1133.54	0	0	0	0	1133.54	0
0.018	2	0.023684211	1133.808534	1.763966	0.018	5	0.02368421	1133.808534	4.409916
0.092	14	0.121052632	1134.913843	12.33574	0.092	34	0.12105263	1134.913843	29.95822
1.087	32	1.430263158	1149.987853	27.82638	1.087	76	1.43026316	1149.987853	66.08765
1.273	34	1.675	1152.850242	29.49212	1.273	103	1.675	1152.850242	89.34378
1.353	43	1.780263158	1154.085764	37.25893	1.353	121	1.78026316	1154.085764	104.8449
1.512	76	1.989473684	1156.549243	65.71272	1.512	154	1.98947368	1156.549243	133.1547
1.621	100	2.132894737	1158.244128	86.33758	1.621	174	2.13289474	1158.244128	150.2274
1.789	135	2.353947368	1160.866179	116.2925	1.789	224	2.35394737	1160.866179	192.9594
1.932	179	2.542105263	1163.107415	153.8981	1.932	243	2.54210526	1163.107415	208.9231
2.087	214	2.746052632	1165.546521	183.6049	2.087	268	2.74605263	1165.546521	229.9351
2.168	235	2.852631579	1166.825225	201.4012	2.168	297	2.85263158	1166.825225	254.5368
2.311	256	3.040789474	1169.089552	218.9738	2.311	332	3.04078947	1169.089552	283.9817
2.479	284	3.261842105	1171.760993	242.3702	2.479	368	3.26184211	1171.760993	314.0572
2.631	302	3.461842105	1174.188554	257.1989	2.631	382	3.46184211	1174.188554	325.3311
2.819	324	3.709210526	1177.205012	275.2282	2.819	369	3.70921053	1177.205012	313.4543
2.991	321	3.935526316	1179.978359	272.0389	2.991	358	3.93552632	1179.978359	303.3954
3.102	316	4.081578947	1181.775083	267.3944	3.102	344	4.08157895	1181.775083	291.0875
3.216	305	4.231578947	1183.626072	257.6827	3.216	339	4.23157895	1183.626072	286.408
3.354	297	4.413157895	1185.874515	250.4481	3.354	335	4.41315789	1185.874515	282.4919
3.518	279	4.628947368	1188.557711	234.7383	3.518	328	4.62894737	1188.557711	275.9647
3.726	271	4.902631579	1191.978305	227.3531	3.726	322	4.90263158	1191.978305	270.1391
3.849	267	5.064473684	1194.010339	223.6162	3.849	311	5.06447368	1194.010339	260.4668

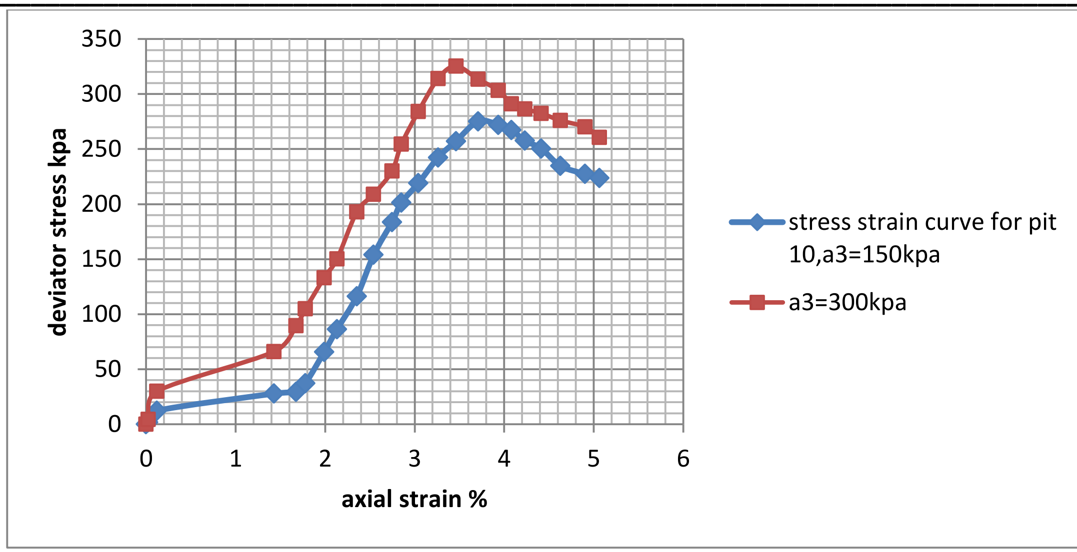

Cell pressure,σ_3 kpa	σ_d (σ_1-σ_3)kpa	σ_1 kpa
150	275.2	425.3
300	325.3	624.7

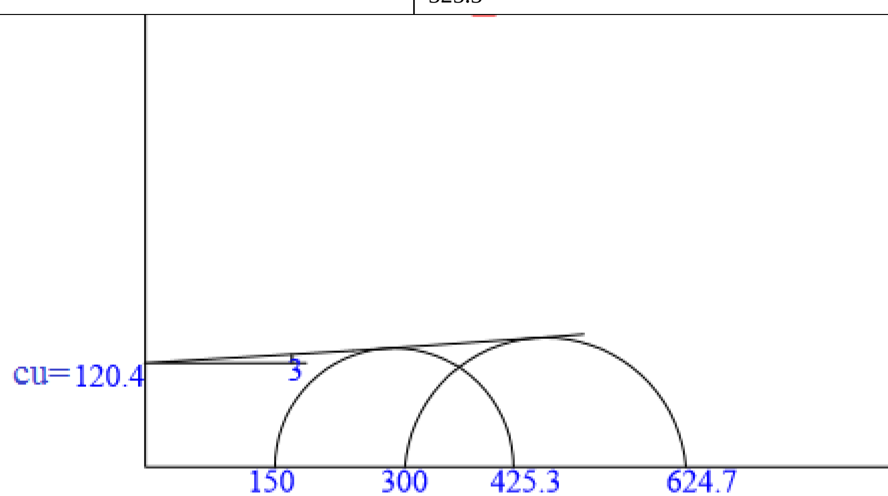

APPENDIX C: general overview of work done

Fig C-1: Hydrometer test

Fig C-2: Mounting sample on tri-axial machine

Fig C-3: sample after shearing

Fig C-4: when extruding sample from mold

Fig C-5: Visual image of soils of study area

Fig C-6: when excavating for taking soil sample